DEVELOPMENT OF AN INNOVATIVE MODULAR STEEL TRUSS SYSTEM

by

Sirou Zhuo

B.Eng., Fujian Agriculture and Forestry University, 2015

A THESIS SUBMITTED IN PARTIAL FULFILLMENT OF

THE REQUIREMENTS FOR THE DEGREE OF

MASTER OF APPLIED SCIENCE

in

THE FACULTY OF GRADUATE AND POSTDOCTORAL STUDIES

(Civil Engineering)

THE UNIVERSITY OF BRITISH COLUMBIA

(Vancouver)

April 2018

Abstract

This thesis proposes an innovative and economical modular steel truss system (MSTS), using modular steel floor system (MSFS) and modular buckling restrained braced truss moment frame (MBRBTMF). The proposed MSTS can be fabricated offsite and then shipped and assembled on site, saving construction time and fabrication expense. This specially designed floor system, MSFS, consists of space trusses and precast concrete slab toppings, and to fully utilize the spaces within the floors, the mechanical, electrical and plumbing (MEP) systems are pre-installed within. The proposed floor system was optimized for both gravity and lateral loads, using a robust structural optimization method conducted in conjunction with the Matlab and OpenSees. Space trusses are utilized to provide sufficient stiffness to support gravity, eliminate vertical deflection and transfer lateral force without significantly increasing floor depth. The buckling restrained braces (BRBs) in MBRBTMF are employed as energy dissipation components, allowing the structures to be repaired efficiently after earthquakes. The seismic performances of a MSTS structure and conventional structures with MSFS were systematically analyzed with OpenSees. The results show that the proposed modular system is highly efficient in resisting gravity and lateral loads, and can be used efficiently for modular constructions worldwide.

Lay Summary

The key purpose of this thesis is to develop an innovative and economical modular steel truss system (MSTS) for building structure. This MSTS consists of modular steel floor system (MSFS) and modular buckling restrained braced truss moment frame (MBRBTMF). The proposed MSTS can be fabricated offsite and then shipped and assembled on site, reducing fabrication errors and saving construction expense.

Detailed design of MSFS and MBRBTMF were conducted, and the optimal design was presented. The seismic behaviors of MSTS and conventional building structures using MSFS were studied, and the results show that the proposed modular steel system, MSTS, is highly efficient, and can be used effectively for modular applications.

Preface

Part of this thesis has been accepted in conference proceedings as detailed below.

1. Chapter 3: Yang TY, Zhuo SR, Li YJ. (2018). “Seismic Behavior and Design of Innovative Modular Steel Floor System”, Key Engineering Materials, Vol. 763, pp. 287-294.

The author of this thesis was responsible for the literature review, model development, data processing, and presentation of results. The manuscripts were drafted by the author of the thesis and revised based on comments by Professor T.Y. Yang at the University of British Columbia.

Table of Contents

List of Tables

List of Figures

List of Symbols

A: area

A_1: area of top and chord chords

A_2: area of web truss chords

A_g: gross area

A_{ne}: effective net area reduced for shear lag

A_{net}: effective net area for tension

A_{nes}: effective net area for shear rupture

C_r: factor compressive resistance of a member or a component

D: dead load

E: earthquake load

F_u: specified minimum tensile strength

F_y: specified minimum yield stress

$F(T)$: site coefficient for spectral acceleration

f_n: natural frequency

g: gravity

H: central height of space truss system

L: live load

M: magnitude

M_p: plastic moment resistance

M_r: factored moment resistance of a member or a component

M_y: yield moment resistance

$\bar{N}_{60}$: average standard penetration resistance

n: parameter for compression resistance

R_1: external radius of top and bottom chords

r_1: inside radius of top and bottom chords

S: elastic section modulus of a steel section

S_1: spacing along length

S_2: spacing along width

S_u: soil undrained shear strength

$S_a(T)$: 5% damped spectral response acceleration for a period of T

$S(T)$: design spectral response acceleration for a period of T

T: fundamental period

T_r: factored tensile resistance of a member of a component

$\bar{V}_{S30}$: average shear wave velocity

Z: plastic section modulus of a steel section

α: displacement demand-capacity ratio

β: force demand-capacity ratio

Δ: deflection

λ: non-dimensional slenderness parameter in column formula

$\emptyset$: resistance factor

List of Abbreviations

ADVE: average drift of vertical element

AP: annual probability

BRBF: buckling restrained braced frame

BRKBTMF: buckling restrained knee braced truss moment frame

DBE: design based earthquake

FEM: finite element model

MBRBTMF: modular buckling restrained braced truss movement frame

MCE: maximum considered earthquake

MDD: maximum diaphragm deflection

MEP: mechanical, electrical and plumbing

MSTS: modular steel truss system

MSFS: modular steel floor system

RT: return period

STFS: space truss floor system

STWFS: space truss with w-beam floor system

TR: period range

TRS: scenario-specific period range

OWSJ: open web steel joists

PGA: peak ground acceleration

UHS: uniform hazard spectrum

Acknowledgements

This work is funded by Canadian Institute of Steel Construction (CISC).

Firstly, I would like to sincerely thank my supervisor Professor T. Y. Yang for his patient instruction, insightful inspiration, kindly encouragement through my MASc program. His knowledge, passion, diligence and devotion extended a broader scope for my study. This work could not have been completed without his generous support. My deep gratitude is also extended to Prof. Lin-hai Han from Department of Civil Engineering of Tsinghua University for reviewing my thesis and providing invaluable advice.

Furthermore, I wish to thank Dr. Dorian Tung, Yuanjie Li and Lisa Tobber for guiding on different projects and help with my studies. Many thanks to my friends and associates, Yuxin Pan, Hongzhou Zhang, Xinwen Zhang and Yingying Wang for their encouragement and support.

Above all, I would like to thank my parents, for their continual and unconditional love and support for my education and life choice.

Dedication

To my parents.

Chapter 1: Introduction

1.1 Modular Construction

Concrete is employed to construct a great number of buildings throughout North America. The Council on Tall Building and Urban Habitat (CTBUH)'s database (Council on Tall Buildings and Urban Habitat, 2017) reveals that, over the last five decades, steel market shares have declined significantly, while those for concrete and composite material have simultaneously increased (as demonstrated in Figure 1.1 and Figure 1.2). This is mostly due to the lack of an efficient steel construction method.

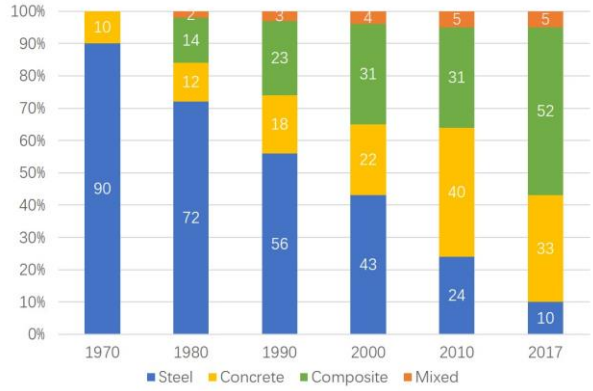

Figure 1.1 Material of the 100 tallest completed buildings, per decade

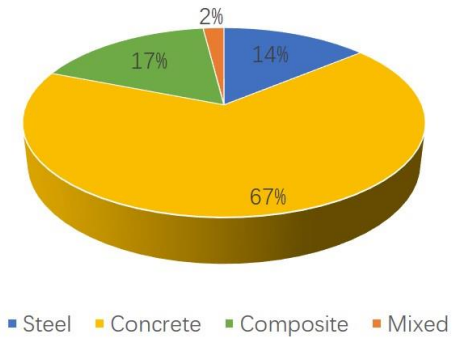

Figure 1.2 Tall buildings 150 meters (492 ft) or taller completed up until 2017: described by type of structural material

With an increasing demand for high quality control and construction speed, modular constructions are becoming increasing popular. Modular construction is a novel industrialized method in which most of the structural elements can be pre-fabricated in factories prior to their on-site assembly. This method is widely used for structures worldwide, some of the applications are described below. Little Hero (as shown in Figure 1.3), the first unitized modular building in Melbourne, Australia

is one of the notable applications of this technology. In China, T30A Tower Hotel, a 30-story building was constructed in 2012 within only 20 days (as shown in Figure 1.4).

Figure 1.3 Little Hero (Hickory Building Innovation, 2010)

Figure 1.4 T30A Tower Hotel (Broad Group, 2012)

This novel technology offers many significant advantages over conventional construction processes (Lawson et al., 2011; Lawson, Richards, 2010):

- Design flexibility: The modular construction method can be adapted to diverse architectural design and applied to various structural systems.

- Manufactural quantity improvement: Compared to on-site construction, the modular construction method has better quality control and assurance. Its intricate and elaborate details are pre-fabricated, while minimizing construction errors.
- Construction time reduction: With the factory performed prefabrication of its structural elements, on-site construction time is significantly shortened. Also, on-site and off-site construction work is able to proceed simultaneously. This greatly reduces construction time, directly translating to construction savings.
- Site condition independence: Site disturbance such as weather and traffic are lessened, since most the structural components are fabricated off-site, lowering both construction time and budget.
- Less material waste: The modules can be disassembled and relocated for a variety of purposes, reducing the demand for raw material and minimizing new demand expenditures.

Overall, the modular construction method provides various merits, compared with traditional structural constructions. However, the seismic performance of modular buildings under severe earthquake shaking may differ significantly from regular structures. Thus, an innovative modular steel truss system (MSTS) consists of both gravity system and seismic force resisting system were introduced and developed in this thesis.

1.2 Review of Floor System

The floor system, as the gravity system, is a significant component of building constructions. It not only supports the gravity load, but also connects the lateral load resisting systems. Over the years, several floor systems have been developed and applied in high-rise structures. The most

common floor systems use cast-in-place concrete, precast concrete, steel and several other emerging floor system materials and methods.

1.2.1 Concrete Floor System

Over the last few decades, concrete floor systems have been commonly used in the building industry. Designers can select from a wide variety of concrete floor systems for practical applications, including cast-in-place and precast concrete floor systems.

Cast-in-place concrete floor systems have been widely used in both residential and commercial applications. These systems are design flexible, and can be applied to a variety of architectural plan. The main advantage of this floor creating system is its continuity of structural system, where such frames as the lateral force resisting system can be implemented. Structural elements and floor system can be cast monolithically, and hence, connectors are not required between beams and columns as they are in most structural systems. Concrete floor systems are known to have good sound and temperature insulation, as well as providing clear surface and fire resistance. These systems are also durable and easy to maintain. Despite their advantages, the main disadvantage of cast-in-place concrete floor systems which is their requirement of a long, on-site curing period and the messy construction environment. The construction is also greatly affected by weather conditions. More importantly, a significant degree of labour is required to construct and deconstruct the formwork for concrete construction, resulting in increased cost.

Precast concrete floor systems are also commonly used in various types of constructions, since these systems provide high manufacture quality control and accuracy. The industry produces

standardized precast slabs, which offers a distinct advantage in construction cost and time. Compared with cast-in-place concrete floor systems, precast systems reduce the time required to set up the formworks and on-site concrete construction. The main drawback is the additional depth needed for the mechanical equipment employed. Furthermore, caulk joints may need to be established between the precast slabs for waterproofing, hence increasing maintenance cost. Although precast concrete floor systems are less affected by weather elements, proper care and maintenance are required for transportation to prevent damage of the precast concrete units. The heavy weight of the concrete slabs also escalates transportation costs and necessitates large crane capacities. Precast concrete hollow-core slabs are frequently employed in many applications as load-bearing floors and roofs (Girhammar, Pajari, 2008). One common type of shallow precast concrete floor is composed of precast prestressed hollow-core planks supported on the lower flange of the structural beams (Hegger et al., 2009). There are several advantages to precast hollow-core floor systems, including light weight, cost saving, high-quality control, fire and sound resistance, excellent deflection and vibrational characteristics. However, the conventional hollow-core floor systems possess laminations of a low span-to-depth ratio and less building design flexibility.

1.2.2 Steel Floor Systems

Steel trusses are commonly utilized in parallel to form steel floor systems. These floor systems provide an open web for mechanical systems, hence eliminating unnecessary waste of space. These systems consist of main steel framing with composite slab toppings. The open web steel joists (OWSJ) used as the main steel framing, illustrated in Figure 1.5, have been used extensively in industrial and structural applications.

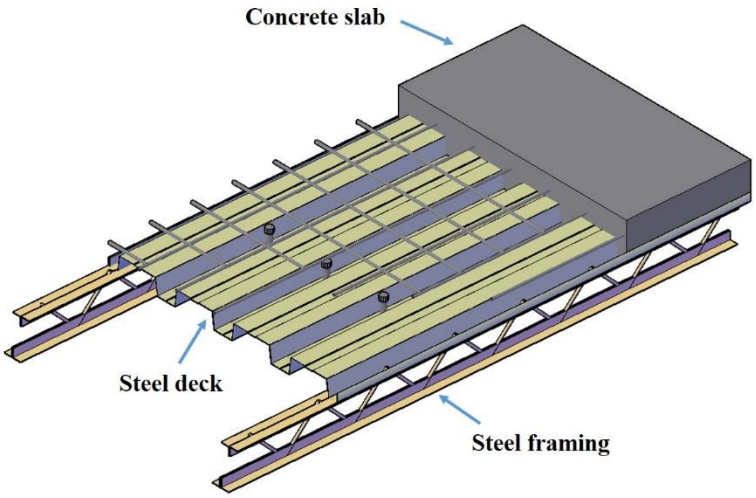

Figure 1.5 Steel framing floor systems

Composite slabs are one of the most common types of slabs used with steel framing floor systems, and consist of steel decking with reinforced concrete toppings. They are commonly used in commercial, industrial and residential buildings due to their rapid construction and general economic advantages. The steel deck sections are used not only as concrete forms during construction, but also as principal tensile reinforcements underlying composite slabs (De Silva et al. 2009). However, these composite slabs exhibit extremely complicated behavior. Additionally, their construction cost is high and require regular maintenance (Daniels et al. 1993).

These systems are further advantageous in that they greatly reduce construction waste, and do not require heavy equipment due to their light weight and easy installation. However, traditional steel floor systems are known to be deep, and toppings are required to cover them, which leads to higher floor depth. Although the mechanical, electrical and pumping systems can be extended between the webs of steel joists, enabling finishing ceilings near the joist's bases, a 16-inch deep steel joists are typically used for a 20 ft. span (Henin et al., 2012).

1.2.3 Emerging Floor Systems

In addition to the traditional floor systems presented above, numerous new floor systems have been developed, including the shallow flat soffit precast concrete floor system, Girder-slab system, Deltabeam system, Cobiax system, and Versa floor, are introduced in this section.

The shallow flat soffit precast concrete floor system has been developed to reduce floor height and construction costs in multistory buildings. Its hollow-core (HC) planks; prestressed beams; and continuous, precast columns are employed as the main structural components of the floor system, while the cast-in-place slabs are used as its topping (Henin et al., 2012; Morcous, Tadros, 2014). The system's detailed construction and installation procedures are detailed in Figure 1.6. This floor system eliminates the need for column corbels and beam ledges in construction and instead provides flat soffit for buildings. Compared with conventional precast concrete flooring, this emerging floor system reduces the depth of the structural floor and improves construction efficiency and quality. However, skilled workers may be needed for the installation of its complicated connections.

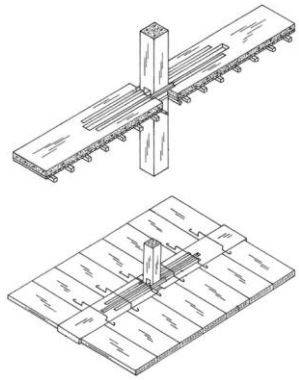

a) Construction sequence (Morcous, Tadros, 2014)

b) Installation of HC-beam connection reinforcement (Henin et al., 2012)

Figure 1.6 The shallow flat soffit precast concrete floor systems

The Girder-slab system is a composite steel and precast flooring system, developed by Girder Slab®, and presented in sectional view in Figure 1.7 (Girder-Slab Technologies, 2016). This floor system is cost-effective and commonly utilized in mid-to-high-rise residential constructions. It utilizes precast concrete panels with a steel beams to form composite slabs. The scheme has a thin depth of 8 to 10 inches, which maximizes its usable and salable floor height and minimizes building height. The Girder-slab system including steel beams and precast slab units, can be fabricated in factories, where construction quality and tolerance can be accurately controlled. However, it may become more difficult to achieve full moment beam connection. Moreover, mechanical equipment cannot be installed within the floor system, resulting in extra space usage and limiting clear floor height.

Figure 1.7 The Girder-slab system (Girder-Slab Technologies, 2016)

The Deltabeam system, as shown in Figure 1.8 (Peikko Group®, 2014), is a slim floor system that can be used in multi-story buildings of any type. The Deltabeam is a hollow composite beam, produced by the Peikko Group®. It offers a flexible layout and high fire resistance. Furthermore, it is also easily to be installed. This floor system can span approximately 30 ft. and carry the required gravity loads to a total depth of roughly 20 inches, shallower than the traditional precast concrete slabs (Dewit, 2012). Although the Deltabeam system is easy assembled, a completely concrete filling is required following its on-site installation, hence adding additional costs in time and materials. Another disadvantage of this system is that the beams and columns cannot be continuous structural elements, which reduces its structural capacity while increasing construction complexity.

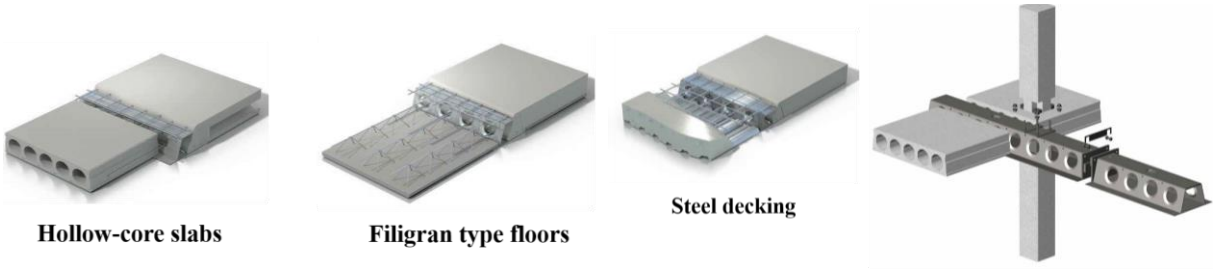

Figure 1.8 The Deltabeam system (Peikko Group®, 2014)

The Cobiax floor system is a novel floor system developed in South Africa and produced by Cobiax®. The design concept and construction of the system are shown in Figure 1.9 (Cobiax®, 2016). This system's scheme is based on void-forming technology which generates specific hollows within reinforced concrete slabs. This system is environmentally friendly, while providing weight reduction, floor height decrease, and large spans. Despite the advantages of the Cobiax floor system, some disadvantages in its practical application include reductions in sectional rigidity and shear capacity. The Cobiax system with large spans could be expensive, which is mainly due to its high Cobiax components (Cobiax cages and spheres) costs (Marais, 2009).

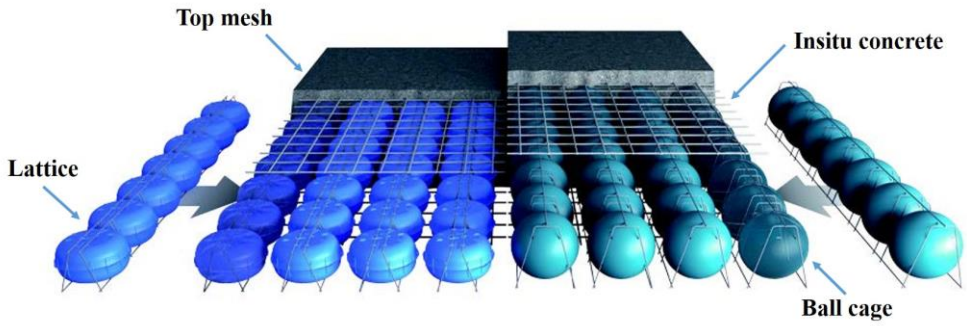

Figure 1.9 The Cobiax floor system (Cobiax®, 2016)

The Versa floor is an innovative structural steel framing solution developed by the Metal Dek Group® and Diversakore™. This floor system as shown in Figure 1.10, combines the speed of steel construction with the mass of concrete. The beams utilize the characteristics of the composite material and provide inherent fire-resistance due to concrete's non-flammability. The main disadvantage of this floor system is the need for frameworks to support its steel members during construction. Additional fire-resistance measures may be desirable since this floor system processes only a 2-hour fire rating (Dewit, 2012).

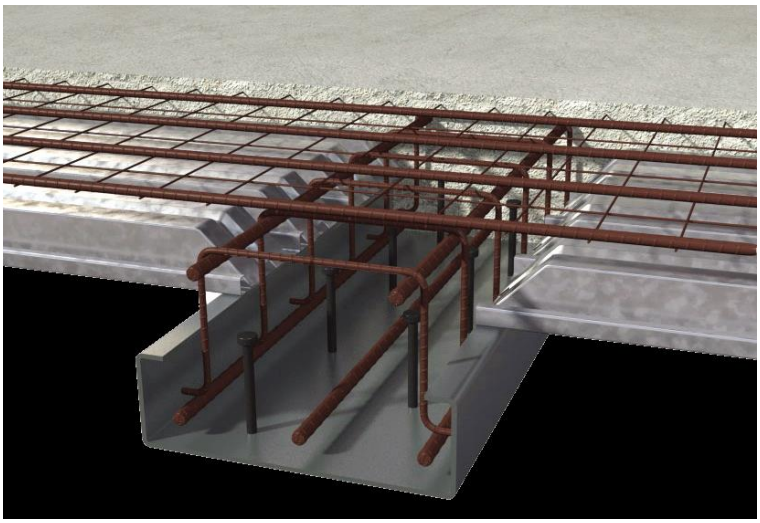

Figure 1.10 The Versa floor (Metal Dek Group & Diversakore, 2010)

1.3 Seismic Force Resistance System (SFRS)

With the design concept emphasis changing from structural strength design to performance based design, the earthquake resistant design has become a critical role of designing new structural systems. To achieve the higher performance objective, many innovative structural seismic force resisting systems (SFRSs) have been developed and studied, including steel moment resisting frame (SMRF), steel plate shear wall (SPSW), and steel braced frame (SBF).

1.3.1 Steel Moment Resisting Frame (SMRF)

Steel moment resisting frame (SMRF), as presented in Figure 1.11, has been in used dating from the earliest steel building constructions, providing large opening and planning flexibility. The SMRF were applied in many 20th century buildings, for its superior earthquake resisting capability. However, more than expected buildings experienced brittle fracturing of beam-column connections after the 1994 Northridge earthquake in America, and 1995 Kobe earthquake in Japan (Hamburger et al., 2009). To increase the connection ductility, various moment connections have

been demonstrated, including reduced beam section connections (Uang, Fan, 2001), end plate connections (Tsai, Popov, 1990), welded unreinforced moment connections (Ricles et al., 2002), and plate-reinforced connections (Kim et al., 2002). However, the main disadvantage of the SMRFs is its low stiffness. Hence, under the similar stiffness, SMRFs are normally more expensive than steel plate shear wall and steel braced frame systems.

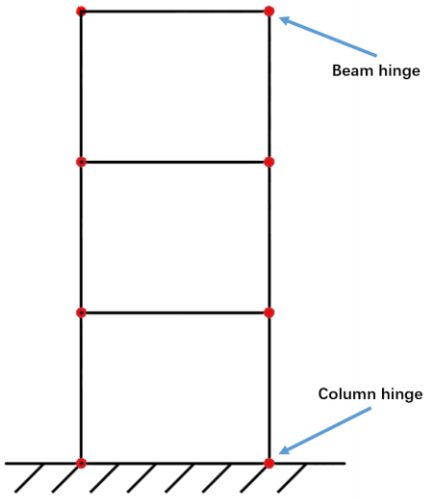

Figure 1.11 Steel moment resisting frame (SMRF)

1.3.2 Steel Plate Shear Wall (SPSW)

Steel plate shear wall (SPSW) as shown in Figure 1.12, is an efficient lateral load resisting system that has been applied extensively in high seismic regions. In comparison with concrete shear wall systems, the SPSW systems are much thinner and lighter, which result in the reduction of gravity loads and overall seismic loads, hence reduce the construction cost. The SPSW systems also have the advantage in construction period, the construction duration can be significant reduced by the fast erection process and less weather effect. The seismic behavior of SPSW systems have been widely studied and tested, and the strip model has been developed for post-buckling strength calculation of SPSW systems (Timler, Kulak, 1983). This model has been experimental verified

and adopted in many current building codes. However, there are still some disadvantages of SPSW systems. In general, the SPSW systems are more flexible, which means the additional flexural stiffness need to be provided. The large steel consumption results in high construction and replacement cost. For the cost optimization, thin steel plate shear wall structures have been studied by many researches to utilize efficiency of material and performance of welding.

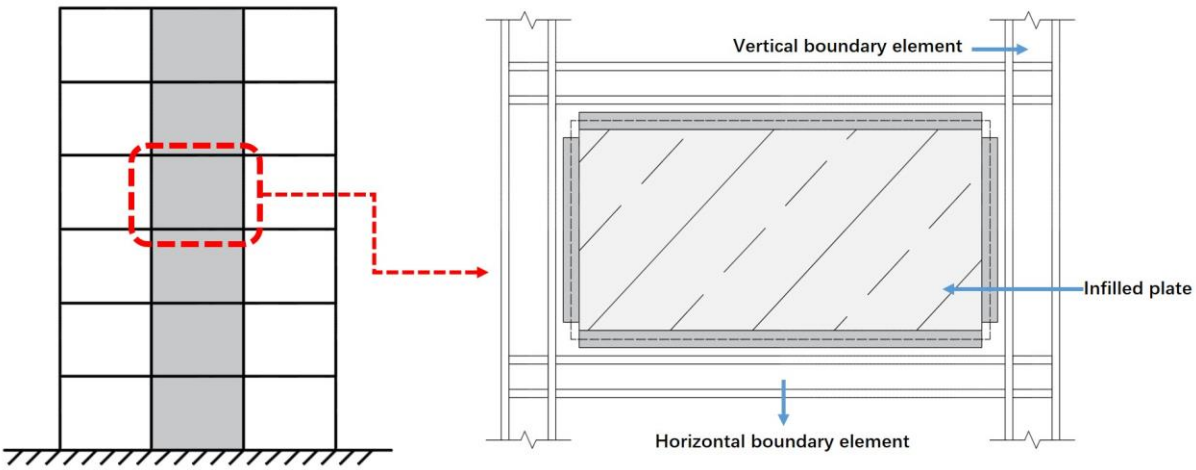

Figure 1.12 Steel plate shear wall (SPSW)

1.3.3 Steel Braced Frame (SBF)

The steel braced frames as shown in Figure 1.13, including steel concentrically braced frame (SCBF), buckling restrained braced frame (BRBF), steel eccentrically braced frame (SEBF), and buckling restrained knee braced truss moment frame (BRKBTMF), have been widely studied.

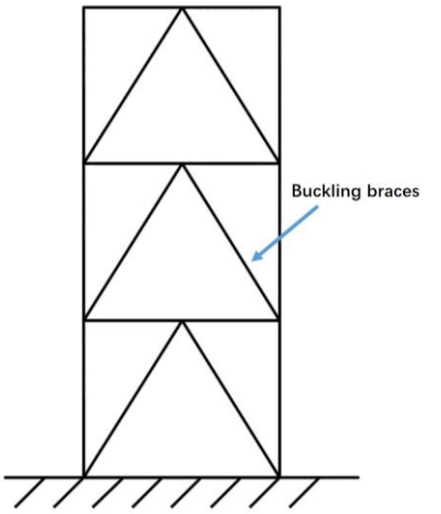

a) Steel concentrically braced frame (SCBF)

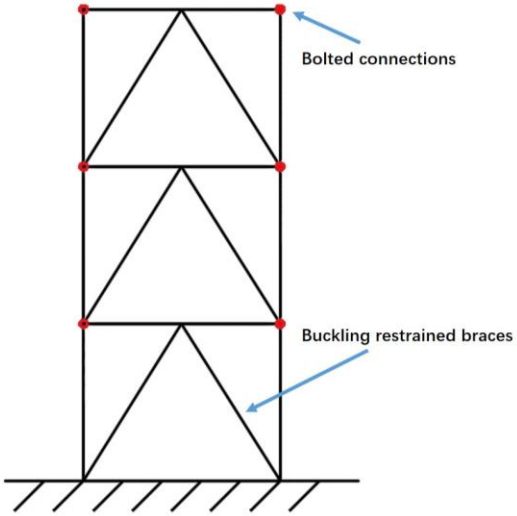

b) Buckling restrained braced frame (BRBF)

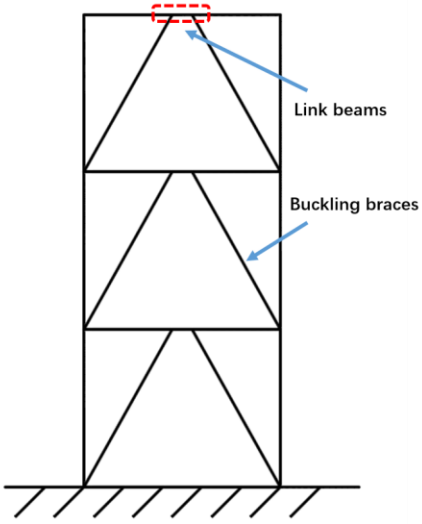

c) Steel eccentrically braced frame (SEBF)

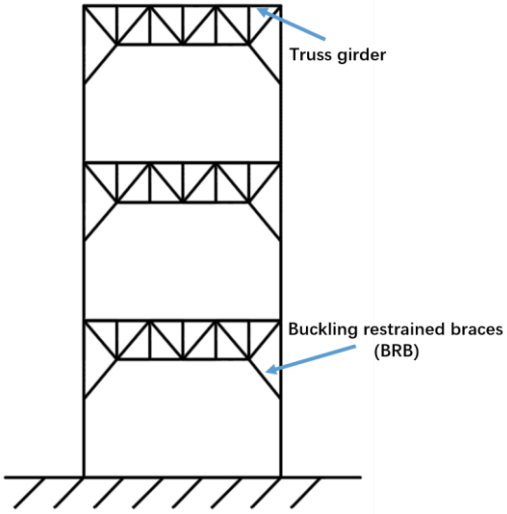

d) Buckling restrained knee braced truss moment frame (BRKBTMF)

Figure 1.13 Steel braced frames (SBFs)

SCBF utilizes the steel braces to increase the lateral structural stiffness, and dissipate the earthquake energy. SCBFs can be arranged in various configurations, among all types, balanced diagonal braced frame is the most common selection. The seismic behaviors of SCBF were analyzed in many past researches, and it is found that the large unbalance vertical forces caused

by brace buckling. To solve this disadvantage, conventional steel braces are replaced by buckling restrained braces (BRBs) in BRBF, and first studied in a North America project (Clark et al., 1999). The experimental results showed high energy dissipation performance of this structural system. SEBF is a relatively new SFRS, proposed by Popov (Popov, Engelhardt, 1988). SEBF combines the features of SMRF and SCBF, while minimizing the disadvantages of both systems. The SEBFs can be classified as shear-controlled or flexural controlled SEBF, according to the link length. The shear-controlled links are favorable with its excellent behavior, while the flexural-controlled links are preferred for its large openings.

To achieve the higher performance objective, an innovative steel SFRS, buckling restrained knee braced truss moment frame (BRKBTMF) was initiated by (Leelataviwat et al., 2012) and further studied by (Yang et al., 2015; Yang et al., 2013). The buckling restrained braces (BRBs) are utilized in the BRKBTMF, as the structural fuses to dissipate energy under severe seismic loadings, providing a robust and resilient structural system towards future earthquakes. More importantly, the structural fuses can be easily and efficiently construction using bolted or pinned connections, and can be more easily replaced after earthquakes. The detailed parameter study of optimization of the BRBKTMF has been conducted, and the results show that the optimal BRB inclinations are either horizontal or connecting directly to the end of the columns. In conclusion, the SBFs provide high performance without adding significant structural weight. However, the SBFs are not favorable by architectures for its opening limitations.

Although the extensively numerical and experimental studies of SRFSs have been conducted over past decades, there are relatively less researches about modular applications of SRFSs. In addition,

most SFRFs are analyzed as two-dimensional models, without considering the combination of floor system and SFRFs.

1.4 Modular Steel Truss System (MSTS)

Based on the literature review, this thesis proposes an innovative and economical modular steel truss system (MSTS), utilizing modular steel floor system (MSFS) in section 1.4.1, and modular buckling restrained braced truss moment frame (MBRBTMF) in section 1.4.2. The designed MSTS is targeted to be effective and efficient in resisting both gravity and seismic loads.

1.4.1 Modular Steel Floor System (MSFS)

Floor system design is influenced by spanning requirements and the loads to be supported. Depending on the variety of floor system employed, the structural strength requires controlling for during the design procedure according to the design standards. Additionally, the maximum deflection of the floor system as defined in NBCC 2015 Table 9.4.3.1 (National Research Council of Canada, 2015). For the system's structural members, including floor beams, joists, and decking, under all cases of supported ceilings, the maximum allowable deflection is that of span/360, and dead loads need not be considered when computing deflections. For load combinations, the deflection limitation criterion is defined as span/240. Thickness is another crucial factor to be considered. For concrete floor systems, concrete thickness is a primary design decision. In residential constructions, nominal 8-inch-thick concrete slabs are readily available, while for office buildings, concrete thickness is usually around 10 inches. For the design of residential and commercial concrete floor system, several requirements are defined by the floor class, as listed in ACI 302.1R-15 (American Concrete Institute, 2015). The guide identifies the various classes of

concrete floors in use, along with their design details, site preparation, and concrete and related material types.

The previous described lack of an efficient steel system curtails the growth and development of the steel constructions. Also, due to the greater number of floors within buildings, the floor systems have a significant impact on construction costs and structural height. This makes the choice of floor system essential, particularly as floor system depth. Traditional steel floor systems are deep, and the space within the floors is not fully utilized, but wasted. Therefore, it is practical for both designers and engineers to increase construction efficiency while minimizing floor depth. More importantly, with increasing trends in steel high-rise structures worldwide, developing a more efficient floor for modular steel constructions is becoming a crucial criterion in maximizing usable space within constructions. As well, in the interest of achieving the steel industry's required environmental and sustainable developmental objectives, it is essential that steel floor systems be constructed more efficiently and create fewer carbon footprints. Also, reducing floor depth would save usable space, allowing for additional floors while maintaining building's structural height. In this thesis, a novel MSFS has been developed to resolve above mentioned issues. To fully utilize the space within floors, the mechanical, electrical and plumbing (MEP) systems are designed to fit within thinner floor depths. Also, the specially designed MEP systems are pre-installed within the proposed floor system.

The design concept of the proposed MSFS is illustrated in Figure 1.14. This modular steel floor is comprised of a structural truss framing system and sandwich non-structural components, as shown respectively in Figure 1.14a and Figure 1.14b, which can significantly minimize the floor depth of

a multi-story steel structure, hence increasing its saleable space. These floor moduli can be used as part of modular constructions in practical projects and improve the efficiency of conventional steel structures. The modular floor system can be shipped to sites as individual units (Figure 1.14c) and then assembled on-site (Figure 1.14d and Figure 1.14e). To facilitate the transportation of modular units, the dimensions of each floor module will be limited to 20 by 8 ft., which are easily stacked and transported using conventional semi-trailer (18-wheeler) trucks.

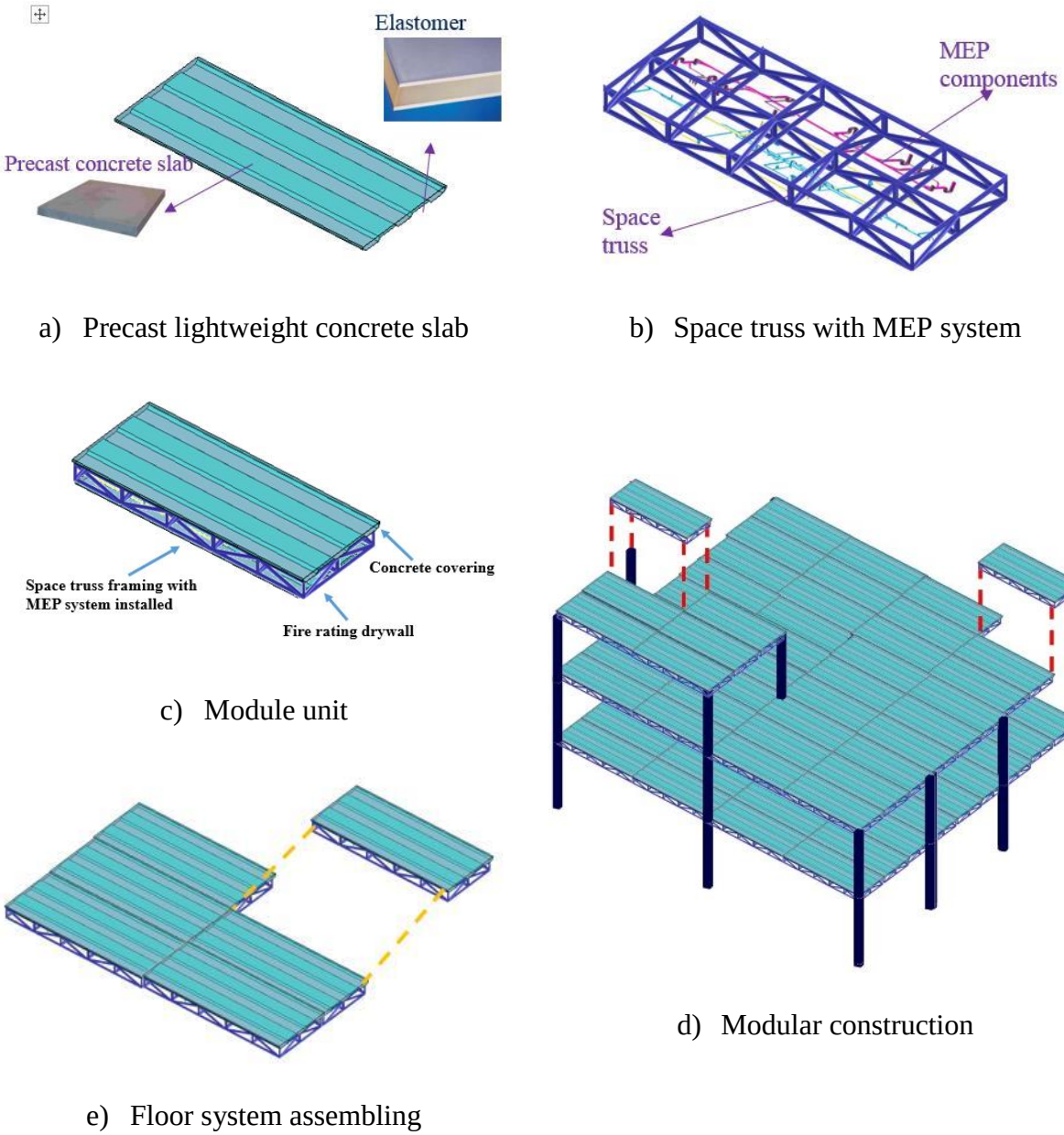

a) Precast lightweight concrete slab

b) Space truss with MEP system

c) Module unit

d) Modular construction

e) Floor system assembling

Figure 1.14 The proposed modular steel floor system (MSFS)

1.4.2 Modular Buckling Restrained Braced Truss Moment Frame (MBRBTMF)

Inspired by BRKBTMF, an innovative modular buckling restrained braced truss moment frame (MBRBTMF), as shown in Figure 1.15, was developed. MBRBTMF consists of steel trusses, and buckling restrained braces (BRBs). BRB, utilizes as a structural fuse in MBRBTMF, is a highly

efficient energy dissipation device, which is capable of absorbing significant energy under seismic loads. The structural fuses can be easily and efficiently construction using bolted or pinned connections and can be more easily replaced after severe earthquake shaking, which makes the structures more resilient towards earthquakes. The performance-based plastic design (PBPD), presented by (Goel, Leelataviwat, 1998) is applied to design this novel structural system, since no prior design guideline was established.

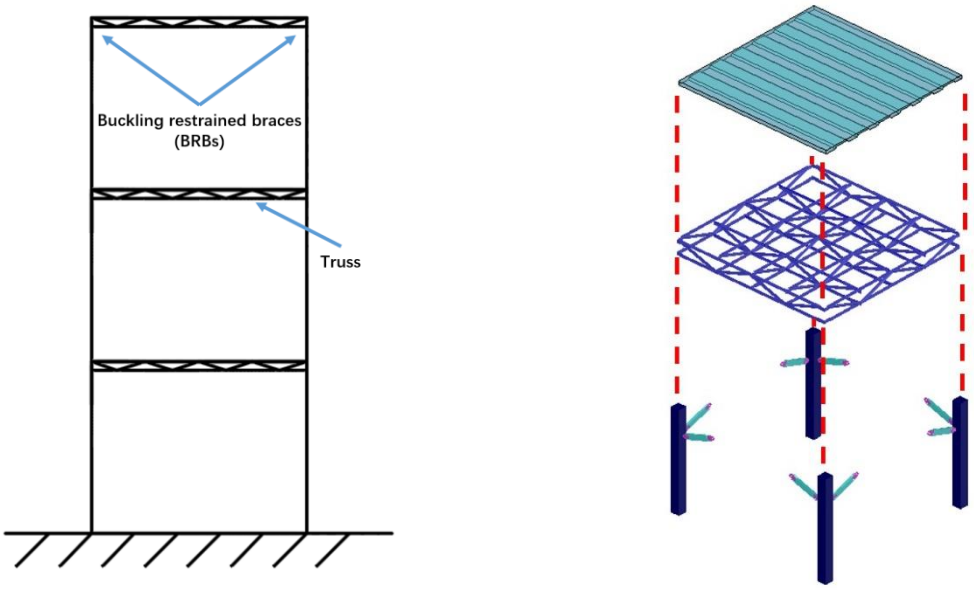

Figure 1.15 Modular buckling restrained braced truss moment frame (MBRBTMF)

To achieve high efficiency and low cost, the modular construction technology is applied. In MSTS, the MBRBTMF is designed to be constructed as a part of floor system, hence, a modular steel floor system (MSFS) is proposed and developed in this thesis. This MSTS can be pre-fabricated in factories, shipped to their required locations, and then assembled on-site. This method would significantly reduce production error, construction waste and the demolition process, which means

less labour, lower costs, and less installation and construction time. In addition, MBRBTMF offers large opening, which is favorable by architectures.

1.5 Research Scope

This study aims to develop an efficient and economically viable modular steel floor system that can be employed worldwide in steel constructions. This would be achieved through

- Providing a preliminary study of previous floor systems and SFRS studies, and then proposing an initial prototype design. Detailed connector designs between modulus floor units will be carefully considered, while ensuring easy construction and installation methods.
- Developing a finite element model of the designed MSFS using OpenSees (Pacific Earthquake Engineering Research (PEER) Center, 2005). Once the model is completed, an optimization algorithm will be developed to optimize the geometry of the floor system in interest of achieving optimal structural efficiency and material usage. Since the optimization process requires an iterative procedure, a programming script will also be developed through the Matlab (The Mathworks, 1998).
- Designing a prototype MBRBTMF system using the PBPD method, a detail design procedure will be presented. Conducting a detailed nonlinear dynamic analysis of both proposed MSTS and conventional structures using MSFS, to confirm the structural efficiency and safety under gravity and seismic loads.
- Upon completion of the prototype design, structural optimization and analytical simulation, a detailed assessment regarding construction cost and time will be conducted and compared with concrete and steel floor systems in conventional structures.

1.6 Thesis Outline

The conceptual and structural design and seismic performance of proposed modular steel floor system will be discussed in the following chapters:

- **Chapter 2 Design and Optimization of Modular Steel Floor System:** A preliminary study of the modular steel floor system and connector designs is provided. At the end of the chapter, an initial structural design of proposed modular steel floor system is presented. For the connector design, the common connectors for space trusses were used, while an innovative concept of honeycomb connector for structural components was proposed. The proposed modular steel floor system was designed using NBCC 2015 (National Research Council of Canada, 2015), CSA S16-14 (Canadian Institute of Steel Construction, 2014) and the AISC steel manual (American Institute of Steel Construction, 2013). The detailed optimization process was conducted to identify the optimal design which uses the least amount of structural material, yet satisfied both strength and deflection limits. Robust structural optimization was conducted using the OpenSees and Matlab programs. A parameter study of the proposed modular steel floor system and a comparison of the modular steel floor, conventional concrete, and steel floor systems were performed. The deflection, natural frequency and mode shape of the proposed modular steel floor system were also analyzed. The serviceability of the floor system under excitation was additionally studied.

- **Chapter 3 Seismic Design of Modular Steel Truss System:** The designed modular steel truss system (MSTS) consists of both gravity and seismic force resisting system. Upon the

completion of MSFS, as the main gravity system, an innovative modular buckling restrained braced truss moment frame (MBRBTMF) was designed using the performance-based plastic design (PBPD) procedure. The PBPD method uses energy-based plastic design approach to satisfy both strength and story drift limitations. The buckling restrained braces (BRBs) were utilized as the structural fuses. The MBRBTMF is targeted to be applied for different hazard levels, without redesign the floor system. A detailed design procedure of MBRBTMF is presented. A prototype 4-story modular steel truss system (MSTS) building was designed. The hazard analysis was conducted for the construction site, and the ground motions were selected and scaled to the target spectrum. The nonlinear analysis was used to quantify the design procedure and the seismic performance of designed modular system. The incremental dynamic analysis was also conducted to provide the collapse assessment of the prototype building.

- **Chapter 4 Application of Modular Steel Floor Systems in Conventional Structural Systems:** To promote the use of modular steel floor systems (MSFSs) for different applications, the performances of structures with conventional SFRSs and MSFSs were studied. The prototype buckling restrained braced frame (BRBF) and buckling restrained knee braced truss moment frame (BRKBTMF) buildings, using MSFS, were designed following PBPD procedure and modelled. A design spectrum was developed, and the ground motions used in the analysis were selected and scaled. Time history analyses of structures are conducted through the OpenSees program to study their seismic performance, and the comparison results of the prototype buildings with the proposed modular steel floor, conventional concrete floor, and steel floor systems are presented. The

construction cost is displayed to provide a visual idea of the advantages of the proposed modular steel floor system. To reduce computational complexity, the study of simplified model with rigid diaphragm was also conducted.

- **Chapter 5 Summary and Conclusions:** A detailed summary of the research results and conclusions for the proposed modular steel building is provided.

Chapter 2: Design and Optimization of Modular Steel Floor System

Based on the literature review, this thesis proposes an innovative modular steel truss system (MSTS), consisting of both gravity and seismic force resisting systems. The modular steel floor system (MSFS), as the main gravity system, was designed and optimized in this thesis. During the prototype design of the MSFS, many parameters, such as the dimensions of the modular unit, structural layouts, and connectors, must be considered and evaluated. The initial design of the proposed modular floor system is determined during this phase.

2.1 Prototype Design

Based on an extensive review, a prototype design was proposed for a MSFS module, as related in Figure 2.1, with the space truss system selected as its main framing.

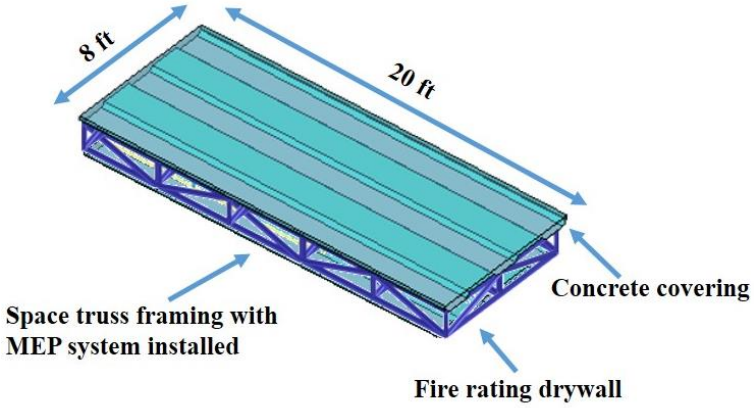

Figure 2.1 The proposed steel floor system (MSFS) module unit

2.1.1 Preliminary Floor Design

Prefabrication is viably achieved in a space truss structural system, due to the modular nature of structural elements, which are produced through accurate geometric measurements. Also, these

structural systems might be further extended or disassembled and reinstalled. This provides higher quality control, less on-site labor usage, and creates less environmental pollution. The dimension for each MSFS modular unit will be limited to 20 by 8 ft., which can be easily transported using conventional trucks.

The proposed MSFS has multiple layers. The top layer one consists of a concrete covering and acts as the foundation for the floor above it. If required, non-structural components such as carpets or tiles can be superimposed largely for additional decorative purposes. The use of the concrete covering serves many advantages, including fire and sound insulation and added stiffness and strength for deflection and load control. Beneath this covering, is a series of specially designed steel space trusses. These trusses are the main structural framing for the proposed modular floor systems. The trusses are designed to be easily connected and provide sufficient stiffness for large span. The space between the steel trusses can produce that required for the mechanical, electrical and plumbing (MEP) systems, and the MEP system is pre-installed within the proposed modular unit.

To reduce construction time and cost, the space truss internal to each modular unit should contain continuous chord member. The connectors between the modular units would be applied for quick and easy installation and assembling. Lastly, a fire rating drywall will be added as the final layer. This will be the finishing stratum of the ceiling for the proceeding floor system. To ensure transportability, the light bulbs will not be pre-installed in the factory, but light wiring will be installed inside within modular steel floor system. The proposed floor system will be designed to

provide sufficient stiffness to minimize deflection under the loads, with a minimum 2-hour fireproof rating and 20-dB noise reduction.

2.1.2 Connector Design

A significant advantage to steel construction is that most structural members can be designed and fabricated in a factory and then quickly assembled on site. However, connectors are usually created uniquely to suit diverse projects, increasing construction cost and time. An efficient way to improve the efficiency of connector construction is to have a flexibly designed connector, which can be modified to any shape or size to fit current architecture demands. The multi angle connectors as shown in Figure 2.2 are used for space trusses, and a concept of honeycomb steel connector for structural elements is proposed.

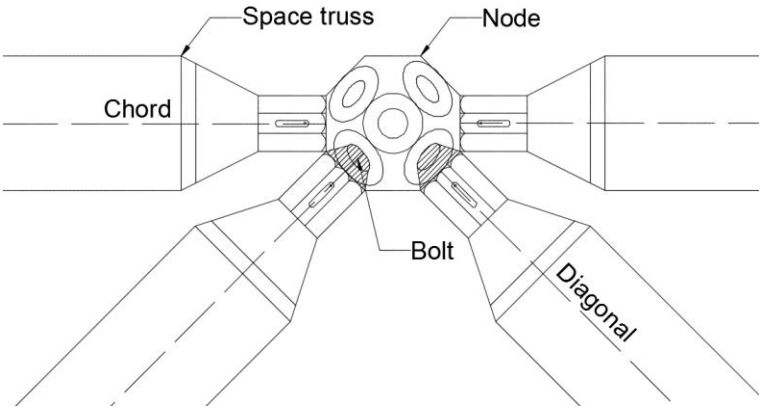

Figure 2.2 Space truss connector

A concept of prototype honeycomb cast steel connector is shown in Figure 2.3, which utilizes the advantages of the natural honeycomb configuration as its seismic energy dissipation device (Figure 2.3a). This connector has more developed redundancy, and greater mechanical properties and stiffness, by taking extraordinary advantages of the natural honeycomb configuration as its interior

structural pattern. In addition, the steel connector will be constructed using an advanced cast steel technology, where three-dimensional honeycombed layers are achieved, and which will significantly increase its energy dissipation capacity and manufacturing efficiency. Steel casting offers a significant design advantages and eliminates the need for additional assemblages and fabrication, meaning lower labor intensity and construction costs. By employing this advanced fabrication technique, the high-stress concentration caused by the welding procedure and the formation of sharp corners will be reduced.

Figure 2.4 shows some conceptual structural connection types, where the connectors can be re-configured to suit dissimilar applications. By making the core design of a modular component, the identical modules can be fabricated more efficiently, significantly increasing the fabrication quality and reducing construction expense. The steel connectors would be versatile and perform as efficient energy dissipation devices to protect the remaining structural elements under extreme seismic events. Overall, the proposed connector is predicted to combine the advantages of the cast steel technique, and the high-energy dissipation capacity of the honeycomb configuration, together with an efficient and economic modular construction scheme to develop the next-generation high-performance steel connectors. Additional details concerning this connector will be investigated in further research.

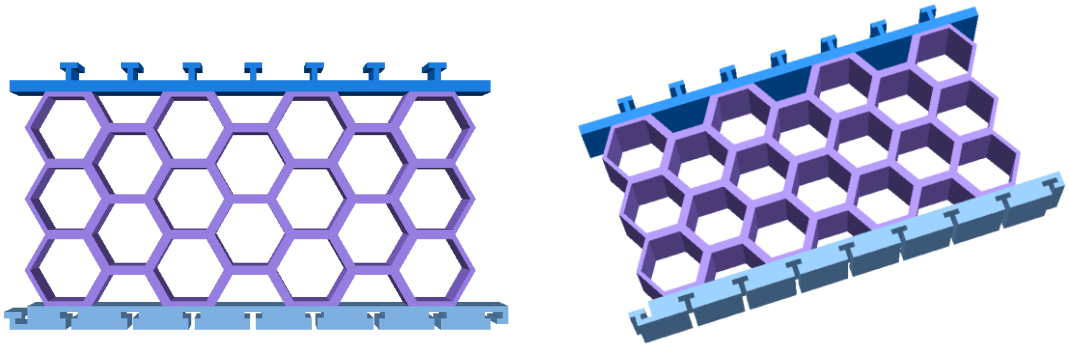

a) Proposed steel connector (Individual module)

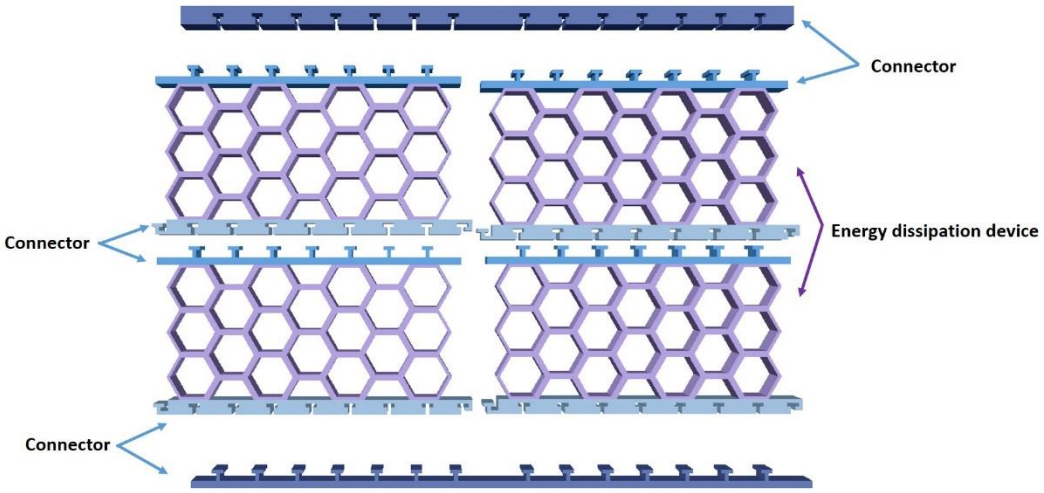

b) Proposed steel connector (assembling module)

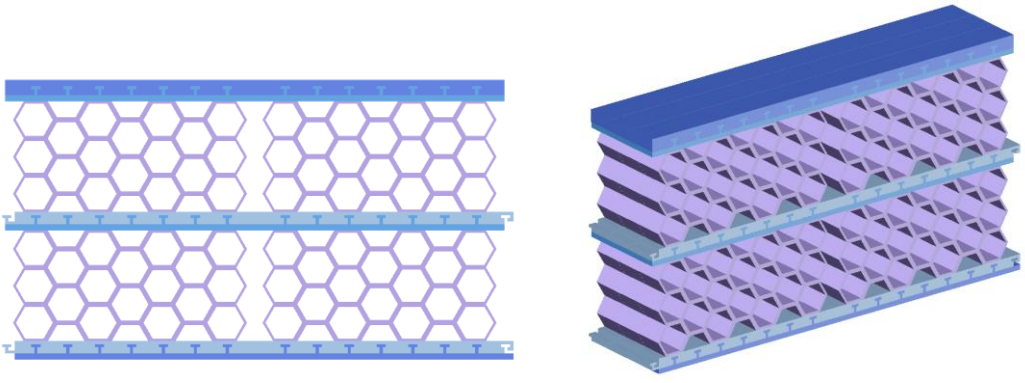

c) Proposed steel connector (assembled configuration)

Figure 2.3 The proposed innovative honeycomb cast steel connector

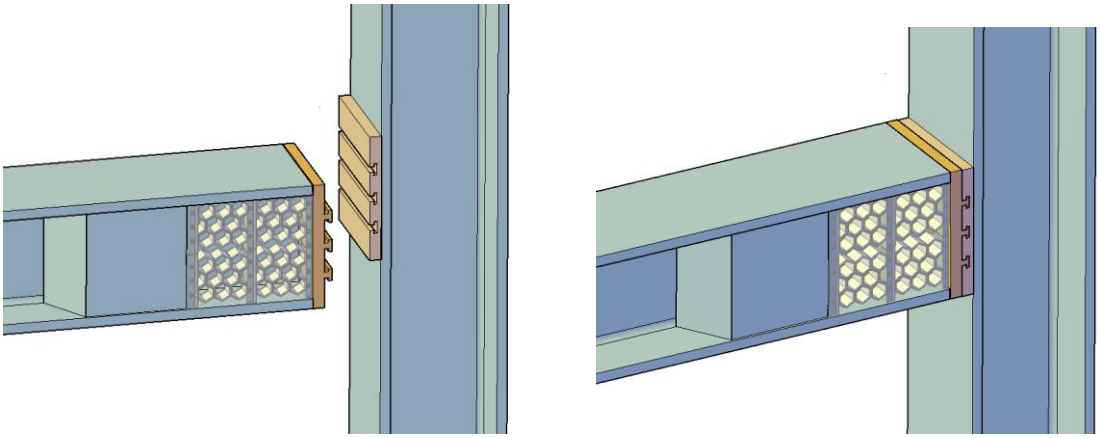

a) Beam-to-column connector case 1

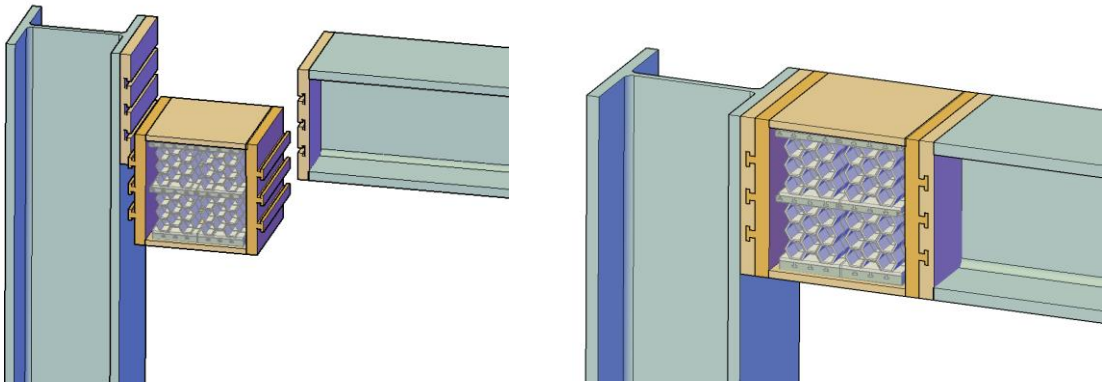

b) Beam-to-column connector case 2

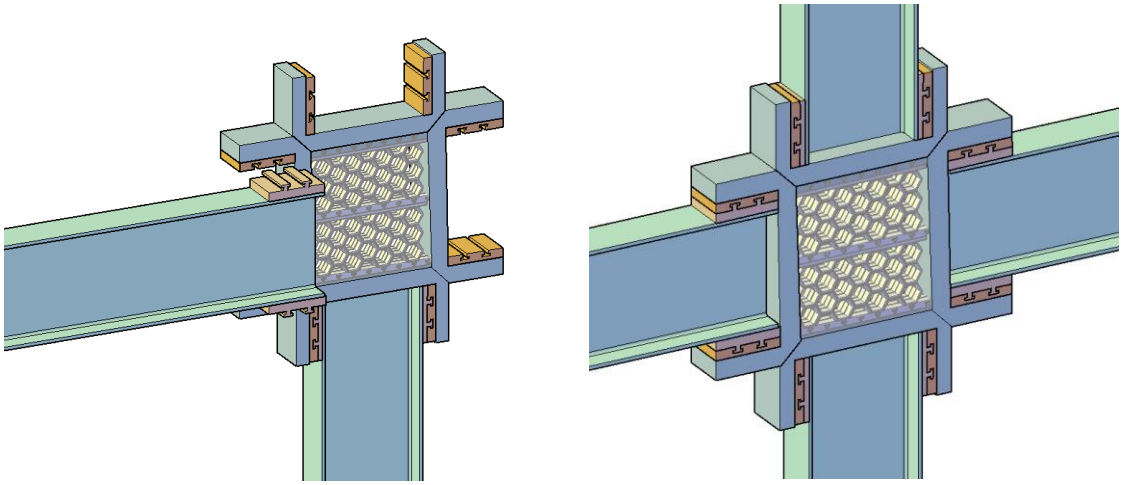

c) Panel zone connector case 1

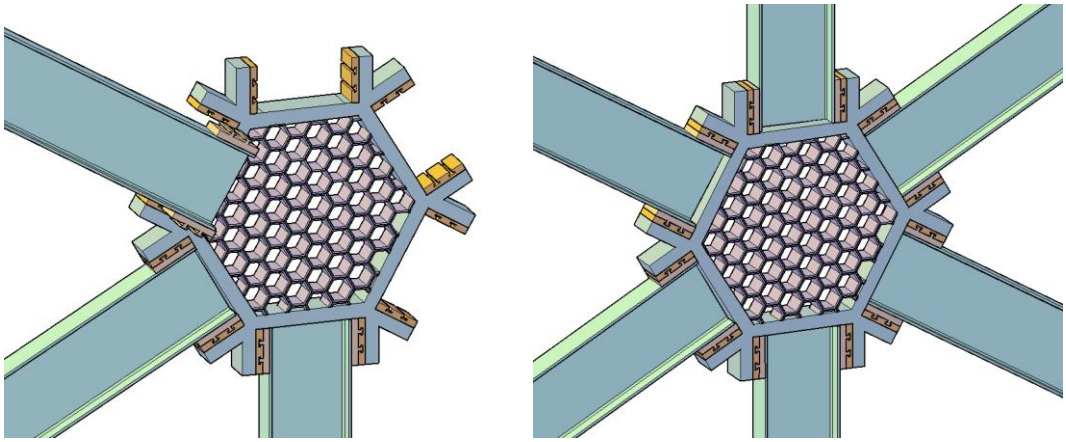

d) Panel zone connector case 2

Figure 2.4 The proposed structural system connector

2.2 Structural Design

The MSFS is designed using space trusses which can provide sufficient stiffness to support the gravity load, minimize vertical deflection, and are able to transfer lateral force without significantly increasing floor depth. Thus, a detailed optimization process is conducted to identify the optimal design utilizing the least amount of structural material yet satisfying both strength and deflection limits as specified in the National Building Code of Canada (NBCC) (National Research Council of Canada, 2015). Robust structural optimization is conducted using OpenSees (Pacific Earthquake Engineering Research (PEER) Center, 2005) and Matlab (The Mathworks, 1998).

Space truss geometry was selected to study the proposed MSFS's optimal design possibilities. Detailed finite element models (FEMs) of this structural system are assembled using a state-of-the-art finite element software, OpenSees, to determine the essential design parameters under diverse load conditions. For the system's design, a live load of 50 psf (2.4 kPa), representative for office buildings, was assigned based on the tributary area for point loads on the nodes. In addition,

an additive dead load of 66.25 psf (3.2 kPa) plus the self-weight were added to the model. The dead loads, used for both gravity and seismic analysis, were calculated based on the structural material presented in Table 2.1, adopted from a steel structural design guide (Goel, Chao, 2008).

Table 2.1 Typical floor gravity and seismic loads

Item	Gravity load (psf)	Seismic load (psf)
Partitions	20	12.5
Floor finish	1	1
LWC + deck (Reducible)	31.25	31.25
Framing self-weight	Calculated	Calculated
Fireproofing	3	3
MEP/Sprinklers	3	3
Clg/Lights	4	3
Misc.	4	3
Dead load	66.25	56.75
Live load (Office)	50	50
Live load (Residence)	40	40

2.3 Design Check

Although the optimal MSFS was designed to be economical, the structural system should still satisfy both the strength and displacement limits, specified in this section. The detailed design checks were based on the specifications of the National Building Code of Canada (NBCC)

(National Research Council of Canada, 2015) and CSA S16-14 (Canadian Institute of Steel Construction, 2014), are listed below.

2.3.1 Load Combination

Different load combinations according to those of NBCC (4.1.3.2), are employed for ultimate limit states. In this study, both wind and snow loads are ignored. Therefore, the load combinations can be summarized as the following three types which listed in Table 2.2, where D represents dead load, L as live load and E as earthquake load.

Table 2.2 Load combination

Item	Case	Load combination
Strength check	1	$1.4D$
	2	$1.25D + 1.5L$
Deflection check	3	$D + L$
	4	L

2.3.2 Capacity Check

The strength of the structural steel member is checked using S16-14 (13). The resistance factor, $\emptyset$, is applied as specified in S16-14 (13.1); for structural steel, $\emptyset$ should be taken as 0.9 and $\emptyset u$ taken as 0.75.

The tension capacity was checked using the factored tensile resistance, T_r. Equation 2.1, and Equation 2.2 shows the factored tensile capacity as specified in S16-14 (13.2). T_r should be equal to the least value of

$$T_r = \emptyset A_g F_y \; or \; T_r = \emptyset_u A_{ne}$$ **Equation 2.1**

And for pin connections, T_r should represent the least value of

$$T_r = 0.75\emptyset A_g F_y \; or \; T_r = \emptyset_u A_{net} F_u \; or \; T_r = 0.6\emptyset_u A_{nes} F_u$$ **Equation 2.2**

The compression capacity was ascertained using the factored compression resistance, C_r. Equation 2.3 shows the compression capacity of elements of doubly symmetric shape as specified in S16-14 (13.3),

$$C_r = \emptyset \frac{AF_y}{(1+\lambda^{2n})^{\frac{1}{n}}}$$ **Equation 2.3**

The bending for the steel member is determined using S16-14(13.5, 13.6). The moment resistance factor, M_r, was calculated using Equation 2.4.

$$M_r = \emptyset Z F_y = \emptyset M_p \; or \; M_r = \emptyset S F_y = \emptyset M_y$$ **Equation 2.4**

2.3.3 Determination of Deflection

The deflection limit of span/360 for live loads only and span/240 for load combinations was employed. For convenience, the demand and capacity ratios for displacement and force are summarized using the variables, α and β, as shown in Equation 2.5 and Equation 2.6, respectively.

$$\alpha = \frac{\text{displacement demand}}{\text{displacement capacity}}$$ **Equation 2.5**

$$\beta = \frac{\text{force demand}}{\text{force capacity}}$$ **Equation 2.6**

If the ratio, α, is less than 1, the maximum displacement of the space truss system still falls under the displacement limit. In other words, the structure is safe, and the optimal result is advisable. Conversely, if α is greater than 1, the structure is unsafe, and the solution is not valid. Similarly, the strength capacity check is also verified using β.

2.4 Structural Optimization

Structural optimization of the MSFS can be separated into three main design parameters; those of sizing, shape, and configuration. The most efficient way to optimize the structural design is to consider all of the parameters simultaneously. The goal of optimization is to find the optimal material usage for the structural system which can also achieve the strength and deflection limits.

2.4.1 Optimization Method

Structural optimization is a highly nonlinear optimization problem (Khatibinia et al. 2014). Hence, efficient and reliable optimization algorithms have been developed to solve. Brutal force and genetic algorithms are commonly utilized to identify the optimal structural design.

The genetic algorithm was introduced by Holland (John, 1992), and was inspired based on Darwin's theory on biological evolutionary algorithms. This method relies on random action, trial and error, and the survival of the fittest to evolve solutions to optimization problems (Auer, 2005). Several advantages are offered by this approach, including the powerful capacity of dealing with discrete problems and a global convergence ability (Ruiyi et al., 2009). However, it is impossible to determine if the optimal solution discovered is the local or global optimum due to its

probabilistic nature, and the genetic algorithm may only converge to local rather than global optimum points as shown in Figure 2.5 (Mardle, Pascoe, 1999).

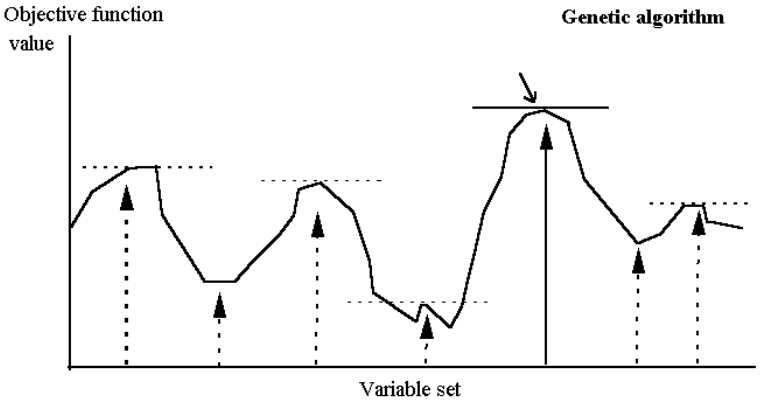

Figure 2.5 The genetic algorithm approach (Mardle, Pascoe, 1999)

The brute force method, based on automatic interaction and matrix calculation, has been carried out as a general problem-solving algorithm. Compared with the genetic algorithm, the brute force method is an optimization algorithm for identifying all possible structural design combinations using advanced computations. Based on this, a structural optimization of modular steel floor system using the brute force method is proposed. Because the optimization process requires an iterative approach, a programming script developed by Matlab was used. The results, which passed both the capacity and deflection checks, were sorted based on the total steel material usage. The optimal MSFS design was the one with less structural thickness, utilizing the least amount of structural material, yet satisfying both the strength and displacement limitations.

The detailed structural optimization was conducted based on the following procedure, along with the detailed optimization method shown in Figure 2.6.

- Calculating and inputting the gravity load using different load combinations for diverse applications and conditions, based on the NBCC guidelines for typical buildings;
- Providing common input method for MSFS, such as material properties, member specifications, and support conditions;
- Defining the basic input range and step size for the design parameters, including the size characteristics of chords and diagonal trusses, and the spacing along both width and length of the structure;
- Generating various geometrical sequences in the OpenSees program, and running a finite element analysis;
- Calculating the total steel usage for each configuration, and recording the combination which satisfies the strength and deflection limits as defined by NBCC and CSA S-16;
- Sorting out the design based on the minimum material usage, and discovering the optimal MSFS design.

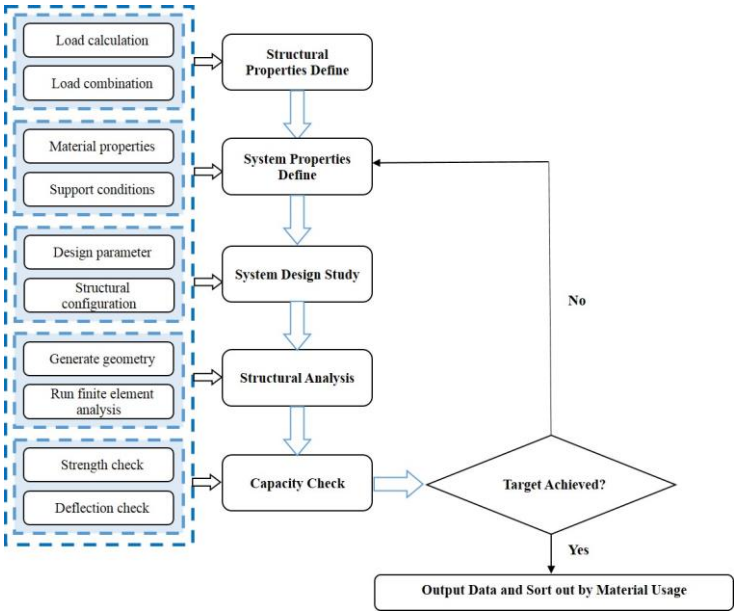

Figure 2.6 The structural optimization procedure

2.4.2 Space Truss Floor System (STFS)

The proposed first design of MSFS, space truss floor system (STFS) model displays a combination of three modules (Figure 2.7a) which are connected using the bolted connectors, the typical configuration type for the proposed modular units is outlined in Figure 2.7b.

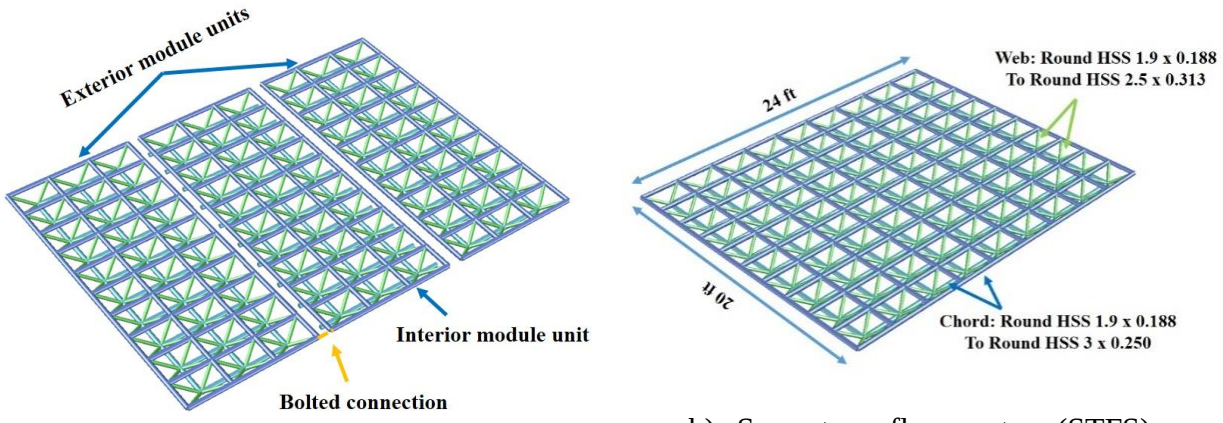

a) Modular unit

b) Space truss floor system (STFS)

Figure 2.7 The proposed space truss floor system (STFS)

Based on experience, the minimal material weight does not equal minimum construction costs, an efficient means to reduce fabrication costs, it is to keep the number of sizes varied and reduce the number of connections. Thus, diminish construction costs, the top and bottom chords were created for use in the same sections, while the truss elements were selected from the commonly available steel sections as listed in the AISC steel manual (American Institute of Steel Construction, 2013). To eliminate sizes of excessive depth (greater than 6 inches), the sections are limited to round HSS, with those of 1.9 x 0.188 to 3 x 0.250 being used for upper and lower chords in this study.

The optimization process was developed based on the Matlab program, with the Matlab codes being used to explore the structural design according to various design variables, including element properties, structural configurations, and spacing between elements. Table 2.3 provides a summary of the range of the design optimization parameter included in the STFS design.

Table 2.3 STFS design parameters

Objective	Symbol	Range
Top and bottom chords	A_1	Round HSS 1.9 x 0.188 to Round HSS 3 x 0.250
Web truss	A_2	Round HSS 1.9 x 0.188 to Round HSS 2.5 x 0.250
Spacing along the length	S_1	2 ft to 20 ft
Spacing along the width	S_2	1ft to 8 ft

The final structural configuration of STFS is that outlined in Figure 2.8, as a structural system with 15-inch spacing along its length and 19-inch along its width. The proposed floor system consists of round HSS 3 x 0.250 as chords and round HSS 2.375 x 0.154 as web trusses. The total depth of the proposed STFS is 11 inches, with 5-inch of clear spacing being provided between chords is provided, for the use in the installation of mechanical, electrical and plumbing (MEP) systems. Most importantly, the total weight of the proposed floor system is 14,320 lbs., which is quite lighter than that of conventional concrete floor system.

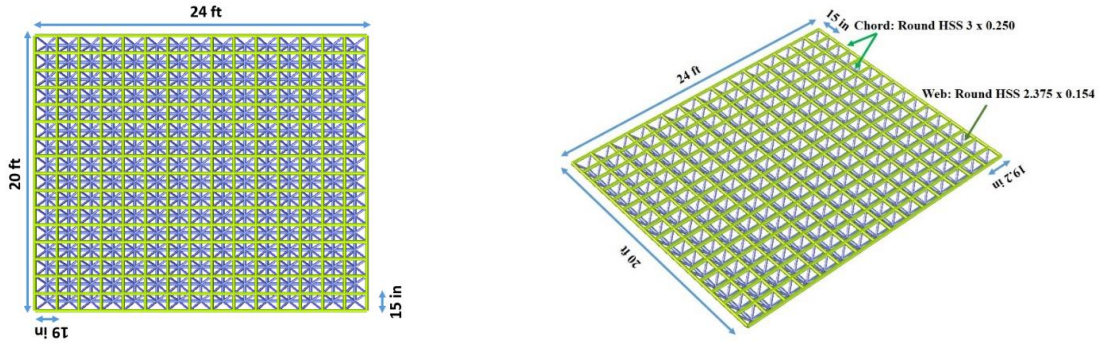

a) Plan view b) Optimal space truss floor system (STFS)

Figure 2.8 The optimal space truss floor system (STFS)

2.4.3 Space Truss with W-beam Floor System (STWFS)

To reduce floor depth, another MSFS design is proposed, using space trusses with w-beam floor system (STWFS). Compared with the STFS, two w-section beams are employed in this design as shown in Figure 2.9. In order to maximize the usable space within the building, the floor thickness (between the central lines of the chords) is reduced to 6 inches.

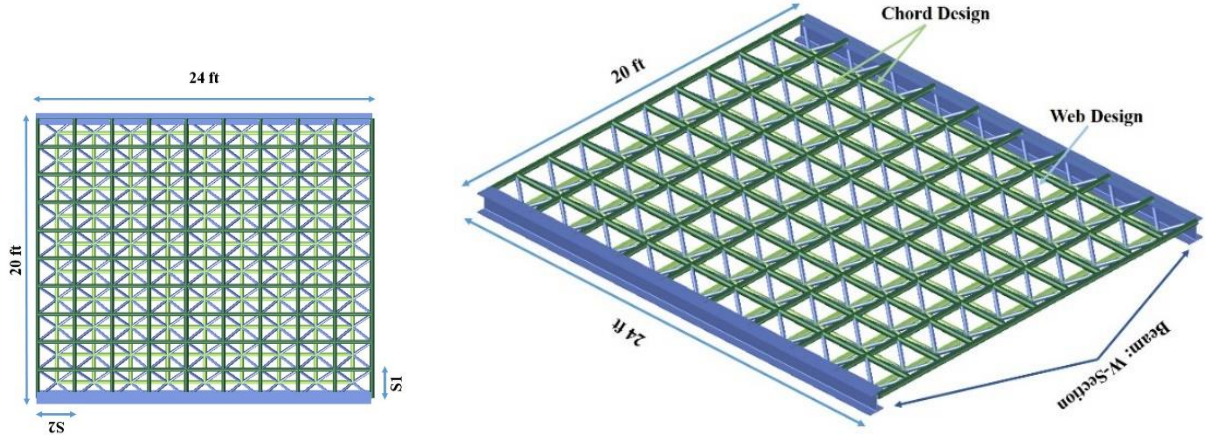

a) Plan view b) Proposed space truss with w-beam floor system (STWFS)

Figure 2.9 The proposed space truss with w-beam floor system (STWFS)

The truss system in this design is constructed from a circular hollow section, and its sizes and topology values are determined by optimization. In order to ensure that the floor system can be easily manufactured, its chord and web members are assumed to have the same cross-section size, respectively. A summary of the ranges of design parameters is included in Table 2.4.

Table 2.4 The STWFS Design parameters

Objective	Symbol	Range
Top and bottom chords	R_1	0.25 inch to 1 inch
	r_1	$0.65R_1$ to $0.95R_1$
Web truss	A_2	0.5 in.^{2} to 2 in.^{2}
Spacing along the length	S_1	1 ft to 10 ft
Spacing along the width	S_2	1 ft to 8 ft

The final structural configuration of the proposed STWFS, outlined in Figure 2.10, is a structural system with 30-inch spacing along its length and 12-inch along its width. The optimal design for the STWFS consists of W12X58 as the structural beams; top and bottom chords with 2-inch external diameters, 1.4-inch internal diameters and 1.6-square-inch areas, as well as 0.5-square-inch area web trusses. The total depth of the proposed floor system is 8 inches, which compares well with a concrete slab of similar span. In addition, the STWFS has 4-inch of clear spacing between the top and bottom chords, which can be used to install mechanical, electrical and plumbing (MEP) systems. The total weight of the STWFS is 11,485 lbs., which is lighter than that of the STFS, and significantly lighter than that of equivalent conventional concrete floor slabs. In order to verify the structure against this design, floor systems using diverse available sections are

also checked. Both the floor systems with Pipe 2-1/2 STD as chords and Pipe 1-1/4 STD as the web and the floor system with Pipe 2 XXS as chords and Pipe 1-1/4 STD as the web passed the structural inspection. These results show that the optimization results are efficient and reliable.

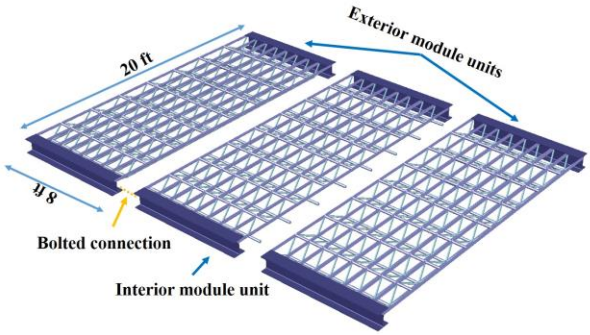

a) Modular unit

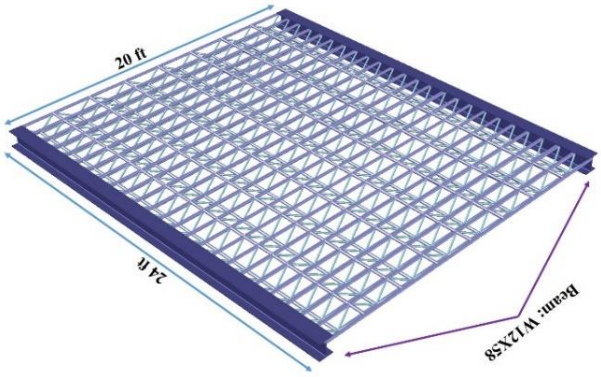

b) Optimal space truss with w-beam floor system (STWFS)

Figure 2.10 The optimal space truss with w-beam floor system (STWFS)

The depths found in this design were compared with different depths found in the various application studied; the relationship of depth to the deflection ratio is displayed in in Figure 2.11.

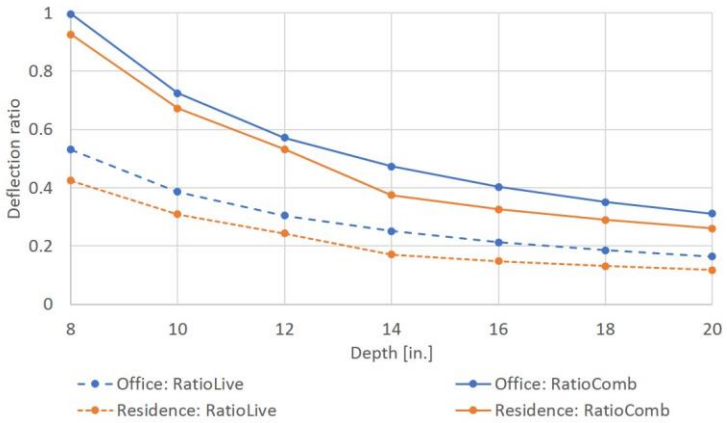

Figure 2.11 The relationship of depth to the deflection ratio

2.5 Parameter Study

A detailed parameter study was conducted by designing floor systems under various applications, including those for office and residential buildings, to study the influence of several parameters affecting optimal design. Applications for both offices and residences were analyzed for both STFS and STWFS. Despite the existing parameters, including structural configurations, element properties and spacing between elements, the central depth was also studied. The parameters used for STFS and the optimal results were outlined in Table 2.5 and Table 2.6.

Table 2.5 A detailed parameter study of STFS

Objective	Symbol	Range
Top and bottom chords	A_1	Round HSS 1.9 x 0.188 to Round HSS 3 x 0.250
Web truss	A_2	Round HSS 1.9 x 0.188 to Round HSS 2.5 x 0.250
Spacing along the length	S_1	2 ft to 10 ft
Spacing along the width	S_2	1ft to 8 ft
Central depth	D	6 inches to 10 inches
Application case		Office and Residence

Table 2.6 Optimal results for STFS

Application	Central depth	Top and bottom chords	Web truss	Spacing along length	Spacing along width
	D (in.)			S_1 (in.)	S_2 (in.)
Office	8	HSS 3 x 0.250	HSS 2.375 x 0.154	15	19.2
	10	HSS 3 x 0.188	HSS 2.375 x 0.250	34.3	32
Residence	8	HSS 3 x 0.250	HSS 2.375 x 0.154	16	24
	10	HSS 3 x 0.250	HSS 2.375 x 0.250	34.3	48

For both office and residential applications, the optimal results for the STFS using a central depth of 6 inches were not applicable. Based on the parameter study, it was revealed that the optimal design for floor systems of residential applications required less material usage. Also, with increment in the floor's central depth, the total material usage decreases.

Similarly, a detailed parameter study of the STWFS is conducted, and the parameters and results are illustrated in Table 2.7 and Table 2.8. Both office and residential applications were studied, and it is revealed that a smaller STWFS depth could be applied. Compared with the STFS, the STWFS's central depth could be reduced to 6 inches. It was also discovered that material usage was reduced when the floor's central depth increased.

Table 2.7 A detailed parameter study of STWFS

Objective	Symbol	Range
Top and bottom chords	R_1	0.25 in. to 1 in.
	r_1	$0.65R_1$ to $0.95R_1$
Web truss	A_2	0.5 in.^{2} to 2 in.^{2}
Spacing along the length	S_1	2 ft to 10 ft
Spacing along the width	S_2	1 ft to 8 ft
Central depth	D	6 inches to 10 inches
Application case		Office and Residence

Table 2.8 The optimal results for STWFS

Application	Central depth	Top and bottom chords		Web truss	Spacing along the length	Spacing along the width
	D (in)	R_1 (in.)	r_1 (in.)	A_2 (in.^{2})	S_1 (in.)	S_2 (in.)
Office	6	1	0.7	0.5	30	12
	8	1	0.65	1.5	120	32
	10	1	0.7	1	120	48
Residence	6	1	0.65	0.5	40	16
	8	1	0.65	1	120	32
	10	0.875	0.6125	1	120	48

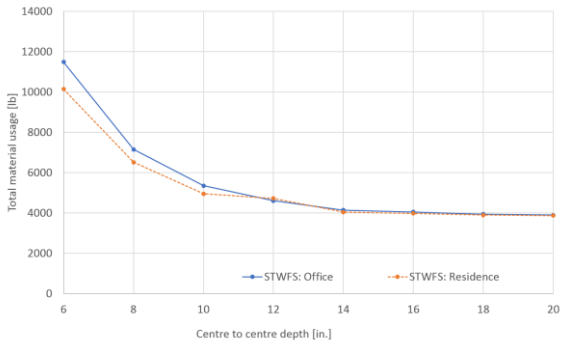

Figure 2.12 The parameter study of STWFS

Optimization results for the STWFS require less material usage than those of the STFS design, due to the shape of the design, all of its elements eliminate material wastes. As shown in Figure 2.12, residential applications' total material usage is smaller than that for offices, mainly due to residences' lower capacity demand. In addition, total material usage and the differences between office and residence applications decrease with increment in STWFS depth.

2.6 Floor Vibration

Floor vibration is considered a severability issue, and is caused by forces applied directly to the floor by human or equipment, or by vibrations transmitted through construction or from the ground (D. E. Allen, Pernica, 1998). The most common source of floor vibration is human activity, such as walking, and the problem is more critical when running, jumping and dancing are involved. Floor vibration is highly related building occupants comfort and/or damage to sensitive equipment. A lack of vibration control causes personal discomfort and increases the fear of structural collapse even though only small displacements and stresses are actually caused.

When designing a steel structure, both stiffness and resonance are main factors in floor vibration. In order to control for floor vibration, deflection limitations have been commonly applied to steel floor systems, and a traditional stiffness criterion for floor constructions limits the live load deflection to an equation of span/360; this is controlled for during design procedures. Resonance is another critical consideration related to most vibration issues; occurs when the fundamental frequency of the designed floor system is close that of the forcing frequency. Typically, the step frequency for human activity is from 2 to 3 Hz, and the fundamental frequency of most floor systems is between 3 and 8 Hz (D. E. Allen, Pernica, 1998). Therefore, in an attempt to control floor vibration, the natural frequency of the designed floor system must be greater than 3 Hz. This ensures that the structural frequency will be higher than the lowest walking harmonic, and avoids resonance at the natural frequency. As shown in Figure 2.13, the least peak acceleration for human comfort recommended for floor systems, for vibrations due to human activities, was at a frequency of between 4 and 8 Hz, implying that severe vibrational effects would not occur at this range.

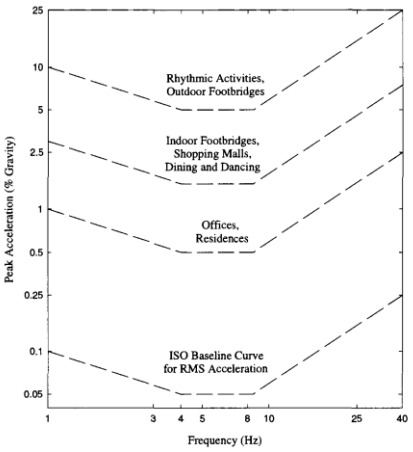

Figure 2.13 The recommended peak acceleration for the human comfort for vibrations due to human activities (D. Allen, Murray, 1993)

Since the most important criteria for the vibration serviceability design and the evaluation of floor systems is a natural frequency, a simple equation (Equation 2.7), can be used to estimate the natural floor frequency, as presented in AISC/CISC Steel Design Guide Series No. 11: Floor Vibrations Due to Human Activity (Construction, 2003).

$$f_{n\,(\mathrm{Hz})} = 0.18\sqrt{\frac{g}{\Delta}} = \frac{18}{\sqrt{\Delta(\mathrm{mm})}} \qquad \textbf{Equation 2.7}$$

where Δ is the total deflection of the floor structure due to the weight supported by all members, including joists, girders, and columns.

Therefore, for the designed STFS, $f_{n1} = 4.4$ Hz, and for the optimal STWFS, $f_{n2} = 4.5$ Hz. To attain a more accurate and detailed assessment of floor vibrations, an Eigen analysis is employed. The results of natural frequency calculated by finite element analysis are shown in Table 2.9, while Figure 2.14 displays the mode shapes of the floor systems, with 30 as a scale factor.

A comparison of these two methods reveals that the manual method results are similar to those for modal analysis. In conclusion, both optimal designs satisfied the minimal floor frequency of 3 Hz, according to SCI-P354 (Smith et al., 2007), to ensure that walking activities will be external to the range which causing resonant or close-to-resonant excitation of the fundamental vibration mode. The natural frequency will increase with the additional steel decks and concrete slab toppings. Further research will perform detailed studies of floor vibration.

Table 2.9 The natural frequency of the floor systems

Floor system	Natural frequency (Hz)		
	Mode 1	Mode 2	Mode 3
STFS	4.2	5.7	6.7
STWFS	4.5	6.3	8.3

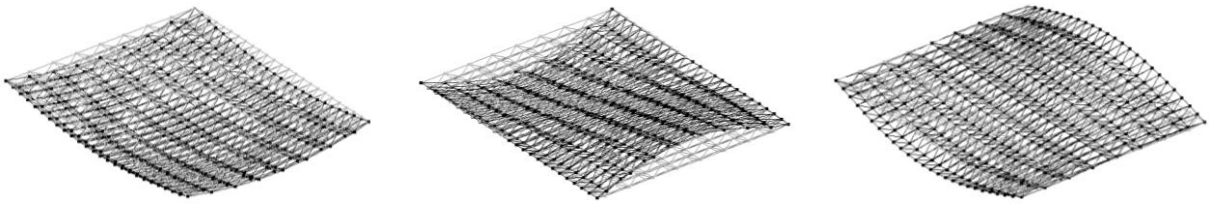

a) Mode 1 b) Mode 2 c) Mode 3

Figure 2.14 The mode shapes of the floor

Chapter 3: Seismic Design of Modular Steel Truss System

The proposed modular steel truss system (MSTS) consists of both gravity system and seismic force resisting system (SFRS) as illustrated in Figure 3.1. In MSTS design, the SFRS is aimed to be adjusted for different hazard levels, without redesigning the gravity system. Thus, an innovative SFRS, modular buckling restrained braced truss moment frame (MBRBTMF) is designed to be coordinated with the designed gravity system, MSFS. In order to maximum the usable space and clear story height, the height of the system is limited to around 11 inches. The buckling restrained braces (BRBs) are utilized as the structural fuses and energy dissipation devices, which can be easily and efficiently construction, and more easily replaced after severe earthquake shaking, making the structures more resilient towards earthquakes. The performance-based plastic design (PBPD) method is adopted for this novel MBRBTMF system, and the detail design procedure is presented in this chapter, and the nonlinear dynamic analysis was conducted to evaluate the performance of the designed MSTS structure.

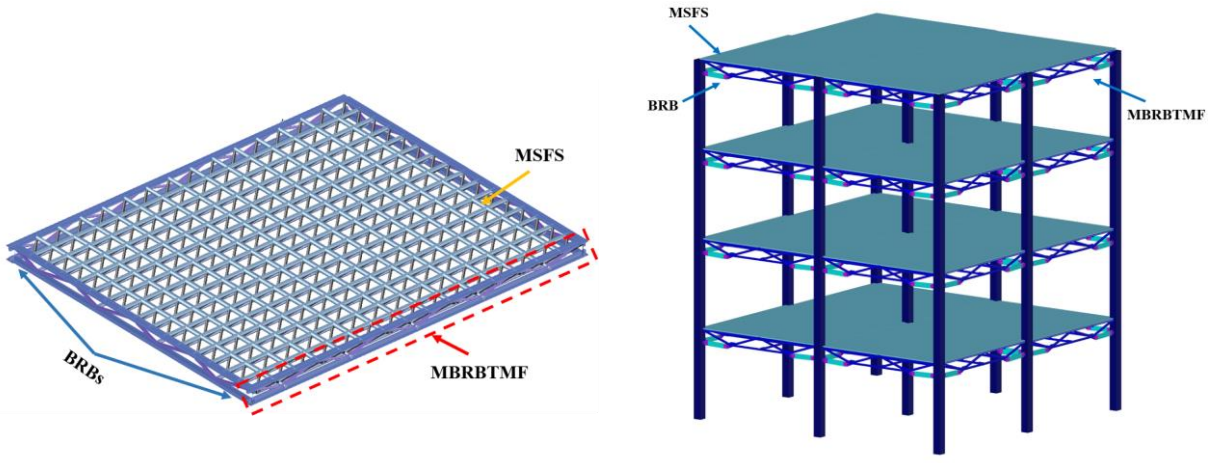

a) MSTS b) MSTS building

Figure 3.1 MSTS concept

3.1 Performance-Based Plastic Design (PBPD) Procedure

The performance-based plastic design (PBPD) procedure was originally developed by Goel (Goel, Leelataviwat, 1998). This design procedure has been successfully used in SMRF (Goel, Leelataviwat, 1998), SCBF (Chao, Goel, 2006b), SEBF (Chao, Goel, 2006a) and BRKBTMF (Yang et al., 2015; Yang et al., 2013) systems.

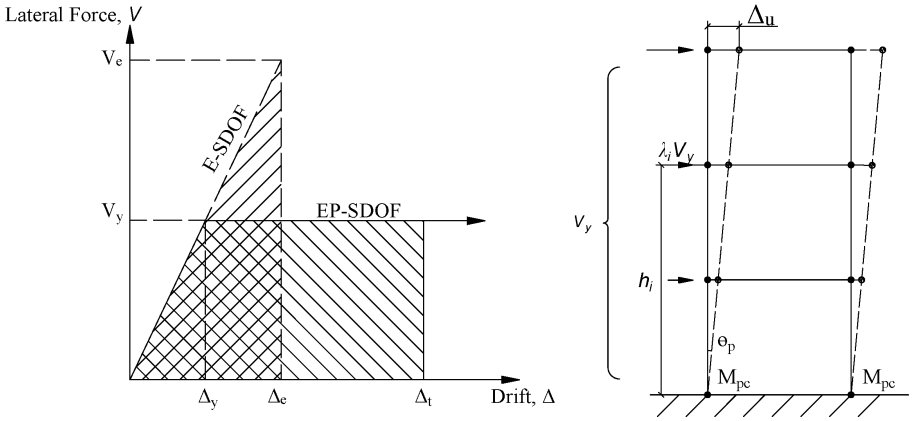

Figure 3.2 PBPD concept

The pre-selected target drift and yield mechanism are used as key performance objectives in PBPD method, while the design base shear is estimated by specified hazard spectrum. Compared to traditional design procedure, both target drift and structural strength are considered in PBPD method, hence, no iteration is needed. The PBPD method assumes that the energy dissipation can be determined by an equivalent elastic-plastic single degree of freedom (EP-SDOF) systems as shown in Figure 3.2, and this method has been extended to multi-story structures (Goel et al., 2010). Based on this, the energy equation can be written as

$$E_e + E_p = \gamma E$$ **Equation 3.1**

where E_e and E_p are the elastic and plastic energy components respectively. The modification factor, γ, can be determined as following equation, depending on the ductility factor, μ_s, and reduction factor, R_μ.

$$\gamma = \frac{2\mu_s - 1}{R_\mu^2}$$ **Equation 3.2**

According to equations above, the base shear coefficient can be achieved following

$$\frac{V_y}{W} = \frac{-\alpha_0 + \sqrt{\alpha_0^2 + 4\gamma S_a^2}}{2}$$ **Equation 3.3**

where

$$\alpha_0 = \frac{8\pi^2}{T^2 g}\left(\sum_{i=1}^{n} \lambda_i h_i\right)\theta_p$$ **Equation 3.4**

In which, λ_i and θ_p are, respectively, the shear distribution factor for floor i, and the global structural inelastic drift ratio.

The story shear distribution factor at level i, β_i, is determined as shown in Figure 3.1, to ensure that the plastic demand evenly distributed along the structural height (Chao et al., 2007).

$$\beta_i = \left(\frac{\sum_{j=1}^{n} w_j h_j}{w_n h_n}\right)^{0.75T^{-0.2}}$$ **Equation 3.5**

where w_j and h_j are, respectively, the seismic weight at level j, and the structural height from ground to level j, while n represents roof level. Then the lateral force at each level can be distributed as

$$F_i = \lambda_i V_y$$ **Equation 3.6**

where

$$\lambda_i = (\beta_i - \beta_{i+1}) \left(\frac{w_n h_n}{\sum_{j=1}^{n} w_j h_j} \right)^{0.75T^{-0.2}}$$ **Equation 3.7**

Using these equations, the design base shear, V_y, can be obtained for any specified hazard level.

3.2 Seismic Design of MBRBTMF

The PBPD method was used to design the proposed MBRBTMF system, based on designed procedure developed by Yang (Yang et al., 2013). In MSTS design, the seismic force resisting system is aimed to be adjusted for different hazard levels, without redesigning the gravity system. The BRBs are selected as the structural fuses, which can be installed and replaced easily and efficiently.

3.2.1 Drift and Base Shear Calculation

The yield drift, Δ_y, and target drift, Δ_t as presented in Figure 3.2 are selected as the first step in PBPD method. A yield drift of 0.75% from pervious BRKBTMF studies, was determined for MBRBTMF. The structural period was determined using the equation from ASCE 2010, then the modification factor, γ, can be calculated. Following the steps, the design base shear can be obtained.

3.2.2 BRB Design

The buckling restrained brace (BRB) are selected as the structural fuses to dissipate energy, and the trusses and columns are designed to remain elastic in MBRBTMF. The plastic energy is calculated using

$$E_p = \sum_{i=1}^{n} 2(\beta_i N_{BRB})\delta_p + 2M_{pc}\theta_p$$ **Equation 3.8**

where N_{BRB} is the BRB's axial strength at roof level, and the plastic moment of column, M_{pc}, and plastic deformation δ_p are determined following

$$M_{pc} = \frac{1.1Vh_{c1}}{4N}$$

$$\delta_p = (D_0 sin\alpha + l_1 cos\alpha)\theta_p \qquad \textbf{Equation 3.9}$$

For pin based, $M_{pc} = 0$. The geometry is shown in Figure 3.3.

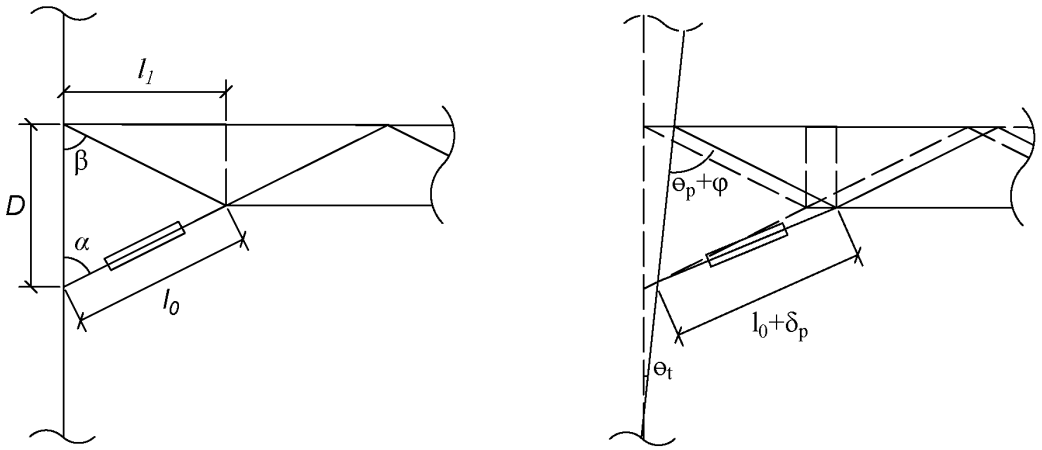

a) Initial geometry b) Deformed geometry

Figure 3.3 Structural geometry

In this design, the BRB inclination was selected as horizontal connecting to column to minimize the depth and maximize the clear story height. The BRB was calibrated using "Steel02" material in OpenSees as illustrated in Figure 3.4, and the elastic modulus, yielding strength and strain hardening ratio parameters are determined by previous model calibration (Black et al., 2004).

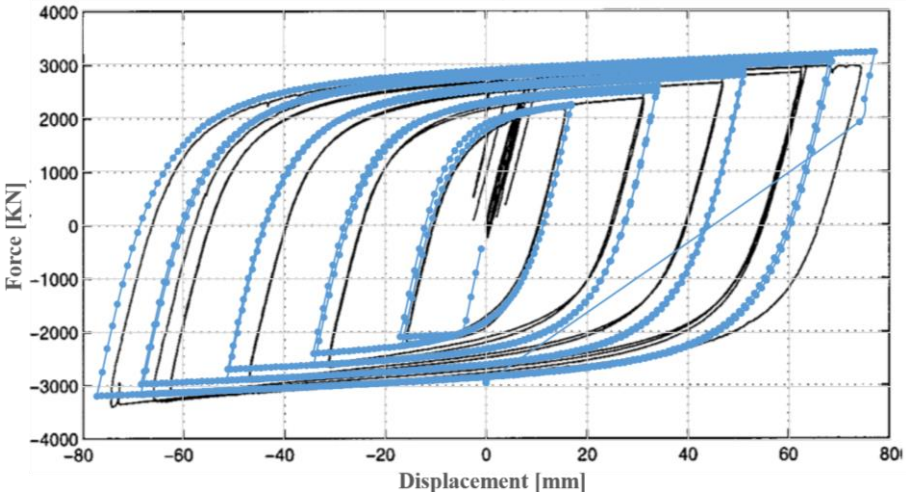

Figure 3.4 BRB Calibration

3.2.3 Truss Design

The truss span and depth was determined based on the dimension of MFSF, thus, the spans were designed as 20 by 24ft., while the central depth is limited as 8 inches. The truss sample under gravity and BRB forces is shown in Figure 3.5. The trusses are assumed to be perfectly pinned to the columns.

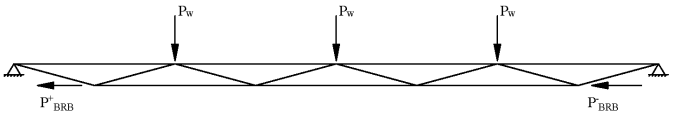

Figure 3.5 Truss sample design

The maximum BBRB forces are calculated following

$$P_{BRB}^{+} = \omega R_y P_y$$

$$P_{BRB}^{-} = \omega \beta R_y P_y \qquad \textbf{Equation 3.10}$$

where P_{BRB}^{+} is the maximum tension force, and P_{BRB}^{-} is the maximum compression force. The strength hardening adjustment factor, ω, compression overstrength, β, and material expected factor, R_y were determined from previous studies (Yang et al., 2013).

3.2.4 Column Design

The columns were designed to remain elastic in this design, and the structural foundation is assumed to be fixed. The BRB's tension and compression forces are assumed to reach the maximum values when the structure reaches the expected strength. The free body diagram of the column tree is shown in Figure 3.6.

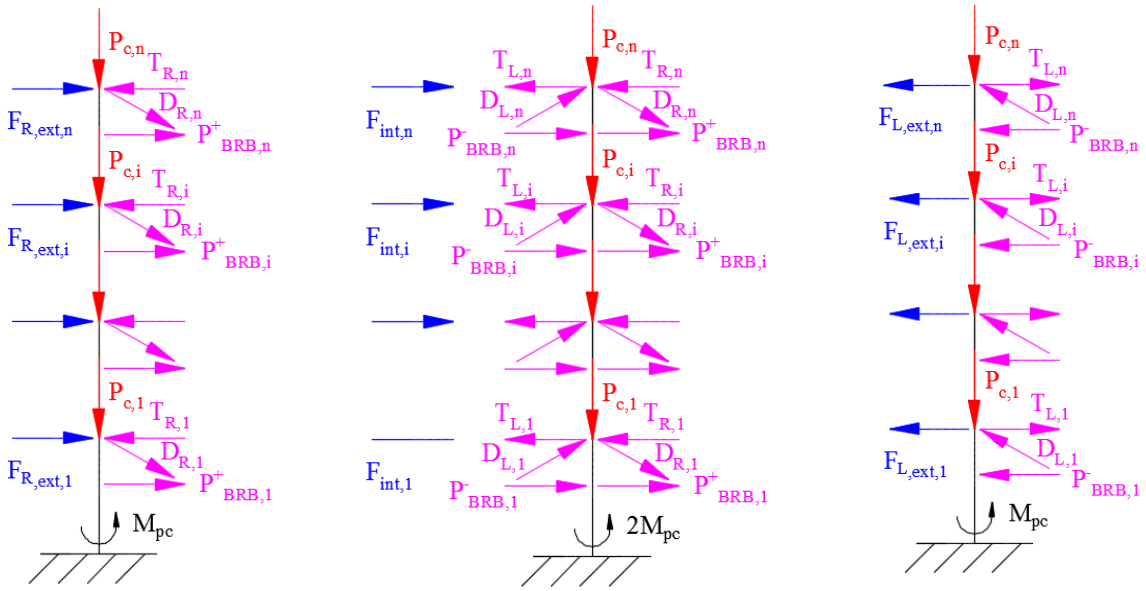

a) Exterior column (lateral force to the right)

b) Interior column

c) Exterior column (lateral force to the left)

Figure 3.6 Free body diagram of column tree

The lateral forces on the columns can be calculated based

$$F_{ext,R,i} = \alpha_i \frac{\sum_{i=1}^{n}(T_{R,j} - D_{R,j} sin\varphi)h_i - \sum_{i=1}^{n}(P^{+}_{BRB,i})(h_i - D) + M_{pc}}{\sum_{i=1}^{n} \alpha_i h_i}$$

$$F_{ext,L,i} = \alpha_i \frac{\sum_{i=1}^{n}(T_{L,j} - D_{L,j} sin\varphi)h_i - \sum_{i=1}^{n}(P^{-}_{BRB,i})(h_i - D) + Mpc}{\sum_{i=1}^{n} \alpha_i h_i}$$

$$F_{ext,R,i} = F_{ext,R,i} + F_{ext,L,i} \quad \textbf{Equation 3.11}$$

where the distribution factor, α_i is determined following

$$\alpha_i = \frac{(\beta_i - \beta_{i+1})}{\sum_{i=1}^{n}(\beta_i - \beta_{i+1})} \quad \textbf{Equation 3.12}$$

3.3 Application of Modular Steel Truss System (MSTS)

Following the PBPD procedure, the structural components of the prototype 4-story MSTS building were designed. To coordinate with the gravity system, the seismic force resisting systems with 11-inch total depth, were designed as frames along the length and width, respectively. To ensure that the performance of the proposed modular steel truss system (MSTS) as shown in Figure 3.1a, a detailed nonlinear dynamic analysis was conducted. The prototype 4-story building located in Berkeley, California, was designed and modelled to confirm the applicability of the designed systems.

3.3.1 Hazard Analysis

A hazard analysis is usually employed as the first step in determining and analyzing the degree of risk. The seismicity of the structural site and hazard spectrum are studied for the prototype structures. Berkeley, is located in the “Pacific Ring of Fire” as shown in Figure 3.7, a seismically active zone belt surrounding the Pacific Ocean. The movements and collisions of tectonic plates results in this region result in strain energy, finally causing earthquakes.

Figure 3.7 The Pacific Ring of Fire (U.S. Geological Survey, 2017)

Cascadia region is the Pacific Northwest region of North American, and one of the most tectonically complex regions in the world. It is well known that convergent boundaries occur where two plates slide toward one another, and that this movement will cause either a subduction zone or continental collision. Specifically, a portion of the Pacific Plate along with the small Juan de Fuca Plate is being subducted beneath the North American Plate, as shown in Figure 3.8. These plate movements and collisions eventually result in a concentration of earthquakes. Hence, more than 100 earthquakes of magnitude 5 or greater have occurred during the past 70 years. Based on the United States Geological Survey (USGS) research, the Cascadia Subduction Zone (CSZ) has suffered magnitude 9.0 and greater earthquakes in the past, and the potential is high for such largest earthquakes to occur again in the future.

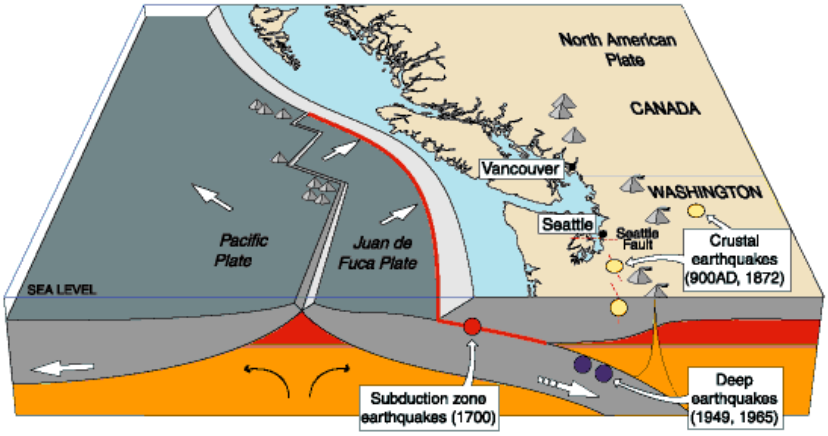

Figure 3.8 Cascadia region (U.S. Geological Survey, 2017)

The construction site was classified as Site Class C, and the information shown in Table 3.1 were determined from U.S. Geological Survey (USGS). Both 10/50 hazard level (DBE level, 2/3 MCE level) and MCE level were considered in structural design.

Table 3.1 Site class information, Berkley

Site class	F_a	S_s (g)	F_v	S_1 (g)	S_{MS} (g)	S_{M1} (g)	S_{DS} (g)	S_{D1} (g)
C	1.2	2.164	1.4	0.835	2.597	1.169	1.732	0.779

According to ASCE, the acceleration value of fundamental period of designed structure can be determined using linear interpolation, as following:

- For $T \leq T_0$, $S_a(T) = S_{DS}(0.4 + 0.6T/T_0)$
- For $T_0 \leq T \leq \mathrm{T_S}$ $S_a(T) = \mathrm{S_{DS}}$
- For $T_S \leq T \leq \mathrm{T_L}$ $S_a(T) = \mathrm{S_{D1}}/T$
- For $T \geq T_L$, $S_a(T) = S_{D1}T_L/T^2$

where $T_0 = 0.09, T_S = 0.45$, and $T_L = 1$. Lastly, the design spectrum of both DBE and MCE level are illustrated in Figure 3.9.

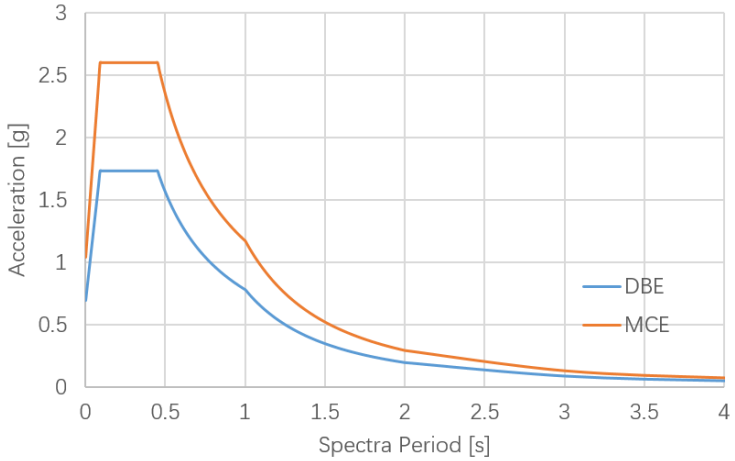

Figure 3.9 Design hazard spectrum, Berkeley

3.3.2 Structural Design and Modelling

The prototype building is a 4-story MSTS building, and the structural height is 53ft. with the 100 by 120 ft. dimension. The first story height is 14ft., and 13ft. for the rest stories. The design parameters used in the PBPD method are listed in Table 3.2.

Table 3.2 Design parameters

Design parameter	10/50 hazard level	2/50 hazard level
S_a	0.78	1.17
T	1.0	1.0
Target drift ratio, θ_u	2.5	3.5
Base shear coefficient	0.16	0.17

The prototype building was designed to achieve two performance objectives: 1) drift ratio less than 3.5% under 2/50 hazard level (MCE level); 2) drift ratio less than 2.5% under 10/50 hazard level (DBE level, 2/3 MCE). Following design procedure in Chapter 2, a design summary of MBRBTMF is listed in Table 3.3.

Table 3.3 MBRBTMF design summary

No.	BRB ($in.^2$)	Column	Frame 1 (along the length)			Frame 2 (along the width)		
			Top chord	Bottom chord	Diagonal chord	Top chord	Bottom chord	Diagonal chord
4	1.5	W27X307	2L3X3X3/16	2L3X3X3/8	2L3X3X1/4	2L3X3X1/4	2L3X3X1/2	2L3X3X1/4
3	2	W27X307	2L3X3X5/16	2L3X3X1/2	2L3X3X3/8	2L3X3X3/8	2L3-1/2X3-1/2X1/2	2L3X3X5/16
2	2	W27X307	2L3X3X5/16	2L3X3X1/2	2L3X3X3/8	2L3X3X1/2	2L3-1/2X3-1/2X1/2	2L3X3X3/8
1	2.5	W27X336	2L3X3X3/8	2L3X3X1/2	2L3X3X3/8	2L3X3X1/2	2L3-1/2X3-1/2X1/2	2L3X3X3/8

The prototype MSTS building was modelled using an advanced finite element analysis software OpenSees. BRB is modelled using truss members with 'Steel02' material, and the elastic modulus, yielding strength, and strain hardening ratio parameters are selected based on past research of BRB (Yang et al., 2015; Yang et al., 2013). The structural columns were defined as "ElasticBeamColumn" elements using Standard AISC steel section. All columns were designed using cross w-section, and were assumed to be perfectly fixed to the ground. The mass contribution in the building model arise from the structural self-weight, including the seismic dead load, design live load and the floor system's self-weight. In addition, the 2.0% Rayleigh damping method at the 1st and 3rd mode is used. The modal period is estimated as 1.0 seconds, which equals the

designed period. The MSFSs can be simplified as rigid diaphragm to reduce the computational complexity, and a detailed study of simplified model is presented in Chapter 4.

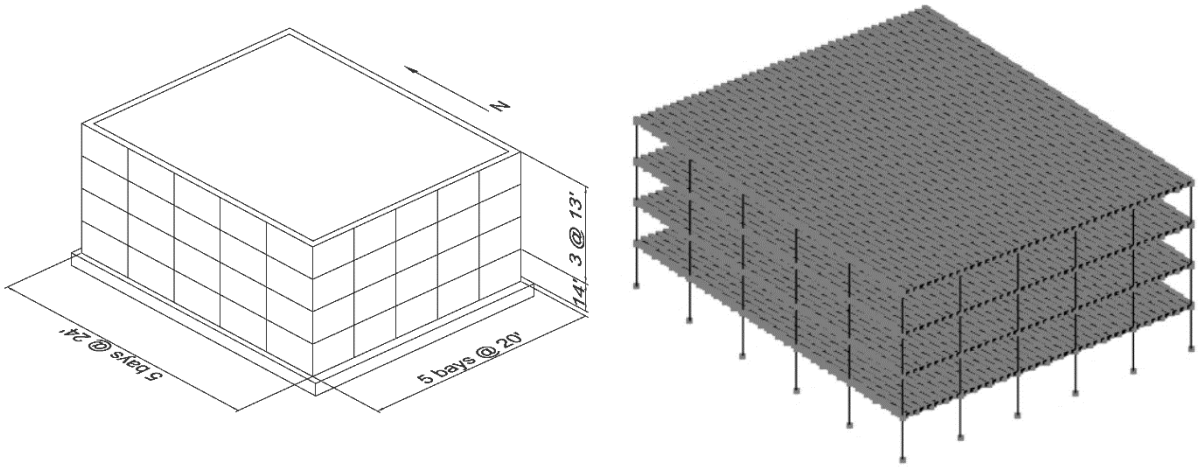

a) The prototype 4-story building b) MSTS model

Figure 3.10 The prototype MSTS building model

3.3.3 Ground Motion Selection

Based on a hazard analysis, ground motions are selected from PEER database (Pacific Earthquake Engineering Research Center, 2010) and listed in Table 3.4, and amplitude-scaled to match the hazard spectrum as illustrated in Figure 3.11. The selected ground motions were scaled to an average value of the 5% damped response spectrum within the period range of 0.2T to 1.5T, where T is the fundamental period of the structure. For ground motion scaling, a square root of the sum of the squares (SRSS) spectrum is conducted for the scaled ground motion. In addition, only an identical scaling factor is applied to both components of each pair.

Table 3.4 Selected ground motion

No.	RSN	Year	Event	Station	M (Mw)	V_{s30} (m/s)	Scaling factor	
							DBE	MCE
1	57	1971	San Fernando	Castaic - Old Ridge Route	6.61	450.28	2.0	3.1
2	164	1979	Imperial Valley	Cerro Prieto	6.53	471.53	2.4	3.6
3	289	1980	Irpinia Italy	Calitri	6.9	455.93	2.3	3.4
4	313	1981	Corinth Greece	Corinth	6.6	361.4	1.9	2.8
5	755	1989	Loma Prieta	Coyote Lake Dam - Southwest Abutment	6.93	561.43	1.6	2.4
6	864	1992	Landers	Joshua Tree	7.28	379.32	1.3	2.0
7	881	1992	Landers	Morongo Valley Fire Station	7.28	396.41	1.9	2.9
8	1083	1994	Northridge	Sunland - Mt Gleason Ave	6.69	402.16	2.6	3.9
9	1633	1990	Manjil Iran	Abbar	7.37	723.95	1.2	1.8
10	3750	1992	Cape Mendocino	Loleta Fire Station	7.01	515.65	2.1	3.2
11	3753	1992	Landers	Fun Valley	7.28	388.63	2.0	3.0

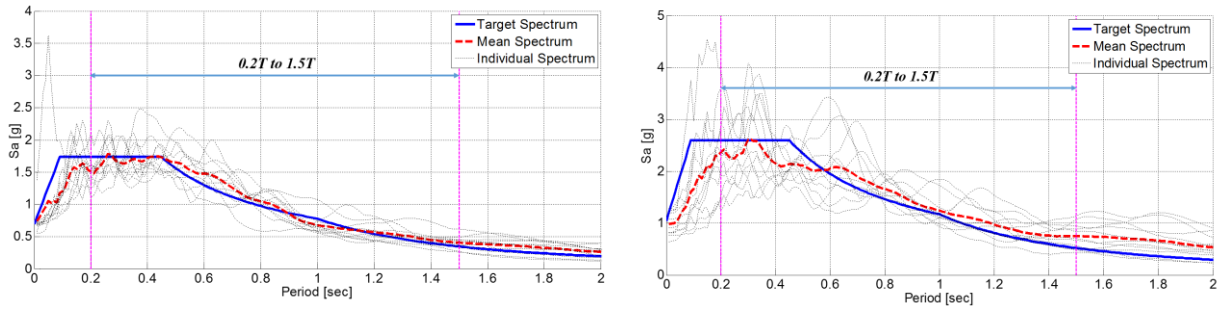

a) 10/50 hazard level (DBE level) b) 2/50 hazard level (MCE level)

Figure 3.11 Response spectrum of scaled ground motions: MBRBTMF building

3.3.4 Structural Performance

The nonlinear response history analysis was conducted to verify the design procedure and seismic performance of the MBRBTMF under earthquakes. Figure 3.12 shows the median peak inter-story drift ratio, and Figure 3.13 presents the peak median story acceleration.

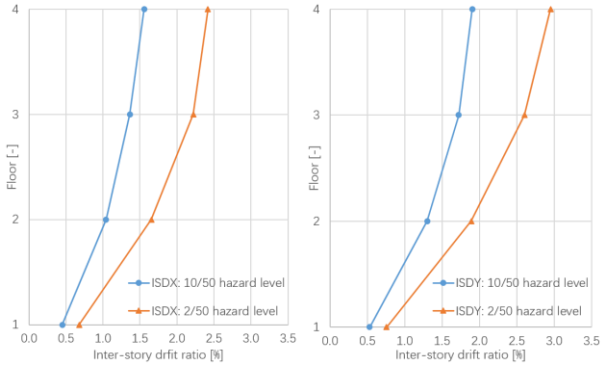

Figure 3.12 Median peak inter-story drift ratio

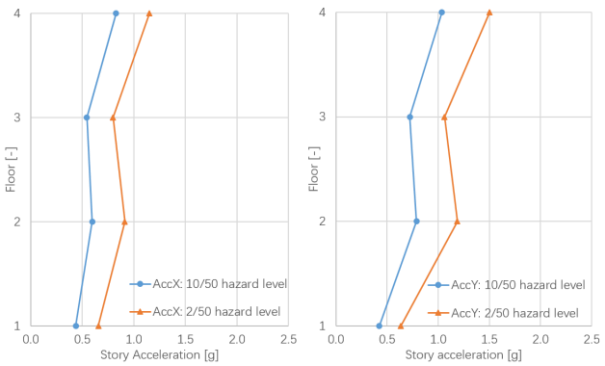

Figure 3.13 Median peak story acceleration

The results show that the performance objectives are achieved, the median peak inter-story drift ratio is less than the target, respectively, 2.5% for 10/50 hazard level and 3.5% under 2/50 hazard level. In addition, the floor accelerations are controlled under two different hazard levels. This indicates that the MBRBTMF is efficient and can be applied for practical applications.

To ensure that the MSTS building structure designed using PBPD can have sufficient performance against collapse, the collapse assessment analysis was conducted. The 44 far-field ground motion records presented in FEMA P695 were selected for this analysis. The incremental dynamic analysis (IDA) is one of the common approaches to assess the collapse capacity of a structure under earthquakes, tracking the relationship between the structural measure and intensity measure. The IDA was performed to estimate the structural performance under different earthquake intensities. During the IDA, the ground motion records were amplitude scaled, and the maximum

inter-story drift ratio was recorded. The IDA curves for the prototype building along with the median response and MCE spectral acceleration are shown in Figure 3.14. The structural demand is taken as the maximum inter-story drift ratio, and the intensity measure is taken as the spectral acceleration of the ground motion at the structural period. This intensity is defined as the collapse intensity for the structure under the specific earthquake.

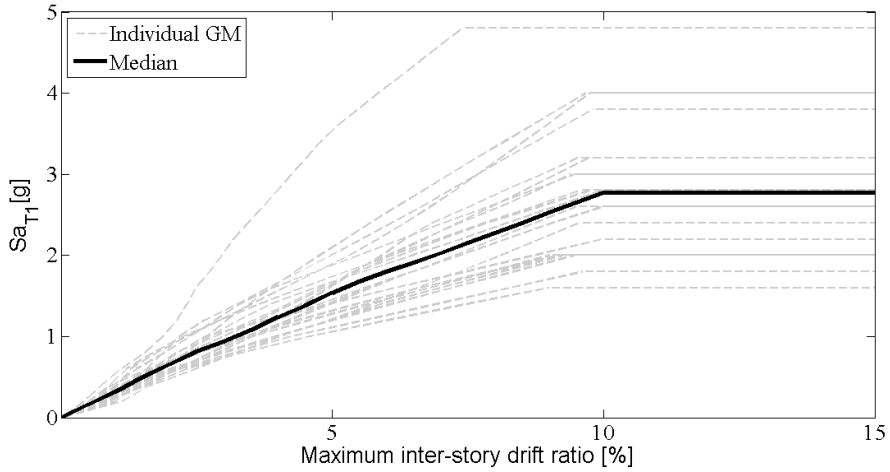

Figure 3.14 IDA curve for the prototype MSTS building

The collapse fragility curve from the IDA results is illustrated in Figure 16. The collapse fragility curve represents the conditional probability of structural collapse for a given ground motion intensity, using a lognormal cumulative distribution function (CDF). The median collapse intensity, $\hat{S}_{CT}$, was obtained from the curve as 2.78 g for the building. The median MCE intensity, S_{MT}, at the fundamental period, was determined as 1.17 g. Thus, the collapse margin ratio (CMR), $\hat{S}_{CT}/S_{MT}$, was computed to be 2.38 for the prototype building.

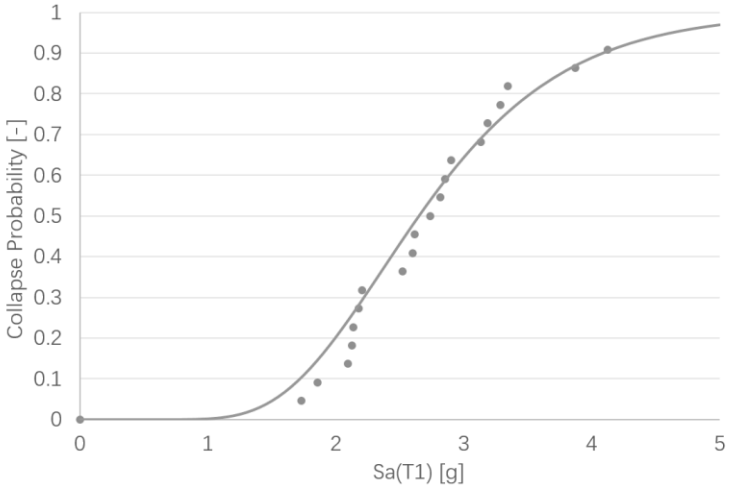

Figure 3.15 Collapse fragility curves for the prototype MSTS building

The collapse probabilities were calculated from the ratio of number of ground motions, causing collapse to the total number of seismic records. It reveals that MSTS had a good seismic performance with less than 10% collapse probability under 2/50 hazard level.

Chapter 4: Application of Modular Steel Floor Systems in Conventional Structural Systems

Besides the use of modular steel floor system (MSFS) in modular steel truss system (MSTS), the MSFS can also work with conventional SFRSs. In this chapter, the prototype buildings with conventional SFRSs and MSFSs are designed and modelled to examine the structural and economic efficiency of the MSFS applied in these structures.

4.1 Application of MSFS in 3-Story BRBF Building

In this case study, a 3-story buckling restrained braced frame (BRBF) building using MSFS, was designed and modelled for location in Vancouver. A comparison of the seismic performance models with equivalent concrete floor, and those with the STWFS, is examined using nonlinear dynamic analysis.

4.1.1 Structural Design and Modelling

A 3-story building for the STWFS and equivalent concrete floor are designed and modeled following past design and research concerning the buckling restrained brace (BRB) frames (Goel, Chao, 2008). In this building design (as shown in Figure 4.1), the floor plan dimensions are determined as being 60 ft. in length by 72 ft. in width, with each story height around 13 ft (4 m).

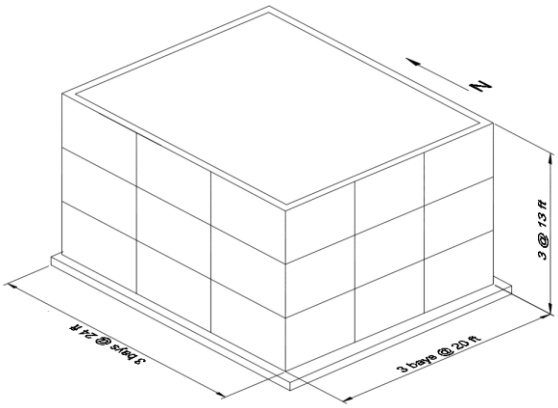

Figure 4.1 An isometric view of the 3-story building

The details of structural design are shown in Table 4.1. It is found that the smaller structural components sizes are applied in the structure with STWFS than the one with an equivalent concrete floor, which implies less material usage and lower construction costs.

Table 4.1 3-Story building design details

Floor system	Floor	Seismic column	Gravity column	Structural beam	BRB size ($in.^2$)
Equivalent concrete floor	1	Box 12 x 12 x 0.375	W12 x 45	W14 x 48	3.5
	2	Box 12 x 12 x 0.375	W12 x 45	W12 x 35	2.5
	3	Box 12 x 12 x 0.375	W12 x 35	W12 x 35	1.5
STWFS	1	Box 12 x 12 x 0.375	W12 x 35	W12 x 35	2
	2	Box 12 x 12 x 0.375	W12 x 35	W12 x 35	2
	3	Box 12 x 12 x 0.375	W12 x 35	W12 x 35	1

Upon the completion of the structural design, the building is modelled using the advanced finite element software OpenSees. Figure 4.2a provides an isometric view of the prototype building with

an equivalent concrete slab while the STWFS is shown in Figure 4.2b. BRB is modelled using truss members with 'Steel02' material, and the structural beam and column are defined as "ElasticBeamColumn" elements using Standard AISC steel section and composite columns. All the structural columns are pin-supported in order to reduce moment demand on the structural foundations.

In general, the concrete slabs are simply replaced by rigid floor diaphragms for simplicity in the dynamic analysis procedure (Lee et al., 2005). In this case, the concrete floor is modelled as rigid diaphragm while the chords of the proposed STWFS are continuous members within the span; hence they are modelled as multiple "ElasticBeamColumn" elements, and the diagonal members are modelled as truss elements. The mass contribution in the building model arise from the structural self-weight, and the 2.0% Rayleigh damping method is used.

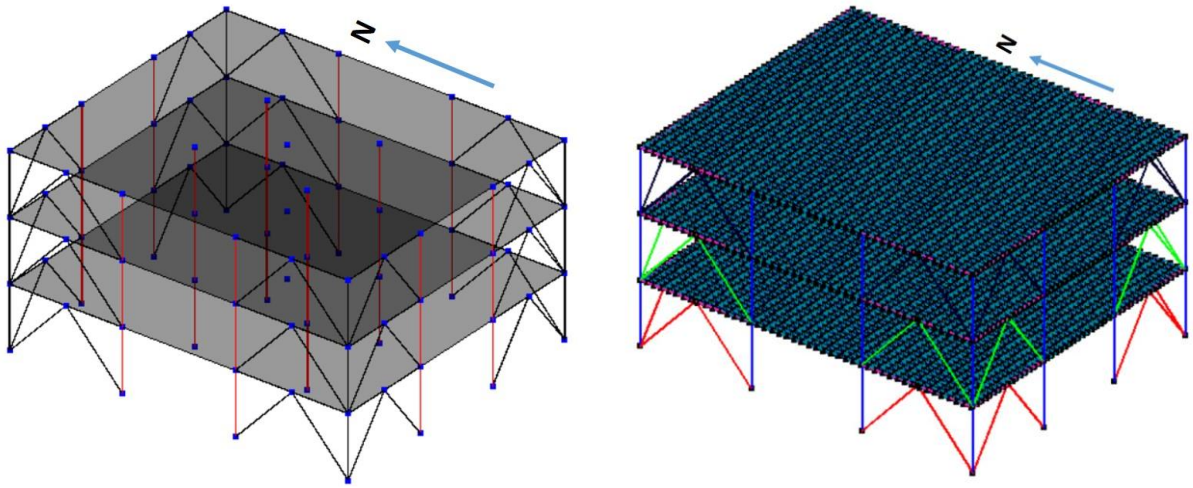

a) Isometric view (building with equivalent concrete floor)

b) Isometric view (building with STWFS)

Figure 4.2 Prototype 3-story building model

4.1.2 Hazard Analysis

The buckling restrained braced frame (BRBF) building construction site has been classified as Site Class C and its detailed description is shown in Table 4.2. The important parameter values for its design spectrum are determined by NBCC 2015. The value of the site's design spectrum coefficient at period T, $F(T)$ was defined as 1.0 in NBCC 4.1.8.4.

Table 4.2 Site class information, Vancouver

Site class	General description	Average shear wave velocity	Average standard resistance	Shear strength
		$\bar{V}_{30}\ (m/s)$	N_{60}	$S_u\ (kpa)$
C	Very dense soil and soft rock	$360 < V_s < 760$	$N_{60} > 50$	$S_u > 100$

In order to properly qualify the seismic risk, the designed structures are subjected to several ground motions scaled at different intensities. In this research study, earthquake records are scaled to the intensities of modified spectrum, and it is necessary to obtain design spectrum for the target hazards. Therefore, the mean seismic hazard values determined using (Natural Resources Canada, 2015) for 2% of exceedance in 50 years are listed in Table 4.3. The probabilities of 2%, 10% and 50% correspond to the return period of 2475, 475 and 72 years. Spectral ($S_a(T)$, where T is recorded in seconds) and the peak ground acceleration (PGA) values are given in units of g (9.81 m/s2).

Table 4.3 Seismic hazard values, Vancouver

Case	$S_a(0.2)$	$S_a(0.5)$	$S_a(1.0)$	$S_a(2.0)$	$S_a(5.0)$	$S_a(10.0)$	PGA
2%/50	0.842	0.749	0.422	0.256	0.081	0.029	0.365

According to NBCC 4.1.8.4, the acceleration value of the fundamental period for the designed structure can be determined using linear interpolations, as follows:

- For $T \leq 0.2s$, $S_a(T) = \max\{\mathrm{F}(0.2)S_a(0.2), \mathrm{F}(0.5)S_a(0.5)\}$
- For $T = 0.5s$, $S_a(T) = \mathrm{F}(0.5)\mathrm{S_a}(0.5)$
- For $T = 1.0s$, $S_a(T) = \mathrm{F}(1.0)\mathrm{S_a}(1.0)$
- For $T = 2.0s$, $S_a(T) = \mathrm{F}(2.0)\mathrm{S_a}(2.0)$
- For $T = 5.0s$, $S_a(T) = \mathrm{F}(5.0)\mathrm{S_a}(5.0)$
- For $T \geq 10.0s$, $S_a(T) = \mathrm{F}(10.0)\mathrm{S_a}(10.0)$

Eventually, the products developed from the above process are called seismic responses and design spectrum. The design spectrum values are shown in Table 4.4 and the design spectrum and mean hazard spectrum are shown in Figure 4.3.

Table 4.4 Values of the design spectrum, Vancouver

Period (s)	0.0	0.2	0.5	1.0	2.0	5.0	10.0
Acceleration (g)	0.840	0.840	0.747	0.421	0.255	0.080	0.028

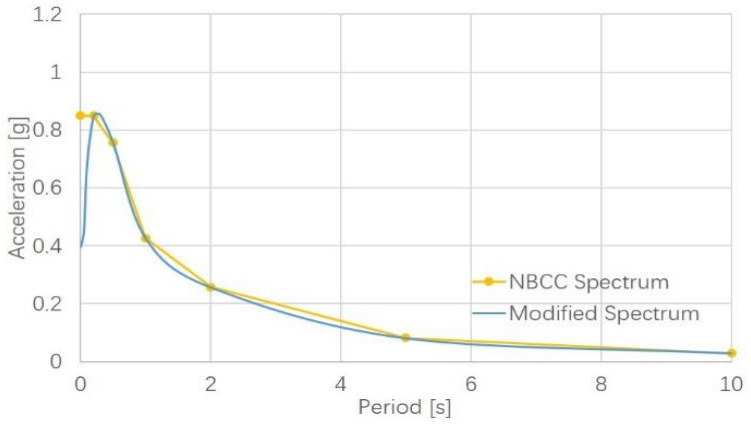

Figure 4.3. Design hazard spectrum

A total hazard spectrum is conducted by EZ-FRISK (EZ-FRISK 2015). Figure 4.4 shows the peak ground acceleration (PGA) at a hazard level of 2% in 50 years, which means an annual probability (AP) of an exceedance of 0.0004. This is calculated using Equation 4.1, where the RT is the return period, and x is the probability of the event being exceeded in y years.

$$\mathbf{AP} = \frac{\mathbf{1}}{\mathbf{RT}} = \mathbf{1} - \mathbf{10}^{\mathbf{log(1-}x\mathbf{)}/y} \qquad \textbf{Equation 4.1}$$

A corresponding GPA obtained from the analysis is 0.363g, which is very close to the 0.365g value from Natural Resource Canada data. Therefore, the EZ-FRISK analysis predicts a PGA of less 1% difference from the valid database, which indicates that the analysis is reliable.

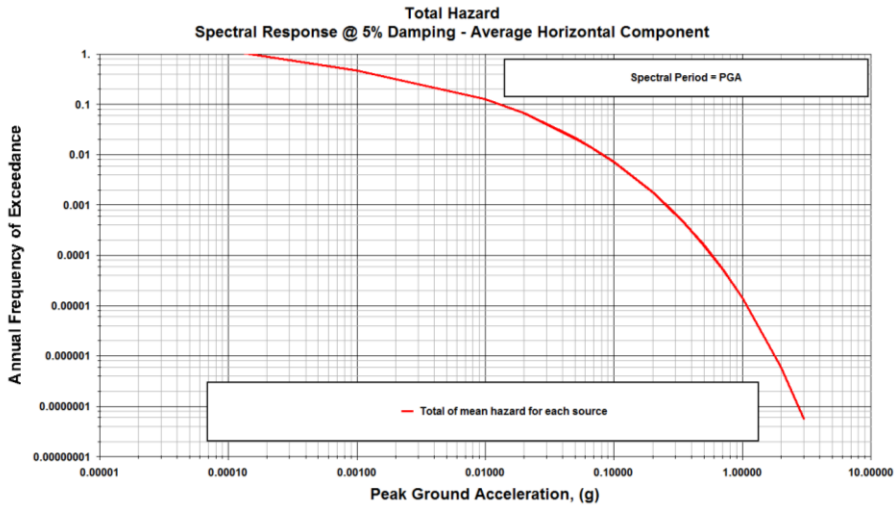

Figure 4.4 Total hazard spectrum

In addition, the hazard is usually represented through a stochastically generated set of all the events that could possibly occur, each associated with a frequency of occurrence (Di Mauro et al., 2013). Figure 4.5 shows the contributions of different seismic sources to the overall hazard risk at the

structural site. It illustrates that the highest weighted source participation to the hazard is the Explorer Interface source.

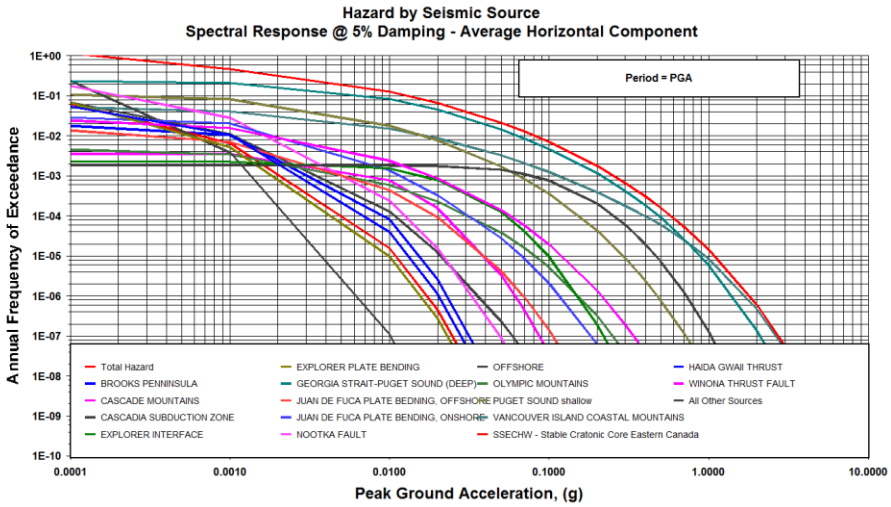

Figure 4.5 Hazard according to the seismic sources

4.1.3 Ground Motion Scaling

According to the preliminary study, the structural periods are achieved and listed in Table 4.5. Although the smaller sizes of the structural elements and BRBs are applied, the fundamental period of the designed building with STWFS has smaller structural period. The obtained structural period is also used for ground motion scaling. The structure with STWFS suffered fewer base shears than the concrete floor, due to its smaller self-weight.

Table 4.5 Structural comparison: 3-Story building

Floor system	Period (sec)		
	Mode 1	Mode 2	Mode 3
Equivalent concrete floor	0.60	0.57	0.43
STWFS	0.55	0.51	0.38

In case study of a 3-story building case study, a pair of 11 ground motions was selected from PEER (Pacific Earthquake Engineering Research Center, 2010) based on hazard analysis, and its amplitude was scaled to match the target spectrum. The ground motions were amplitude scaled between 0.2T and 1.5T, where T is the fundamental period of the structure, so that the mean spectrum did not fall below the target spectrum by greater than 10% within the period range. In this case, the fundamental period of the designed building was around 0.6 seconds for both systems. Table 4.6 shows a summary of the scaled ground motions, and Figure 4.6 shows the scaled and mean spectrum.

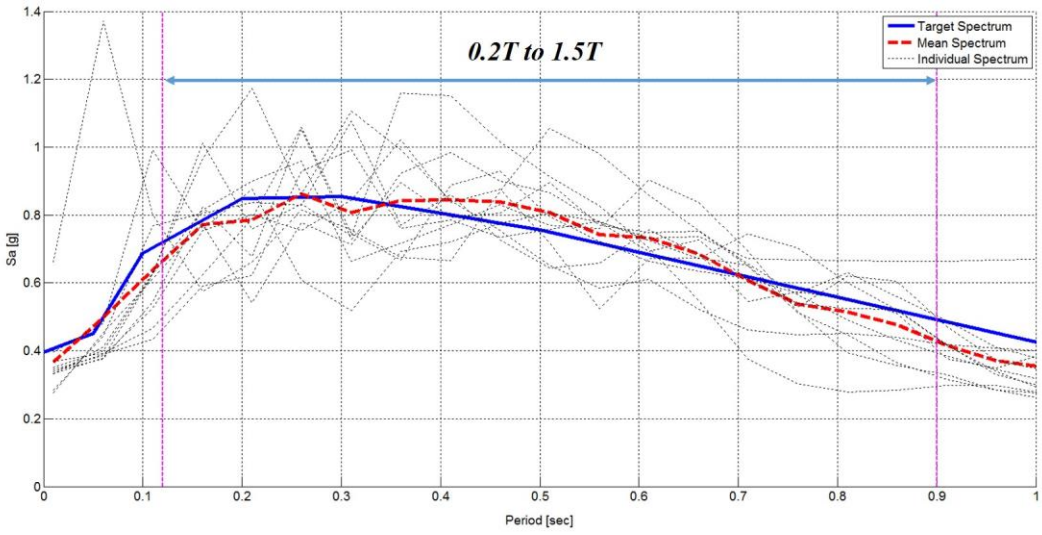

Figure 4.6 Response spectrum of scaled ground motions: 3-story building

Table 4.6 Scaled ground motions: 3-story building

No.	RSN	Year	Event	Station	M (Mw)	V_{s30} (m/s)	Scaling factor
1	15	1952	Kern County	Taft Lincoln School	7.36	385.43	0.71
2	125	1976	Friuli Italy	Tolmezzo	6.5	505.23	1.43
3	164	1979	Imperial Valley	Cerro Prieto	6.53	471.53	1.23
4	285	1980	Irpinia Italy	Bagnoli Irpini	6.9	649.67	1.72
5	292	1980	Irpinia Italy	Sturno (STN)	6.9	382	0.84
6	313	1981	Corinth Greece	Corinth	6.6	361.4	0.97
7	496	1985	Nahanni Canada	Site 2	6.76	605.04	1.02
8	587	1987	New Zealand	Matahina Dam	6.6	551.3	0.94
9	739	1989	Loma Prieta	Anderson Dam	6.93	488.77	0.97
10	741	1989	Loma Prieta	BRAN	6.93	476.54	0.41
11	753	1989	Loma Prieta	Corralitos	6.93	462.24	0.42

4.1.4 Comparison Results

To determine the seismic influence on the structure with the proposed floor system, a comparison was performed with models of 3-story building using an equivalent concrete floor and STWFS. The median responses were obtained from a time history analysis, and the dynamic loads were applied simultaneously to the structure as two acceleration time histories in the N-S and E-W directions. Figure 4.7 and Figure 4.8 present the median peak inter-story drift and floor acceleration while Figure 4.9 and Figure 4.10 display a sample time history and BRB hysteresis, respectively, from one of the earthquake records.

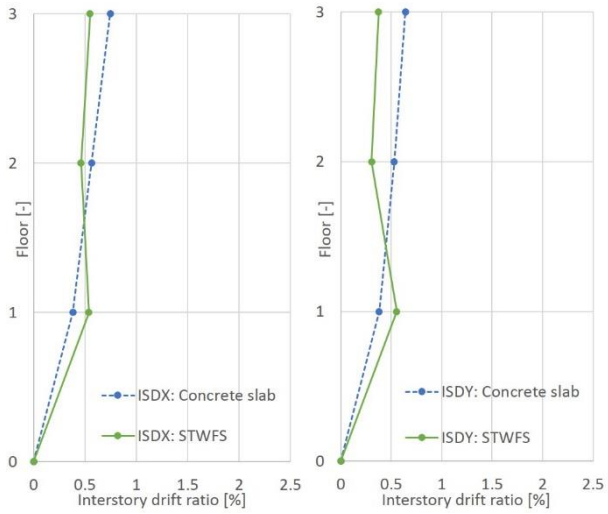

Figure 4.7 Median peak inter-story drift ratio

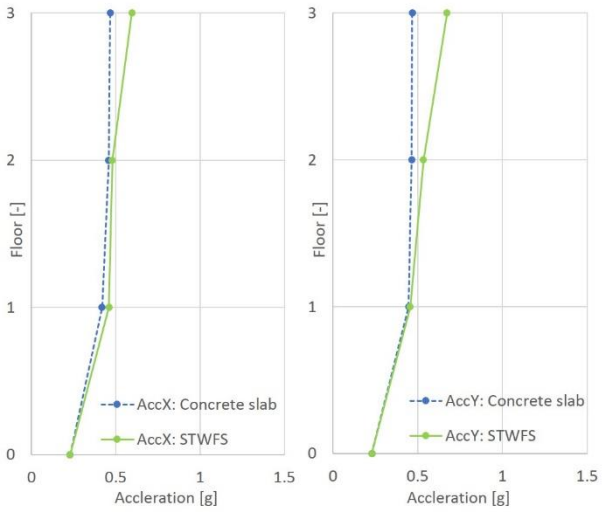

Figure 4.8 Median peak story acceleration

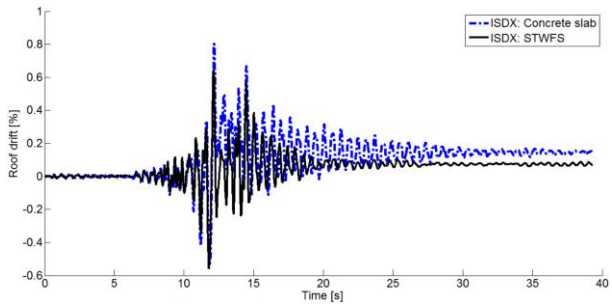

a) Roof drift: X-direction

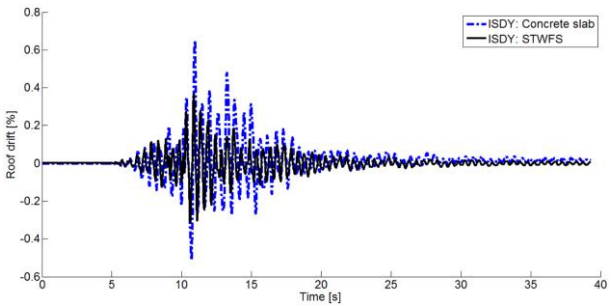

b) Roof drift: Y-direction

Figure 4.9 Roof drift time history curve: 3-story building

According to Figure 4.7, both buildings satisfied the inter-story drift limit of 2.5%. Although, a smaller BRB and structural element sizes are applied to the STWFS structure, there was only a small difference on the 1st floor between the inter-story drifts with equivalent concrete floors. Furthermore, both Figure 4.7 and Figure 4.9 shows that the building with equivalent concrete floors tends to have a larger inter-story drift on its upper floors. Additionally, the construction with concrete slabs has more residual drifts than the one with STWFS.

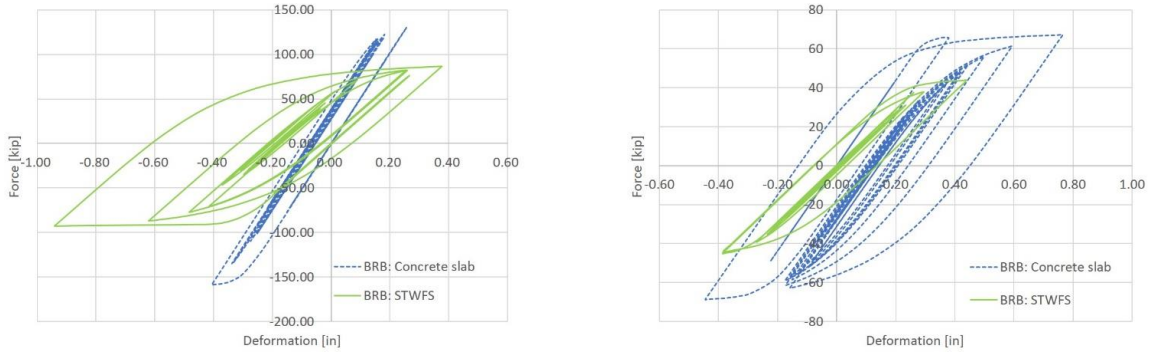

a) BRB behavior: 1st floor

b) BRB behavior: 3rd floor

Figure 4.10 BRB behavior: 3-story building

Figure 4.10 shows the BRB behavior of the 3-story building on 1st and 3rd floors. The BRBs of the structure with the concrete floors yielded, while the one with the STWFS showed less upper floor deformation as shown in Figure 4.10b, which means the building with the proposed steel system is sufficiently strong and the designed floor can efficiently transfer lateral force to the SFRS to resist lateral loads. Comparable results are found for STFS, and will not be discussed in this thesis.

4.2 Application of MSFS in 12-Story BRBF Building

In addition, a 12-story buckling restrained braced frame (BRBF) building using MSFS, was designed and modelled in order to examine the structural and economic efficiencies of the proposed modular steel floor when applied in high-rise buildings. A comparison of the seismic performance models with concrete floor, conventional steel floor, and those with the STWFS, is examined using nonlinear dynamic analysis.

4.2.1 Building Design and Modelling

The structure is designed in the same way as the 3-story building, to be more practical, the floor dimension was expanded to 100 ft in length by 120 ft in width as shown in Figure 4.11.

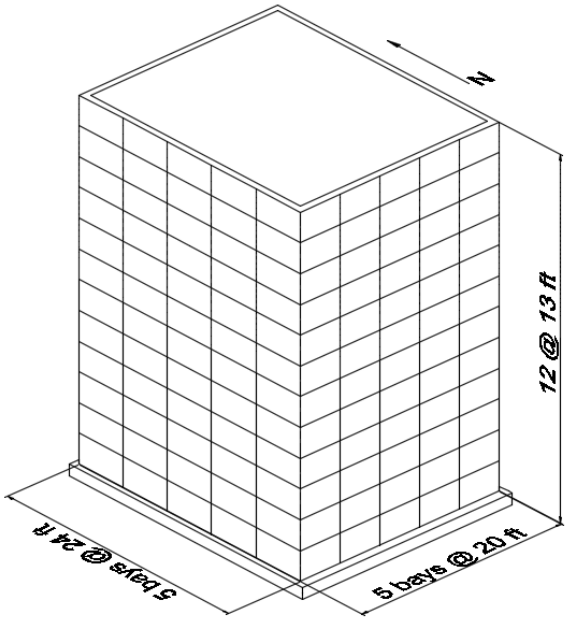

Figure 4.11 An isometric view of the 12-story building

The design details are shown in Table 4.7, Table 4.8 and Table 4.9. Compared with the 3-story building's design, it is obvious that the 12-story building with the proposed floor system requires much less (by around 40% less) total material usage than the one with the equivalent concrete floors, leading to a significant reduction in construction cost. Although the total material usage in the building with STWFS is relatively greater than that of the one with the conventional steel floors, the total depth of the STWFS is only half the depth of the conventional steel floor, which means that, under the same height restrictions, the building with STWFS can provide more usable space and flooring. It can be expected that the higher and larger construction with STWFS will be even more economical and efficient.

Table 4.7 12-Story building design details: equivalent concrete floor

Floor	Seismic column	Gravity column	Structural beam	BRB size ($in.^2$)
1 & 2	Box 24 x 24 x 2	W21 x 111	W21 x 93	8.5
3 & 4	Box 24 x 24 x 1.5	W12 x 96	W21 x 83	8
5 & 6	Box 18 x 18 x 1.5	W14 x 82	W21 x 83	7.5
7 & 8	Box 16 x 16 x 1	W14 x 68	W18 x 71	6.5
9 & 10	Box 12 x 12 x 0.625	W12 x 50	W 18 x 65	5
11 & 12	Box 12 x 12 x 0.375	W12 x 35	W12 x 45	3

Table 4.8 12-Story building design details: conventional steel floor

Floor	Seismic column	Gravity column	Structural beam	BRB size ($in.^2$)
1 & 2	BOX18X18X1.5	W14X68	W14X48	3.5
3 & 4	BOX16X16X1	W14X53	W14X48	3.5
5 & 6	BOX16X16X0.625	W12X45	W14X48	3.5
7 & 8	BOX12X12X0.625	W12X45	W14X48	3.5
9 & 10	BOX12X12X0.375	W12X35	W12X35	2.5
11 & 12	BOX12X12X0.375	W12X35	W12X35	1.5

Table 4.9 12-Story building design details: STWFS

Floor	Seismic column	Gravity column	Structural beam	BRB size ($in.^2$)
1 & 2	Box 18 x 18 x 1.5	W14 x 68	W16 x 57	4.5
3 & 4	Box 18 x 18 x 1	W14 x 68	W16 x 57	4.5
5 & 6	Box 16 x 16 x 1	W18 x 65	W14 x 53	4
7 & 8	Box 14 x 14 x 0.5	W12 x 45	W14 x 48	3.5
9 & 10	Box 12 x 12 x 0.375	W12 x 45	W14 x 48	3.5
11 & 12	Box 12 x 12 x 0.375	W12 x 35	W12 x 35	1.5

Similarly, for the 3-story building, the beam and column elements are designed to be remain elastic, hence, they are modelled using "ElasticBeamColumn" elements, and the base of the columns is pinned. The buckling restrained braces (BRBs) were modelled using truss elements with "Steel02" material. The mass contribution in the building model derives from the structural self-weight, and the 2.0% Rayleigh damping method at the 1st and 3rd mode was used. The equivalent concrete floor systems were simply replaced by rigid diaphragms in the dynamic analysis procedure, while the conventional steel floor systems were modelled with steel decking and planar trusses. To reduce the computational complexity, for the building model with the STWFS, the floor was modelled using the truss element in the OpenSees program. Figure 4.12a shows the prototype building model with its equivalent concrete floor modelled as a rigid diaphragm, while Figure 4.12b illustrates the one with its conventional steel floor, and Figure 4.12c shows the model with the proposed modular steel floor system.

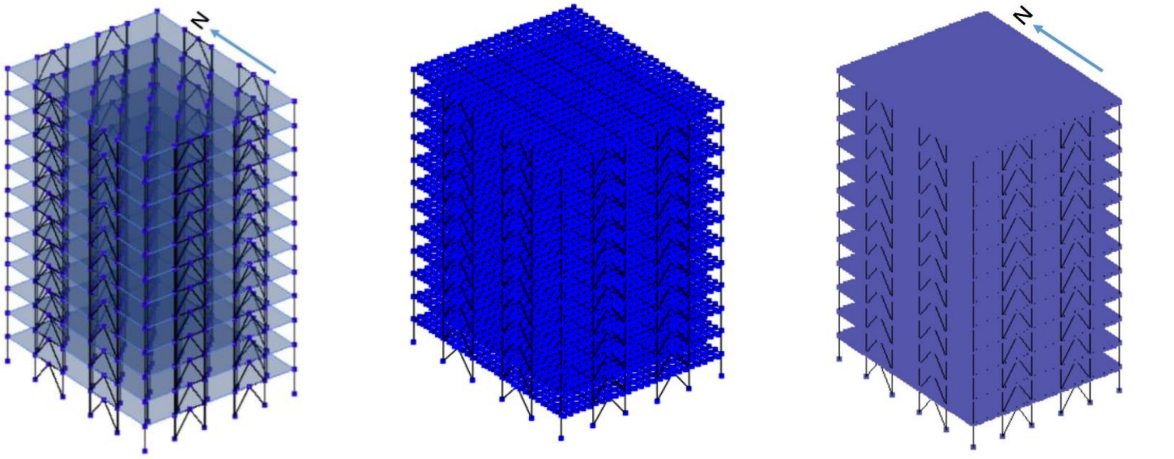

a) Isometric view (equivalent concrete floor)

b) Isometric view (conventional steel floor)

c) Isometric view (STWFS)

Figure 4.12 Prototype 12-story building model

4.2.2 Ground Motion Scaling

To determine the difference between the structures, a comparison was conducted with the 12-story building. Table 4.10 shows the comparison of the modal periods. The designed building with the proposed floor system has the smallest period. In addition, the period of the structure with STWFS was closer to the one with the equivalent concrete floors, mainly due to larger elements and BRB sizes being employed in the structure with concrete slabs. If the same conditions applied, the structural period for the proposed floor system will decrease significant. A significant reduction was found in the building with the STWFS, where the structure suffered 40% fewer base shears than the one with concrete floors. This is mainly because of the smaller self-weight of the structure with STWFS.

Table 4.10 Structural period: 12-story building

Floor system	Period (sec)		
	Mode 1	Mode 2	Mode 3
Equivalent concrete floor	2.20	2.06	1.22
Conventional steel floor	2.40	2.27	1.51
STWFS	2.18	2.05	1.33

In this case study, the ground motion selection was based on the guideline of the NBCC 2015 Commentary. For South-West British Columbia, where shallow crustal, subcrustal and subduction earthquakes are expected. Thus, the 3 suites involve different tectonic sources, and each suite including 11 ground motions are selected and amplitude scaled to match the target spectrum. This scaling procedure is consistent with the procedure presented in the NBCC 2015 Commentary. The ground motions are amplitude scaled at between 0.15T and 2.0T, where T is the fundamental period of the structure. In this case, the fundamental period is around 2.20 seconds as shown in Table 4.10. The scaling factor is limited between 0.25 and 4.

For location where earthquakes from different tectonic sources contribute to the hazard, the ground motion suites should be selected to cover appropriate segments of the period range, TR, and each of the period segments should constitute a scenario-specific period range, TRS. For a building located in Vancouver, the TRS and the response spectrum of scaled ground motions is presented in Figure 4.13. Details of ground motions are shown in Table 4.11, Table 4.12 and Table 4.13. For each suite, 11 ground motion records are selected and scaled for different earthquake sources contributing to the hazard, and a common scaling factor for each suite is calculated to ensure that

the mean spectrum does not fall below the scenario-specific target spectrum by greater than 10% within the period range of interest TRS.

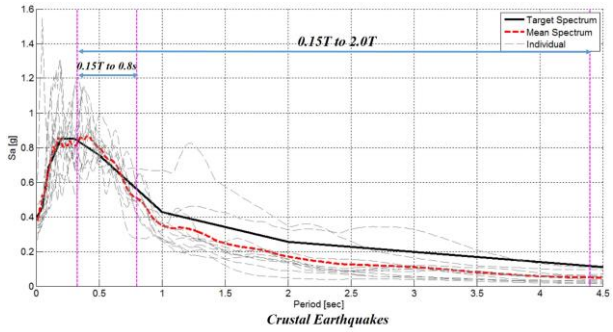

a) The response spectrum of scaled crustal ground motion

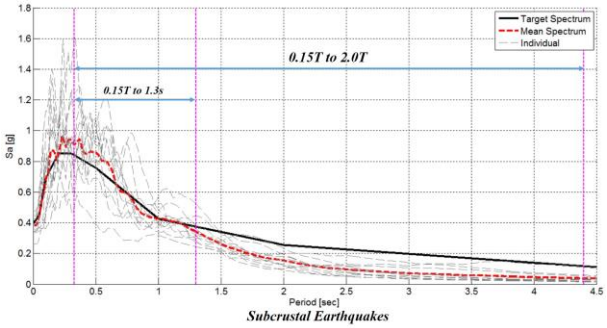

b) The response spectrum of scaled subcrustal ground motion

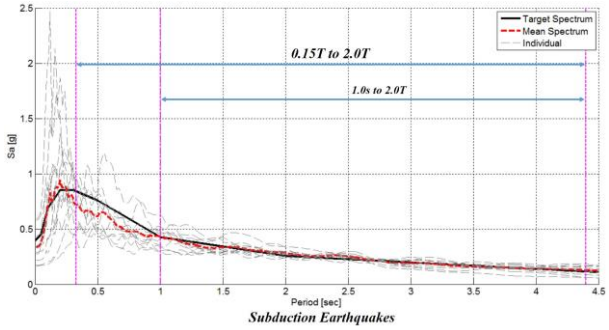

c) The response spectrum of scaled subduction ground motion

Figure 4.13 Ground motion scaling

Table 4.11 Scaled crustal ground motions: 12-story building

No.	RSN	Year	Event	M (Mw)	V_{s30} (m/s)	D5-95 (sec)	Scaling factor	Final scaling factor
1	15	1952	Kern County	7.4	385.43	30.3	1.27	1.30
2	139	1978	Tabas Iran	7.3	471.53	11.3	2.05	2.10
3	164	1979	Imperial Valley	6.5	471.53	11.3	1.85	1.90
4	285	1980	Irpinia Italy	6.9	649.67	36.4	2.42	2.48
5	292	1980	Irpinia Italy	6.9	382.00	19.6	1.31	1.34
6	313	1981	Corinth Greece	6.6	361.40	15.2	1.39	1.42
7	496	1985	Nahanni Canada	6.8	605.04	15.4	1.33	1.36
8	587	1987	New Zealand	6.6	551.30	7.3	1.26	1.29
9	739	1989	Loma Prieta	6.9	488.77	8.4	1.35	1.38
10	741	1989	Loma Prieta	6.9	476.54	10.9	0.55	0.56
11	753	1989	Loma Prieta	6.9	462.24	9.8	0.61	0.62
Suite scaling factor				1.02				

Table 4.12 Scaled subcrustal ground motions: 12-story building

No.	Year	Event	Station	M (Mw)	V_{s30} (m/s)	D5-95 (sec)	Scaling factor	Final scaling factor
1	2001	Geiyo	Kiknet Station EHMH005	6.4	501.42	13.1	3.00	3.27
2	2001	Geiyo	Kiknet Station EHMH008	6.4	560.58	9.5	1.35	1.47
3	2001	Geiyo	Kiknet Station YMG018	6.4	499.35	9.1	1.28	1.39
4	1997	Michoacan	UNR Station UNIO	7.3	403.41	21.5	4.00	4.35
5	1997	Michoacan	UNR Station VILE	7.3	627.95	15.8	4.00	4.35
6	2005	Miyagi_Oki	KNET Station MYG006	7.2	205.38	48.6	2.41	2.62
7	2005	Miyagi_Oki	KNET Station MYG010	7.2	204.82	34.4	1.85	2.01
8	2001	Nisqually	USGS station 7010	6.8	361.00	24.1	2.34	2.55
9	2001	Nisqually	USGS station 7032	6.8	327.66	18.7	2.11	2.29
10	2001	Nisqually	USGS station 7030	6.8	347.17	17.3	2.04	2.22
11	1949	Olympia OLY0A	Olympia Hwy Test Lab	6.9	485.51	23.7	1.80	1.96
Suite scaling factor				1.09				

Table 4.13 Scaled subduction ground motions: 12-story building

No.	Year	Event	Station	M (Mw)	V_{s30} (m/s)	D5-95 (sec)	Scaling factor	Final scaling factor
1	1952	Hokkaido	Station HKD087	8.0	189	40.15	2.52	2.52
2	1952	Hokkaido	Station HKD094	8.0	381.1	65.34	2.45	2.45
3	1952	Hokkaido	Station HKD105	8.0	567.6	33.34	1.23	1.23
4	1952	Hokkaido	Station HKD127	8.0	602.51	44.59	3.25	3.25
5	1952	Hokkaido	Station HKD182	8.0	250.58	385.62	3.55	3.55
6	2010	Maule	Stgolaflorida	8.8	685.00	41.6	2.72	2.72
7	1985	Michoacan	UNR Station AZIH	8.0	461.97	19.8	2.73	2.73
8	2011	Tohoku	KNET Station CHB022	9.0	378.84	111.16	3.04	3.04
9	2011	Tohoku	KNET Station KNG007	9.0	488.45	116.17	3.16	3.16
10	2011	Tohoku	KNET Station SIT009	9.0	392.4	76.6	3.18	3.18
11	2011	Tohoku	KNET Station TKY006	9.0	411.33	101.72	3.14	3.14
Suite scaling factor				1.00				

4.2.3 Comparison Results

To determine the seismic influence of the floors, the median responses are obtained from time history analysis, and the dynamic loads were applied simultaneously to the structure as two acceleration time histories in the N-S and E-W directions. Following the same procedure of dynamic analysis, the comparison results are obtained. Figure 4.14 presents the median peak inter-story drift and Figure 4.15 shows the floor acceleration while Figure 4.16 shows a sample time history from one of the earthquake records.

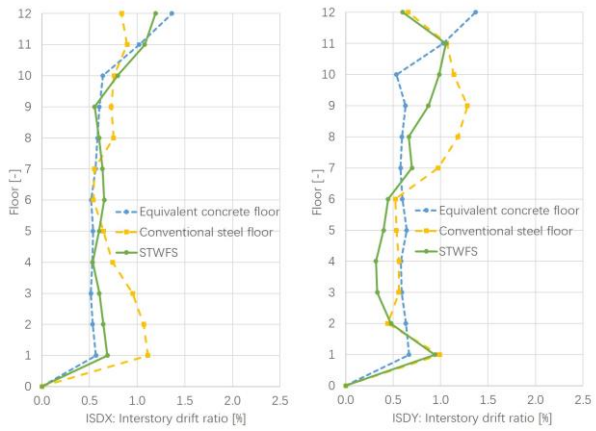

Figure 4.14 Median peak inter-story drift ratio

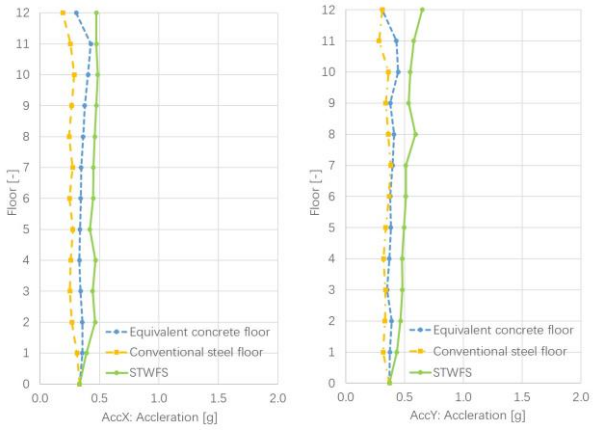

Figure 4.15 Median peak story acceleration

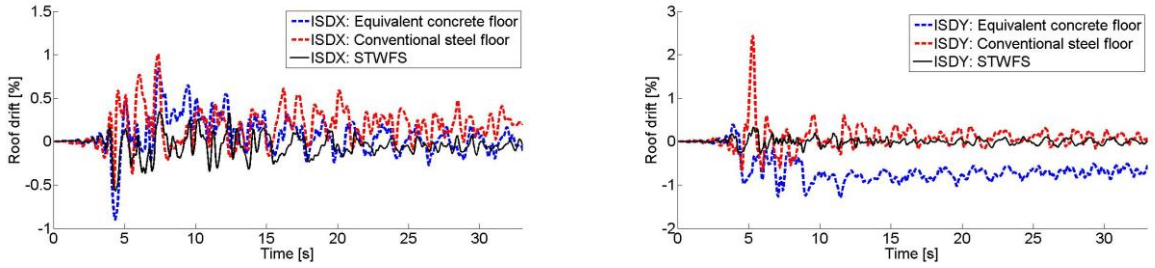

a) Roof drift: X-direction

b) Roof drift: Y-direction

Figure 4.16 Roof drift time history curve: 12-story building

The seismic performance of the building with the proposed floor system is very comparable with the ones of equivalent concrete and conventional steel flooring. Based on Figure 4.14, all the

buildings satisfied the inter-story drift limit of 2.5%, and the similar behavior of peak accelerations is also shown in Figure 4.15. Overall, the structural behavior or STWFS is good in both directions. Moreover, the inter-story drift of roof level is shown to be smaller and less residuary in the building with the STWFS as shown in Figure 4.16.

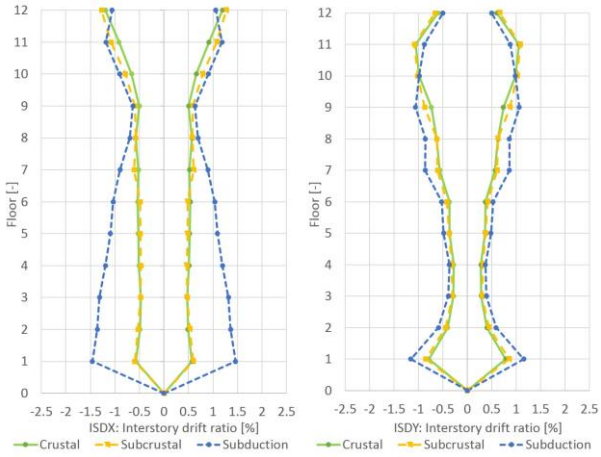

Figure 4.17. Median inter-story drift responses for different seismic sources

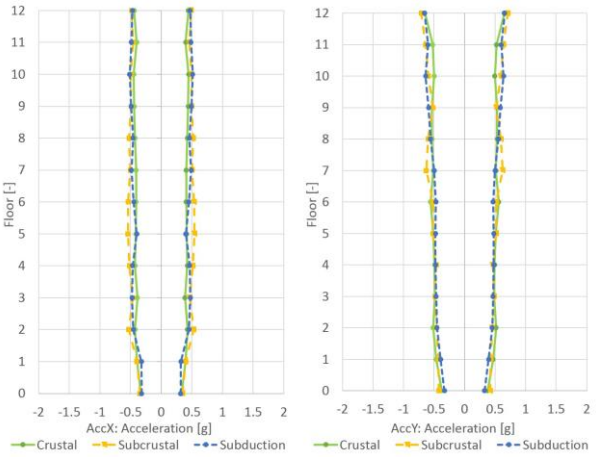

Figure 4.18. Median inter-story drift responses for different seismic sources

As shown in Figure 4.17 and Figure 4.18, structural behavior is similar for both crustal and subcrustal earthquakes, although their intensities are different; this is mainly because they are selected and scaled according to the same hazard level, and overlapped within the TRS based on the requirements in the NBCC 2015 Commentary. Figure 4.17 shows a comparison of median peak inter-story drift responses for crustal, subcrustal and subduction earthquakes, and for all tectonic sources, the peak inter-story drift ratio is no greater than 1.5%, implying that the adequate seismic performance can be achieved by the proposed STWFS. In addition, it is found that larger seismic demands are caused by subduction ground motions, due to their long-period and long-duration excitations. In the structural design, different BRB sizes are used for each building so that

each might achieve the same design target. The structure with STWFS has a greater deformation, mostly due to the application of smaller structural elements and BRB sizes. However, the upper level of the structure with the STWFS was less deformed. It was also found that the BRB behavior of most floor levels with the proposed floors within the building was satisfied, and the comparable results are found with STFS, implying that the building with the proposed floor was sufficiently strong and that the designed MSFS can efficiently transfer lateral forces to the SFRS to resist lateral loads. In addition, the total material usage comparison of structure with equivalent concrete flooring, conventional steel floor and STWFS was conducted. It is observed that the total material usage decreases significantly with increments in story height and dimensions. In other words, the proposed MSFS is economical, especially for high-rise buildings.

4.3 Simplified Model for Seismic Analysis

To reduce the computational complexity, a simplified model using rigid diaphragm was built. The comparison of the model with MSFS and rigid diaphragm was conducted to verify the feasibility of the simplified model.

4.3.1 Simplified Model of BRBF Building with MSFS

For the 12-story buckling restrained braced frame (BRBF) building model with proposed MSFS, numerous nodes and elements were modelled, and the proposed floor was modelled using the truss elements in OpenSees to reduce computational complexity. However, the performance of computational efficiency was not satisfied. Therefore, to reduce the computational complexity and increase its efficiency, a simplified model for a 12-story building using rigid diaphragm was

modelled and compared. The design of the structure was the identical to the one with proposed floor, and the ground motions are applied to the structure in the N-S and E-W directions.

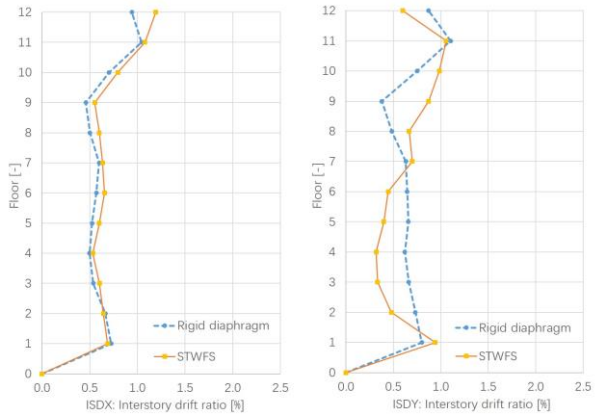

Figure 4.19 Median peak inter-story drift ratio

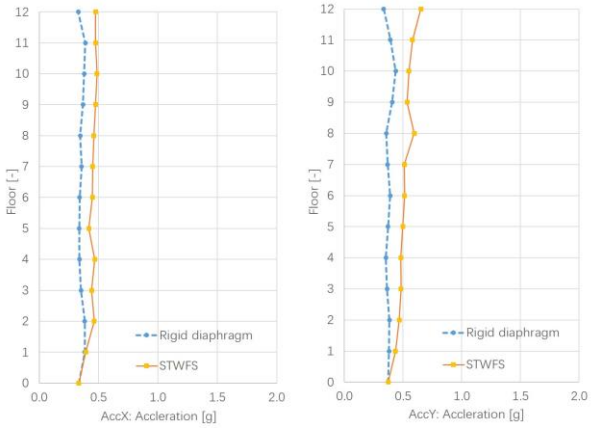

Figure 4.20 Median peak story acceleration

Figure 4.19 presents the median peak inter-story drift and Figure 4.20 shows the floor acceleration. As shown in the figures, the structural behaviors were quite close. For inter-story drift, the performances in the X-direction are almost the same, and the overall behavior is similar. Although there is difference in the Y-direction, the structural behaviors are subjected to same trend. In this case, the model can be simplified to that of a rigid diaphragm for seismic analysis.

4.3.2 Simplified Model of BRKBTMF Building with MSFS

The prototype building was a 4-story building with buckling restrained knee braced truss moment frame (BRKBTMF) and proposed MSFS, consisted of 5 bays of frames. The building dimensions were 100 ft. by 120 ft. with structural height at 53 ft., and the story height was 14 ft. (11.5 ft. clear height) for the 1st floor and 13 ft. (10.5 ft. clear height) for the upper floors. The BRKBTMF design using PBPD method was employed, based on the angel and span as illustrated in Figure

4.21. For frame 1 (along the length), an angle of 63° BRB inclination was selected, while for Frame 2, 63° BRB inclination was decided.

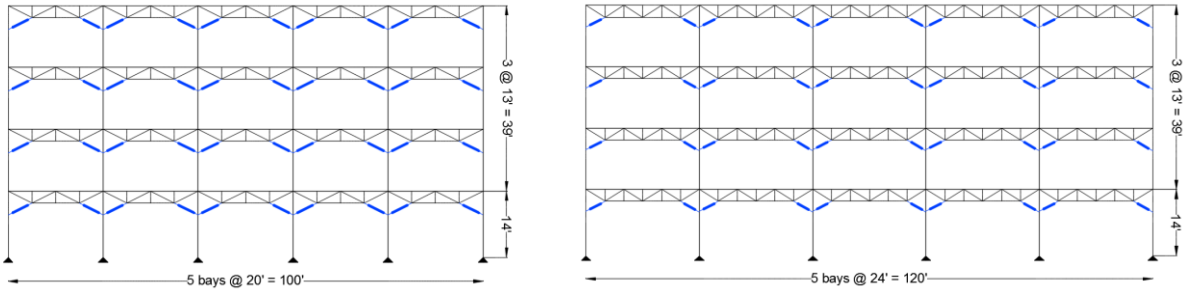

a) Frame 1 (along the length) b) Frame 2 (along the width)

Figure 4.21 The prototype building description

The prototype building was designed based on performance based plastic design (PBPD) method (Goel, Chao, 2008), and the prototype building was designed to satisfy two performing objectives, drift ratio less than 2.5% under 10/50 hazard level (2/3 MCE level), and less than 3.5% under 2/50 hazard level (MCE level). The yield drift is selected as 0.75%, and the structural period is estimated as 1 second. Table 4.14 and Table 4.15 show the final design of structural components and frame.

Table 4.14 Structural components design

Floor	Exterior column	Interior column	Gravity column	BRB size ($in.^2$)
1	W30X116	W30X173	W12X40	1
2	W30X116	W30X173	W12X40	1.5
3	W30X261	W30X292	W12X65	1.5
4	W30X261	W30X292	W12X65	2

Table 4.15 Frame design

Floor	Frame 1				Frame 2			
	Top chord	Bottom chord	Vertical chord	Diagonal chord	Top chord	Bottom chord	Vertical chord	Diagonal chord
4	W12X14	2L2X2X3/8	2L2X2X1/8	2L3X3X1/4	W12X58	2L3X3X1/4	2L2X2X1/8	2L3X3X1/4
3	W12X14	2L3X3X1/4	2L2X2X1/8	2L3X3X5/16	W12X58	2L3X3X1/4	2L2X2X1/8	2L3X3X5/16
2	W12X14	2L3X3X1/4	2L2X2X1/8	2L3X3X/3/8	W12X58	2L5X5X7/8	2L2X2X1/8	2L5X5X7/8
1	W12X14	2L3X3X5/16	2L2X2X1/8	2L3X3X7/16	W12X58	2L5X5X7/8	2L2X2X1/8	2L5X5X7/8

The structural performances under 10/50 hazard level (DBE level) and 2/50 hazard level (MCE level) were evaluated, and compared with the model using rigid diaphragm. Figure 4.22 shows the peak median inter-story drift ratio, and Figure 4.23 presents the peak median story acceleration.

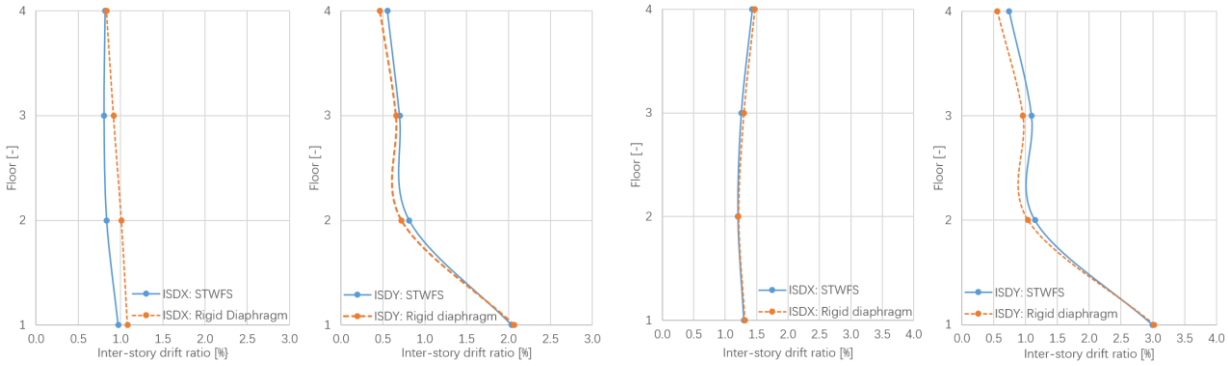

a) 10/50 hazard level b) 2/50 hazard level

Figure 4.22 Peak median inter-story drift ratio

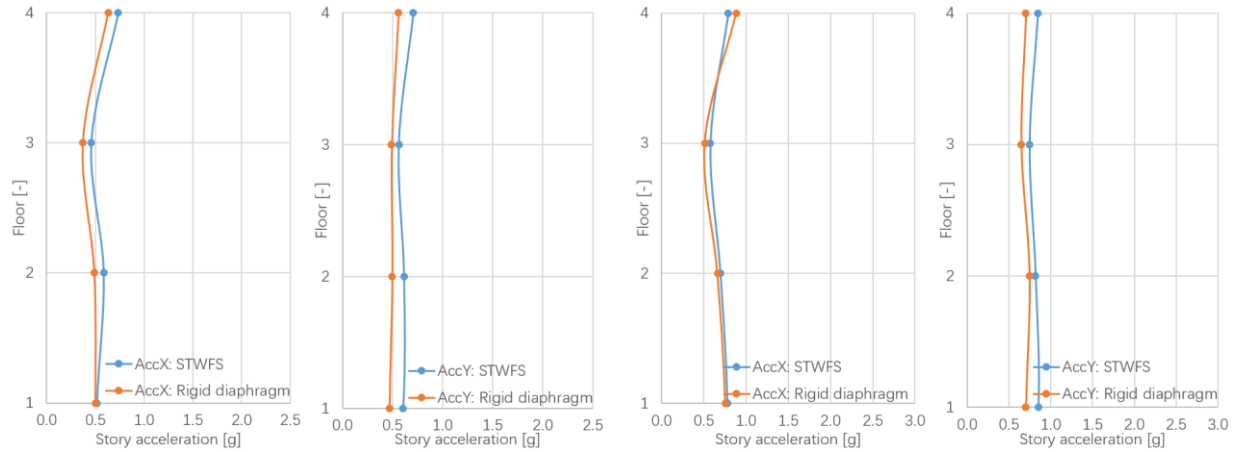

a) 10/50 hazard level b) 2/50 hazard level

Figure 4.23 Peak median story acceleration

Overall, the structural behaviors of model with proposed STWFS and the one using rigid diaphragm are similar, and the comparable results are found with the model using STFS. The results indicate that the proposed MSFS can transfer the seismic force efficiently. Moreover, the building with MSFS can be analyzed utilizes simplified model using rigid diaphragm. However, further research is required to validate the simplified model in various structural systems and applications.

Chapter 5: Summary and Conclusions

In this study, an economical and innovative modular steel truss system (MSTS) is introduced and developed for modular constructions. The MSTS consists of modular steel floor system (MSFS) and modular buckling restrained braced truss moment frame (MBRBTMF). Two types of MSFS, including the space truss floor system (STFS) and space truss with w-beam floor system (STWFS), were designed and optimized. The specially designed space trusses are utilized in the floor system to provide sufficient stiffness to support gravity, eliminate vertical deflection and transfer lateral force without significantly increasing floor depth. The MBRBTMF was designed following the performance based plastic design (PBPD) method. To promote the use of the introduced system, the design and optimization procedure was presented.

The optimal design of the STFS is a structural system with a 15-inch spacing along its length and 19-inch spacing along its width. The STFS consists of round HSS 3 x 0.250 as top and bottom chords, and round HSS 2.375 x 0.154 as web trusses. The total depth of the proposed floor system is 11 inches, and a 5-inch clear spacing between the top and bottom chord is provided. In addition, the optimization results for STWFS showed that an optimal configuration of a 6-inch height (centre line of elements) was the structural system, with 30-inch spacing along its length and 12-inch spacing along its width. The proposed floor system consists of W12X58 as the structural beam, top and bottom chords with 2-inch external diameters, 1.4-inch internal diameters and 1.6-square-inch areas, as well as the 0.5-square-inch area web trusses. The total floor depth is 8 inches, which is very comparable with the conventional concrete slabs, and this creates a 4-inch gap to allow mechanical, electrical and plumbing (MEP) systems to pass through. To be more practical, the

floor system using the available section is also checked, and these results show that the optimization results are efficient and reliable.

The information on structure and site condition were introduced, and a prototype 4-story MSTS building was designed and modelled. The MBRBTMFS, as the seismic force resisting frame, was designed following the PBPD procedure. The buckling restrained braces (BRBs) were selected as the structural fuses and energy dissipation devices, where the rest structural components were designed to remain elastic. The structure was modelled in an advanced finite element analysis software OpenSees. The hazard analysis was conducted, and ground motions were selected and amplitude scaled to match the target spectrum. The results showed that the MBRBTMF is efficient and the seismic performance of the prototype building is excellent. The structures with conventional SFRS were also designed, and it was found that the building with the proposed floor system, requires less material usage for both its structural elements and BRBs, which means less construction costs. In addition, more usable space height can be provided by the designed floor, and it can be expected that higher and larger construction with the proposed floors would be even more economical and efficient. The seismic performances of various floors were studied, and the results of the analyses reveal that the structure with the proposed floor has satisfied seismic performance. This implies that the building with the designed STFS is sufficiently strong and that the proposed floor can efficient transfer lateral force to the different SFRSs to resist lateral loads. In conclusion, the proposed MSTS shows a promising performance for practical applications.

Bibliography

Allen, D., & Murray, T. (1993). Design criterion for vibrations due to walking. *Engineering Journal, 30*(4), 117-129.

Allen, D. E., & Pernica, G. (1998). *Control of floor vibration*: Institute for Research in Construction, National Research Council of Canada.

American Concrete Institute. (2015). ACI 302.1R-15: Guide for Concrete Floor and Slab Construction.

American Institute of Steel Construction. (2013). AISC Shapes Database V14.1: American Institute of Steel Construction.

Auer, B. J. (2005). *Size and shape optimization of frame and truss structures through evolutionary methods*.

Black, C. J., Makris, N., & Aiken, I. D. (2004). Component testing, seismic evaluation and characterization of buckling-restrained braces. *Journal of Structural Engineering, 130*(6), 880-894.

Broad Group. (2012). T30A Tower Hotel.

Canadian Institute of Steel Construction. (2014). CSA-S16-14: design of steel structures *Canadian Standards Association, Mississauga, Ontario, Canada*.

Chao, S.-H., & Goel, S. C. (2006a). Performance-based seismic design of eccentrically braced frames using target drift and yield mechanism as performance criteria. *ENGINEERING JOURNAL-AMERICAN INSTITUTE OF STEEL CONSTRUCTION INC, 43*(3), 173-200.

Chao, S.-H., & Goel, S. C. (2006b). *A seismic design method for steel concentric braced frames for enhanced performance.* Paper presented at the 4th International Conference on Earthquake Engineering.

Chao, S.-H., Goel, S. C., & Lee, S.-S. (2007). A seismic design lateral force distribution based on inelastic state of structures. *Earthquake Spectra, 23*(3), 547-569.

Clark, P., Aiken, I., Kasai, K., Ko, E., & Kimura, I. (1999). *Design procedures for buildings incorporating hysteretic damping devices.* Paper presented at the Proceedings 68th annual convention.

Cobiax®. (2016). Cobiax® Lightweight concrete slabs. from www.cobiax.com/home

Construction, A. I. o. S. (2003). AISC/CISC Steel Design Guide Series No. 11: Floor Vibrations Due to Human Activity.

Council on Tall Buildings and Urban Habitat, C. (2017). The Global Tall Building Database of the CTBUH. from http://www.skyscrapercenter.com/

Dewit, N. (2012). A Composite Structural Steel and Prestressed Concrete Beam for Building Floor Systems.

Di Mauro, M., McLean, L., Guha-Sapir, D., Wirtz, A., Eichner, J., & Dilley, M. (2013). *Risk Information Issues and Needs: An Overview.* Paper presented at the Geneva, Switzerland. http://www. wmo. int/pages/prog/drr/projects/Thematic/HazardRisk/2013-10-TC-Prog-FP-Meeting/documents/Doc.

Girder-Slab Technologies, L. (2016). The GIRDER-SLAB® System Design Guide v3.3. from www.girder-slab.com/

Girhammar, U. A., & Pajari, M. (2008). Tests and analysis on shear strength of composite slabs of hollow core units and concrete topping. *Construction and Building Materials, 22*(8), 1708-1722.

Goel, S. C., & Chao, S.-H. (2008). *Performance-based plastic design: earthquake-resistant steel structures*: International Code Council.

Goel, S. C., & Leelataviwat, S. (1998). Seismic design by plastic method. *Engineering Structures, 20*(4-6), 465-471.

Goel, S. C., Liao, W. C., Reza Bayat, M., & Chao, S. H. (2010). Performance‐based plastic design (PBPD) method for earthquake‐resistant structures: an overview. *The structural design of tall and special buildings, 19*(1‐2), 115-137.

Hamburger, R. O., Krawinkler, H., Malley, J. O., & Adan Scott, M. (2009). Seismic design of steel special moment frames. *NEHRP Seismic Design Technical Brief*(2).

Hegger, J., Roggendorf, T., & Kerkeni, N. (2009). Shear capacity of prestressed hollow core slabs in slim floor constructions. *Engineering Structures, 31*(2), 551-559.

Henin, E., Morcous, G., & Tadros, M. K. (2012). Shallow Flat Soffit Precast Concrete Floor System. *Practice Periodical on Structural Design and Construction, 18*(2), 101-110.

Hickory Building Innovation. (2010). Little Hero.

John, H. (1992). Holland, Adaptation in Natural and Artificial Systems: An Introductory Analysis with Applications to Biology, Control and Artificial Intelligence: MIT Press, Cambridge, MA.

Kim, T., Whittaker, A., Gilani, A., Bertero, V., & Takhirov, S. (2002). Experimental evaluation of plate-reinforced steel moment-resisting connections. *Journal of Structural Engineering, 128*(4), 483-491.

Lawson, R. M., Ogden, R. G., & Bergin, R. (2011). Application of modular construction in high-rise buildings. *Journal of architectural engineering, 18*(2), 148-154.

Lawson, R. M., & Richards, J. (2010). Modular design for high-rise buildings. *Proceedings of the Institution of Civil Engineers-Structures and Buildings, 163*(3), 151-164.

Lee, D.-G., Ahn, S.-K., & Kim, D.-K. (2005). Efficient seismic analysis of building structure including floor slab. *Engineering Structures, 27*(5), 675-684.

Leelataviwat, S., Goel, S., Rai, D., Liao, W., Bayat, M., Chao, S., & Stojadinovic, B. (2012). *A Collaborative Research Program on Performance-Based Design of Innovative Structural Systems for Earthquake Resistance: An Overview*. Paper presented at the 15th World Conference on Earthquake Engineering (15 WCEE), Lisbon, Portugal. 本人為通訊作者.

Marais, C. C. (2009). *Design adjustment factors and the economical application of concrete flat-slabs with internal spherical voids in South Africa.* University of Pretoria.

Mardle, S., & Pascoe, S. (1999). An overview of genetic algorithms for the solution of optimisation problems. *Computers in Higher Education Economics Review, 13*(1), 16-20.

Metal Dek Group & Diversakore. (2010). Vibration Performance of Composite Steel Frame-and-Dek Floor System. from http://www.diversakore.com/

Morcous, G., & Tadros, M. (2014). Shallow flat soffit precast concrete floor system: Google Patents.

National Research Council of Canada. (2015). National Building Code of Canada. Ottawa, ON.

Natural Resources Canada. (2015). Natural Resources Canada, .

Pacific Earthquake Engineering Research (PEER) Center. (2005). OpenSees command language manual. *264*.

Pacific Earthquake Engineering Research Center, P. (2010). Ground motion database. from Univ. of California, Berkeley

Peikko Group®. (2014). DELTABEAM® Slim Floor Structures, Technical Manual. from www.peikko.com/

Popov, E. P., & Engelhardt, M. D. (1988). Seismic eccentrically braced frames. *Journal of Constructional Steel Research, 10*, 321-354.

Ricles, J. M., Mao, C., Lu, L.-W., & Fisher, J. W. (2002). Inelastic cyclic testing of welded unreinforced moment connections. *Journal of Structural Engineering, 128*(4), 429-440.

Ruiyi, S., Liangjin, G., & Zijie, F. (2009). *Truss topology optimization using genetic algorithm with individual identification.* Paper presented at the Proceedings of the world congress on engineering.

Smith, A., Hicks, S., & Devine, P. (2007). SCI P354: Design of Floors for Vibration: A New Approach: The Steel Construction Institute, Silwood Park, Ascot, Berkshire, UK.

The Mathworks. (1998). Guide, MATLAB User's. *Inc., Natick, MA, 5*, 333.

Timler, P. A., & Kulak, G. L. (1983). Experimental study of steel plate shear walls.

Tsai, K.-C., & Popov, E. P. (1990). Cyclic behavior of end-plate moment connections. *Journal of Structural Engineering, 116*(11), 2917-2930.

U.S. Geological Survey, U. (2017). U.S. Geological Survey, USGS.

Uang, C.-M., & Fan, C.-C. (2001). Cyclic stability criteria for steel moment connections with reduced beam section. *Journal of Structural Engineering, 127*(9), 1021-1027.

Yang, T., Li, Y., & Goel, S. C. (2015). Seismic Performance Evaluation of Long-Span Conventional Moment Frames and Buckling-Restrained Knee-Braced Truss Moment Frames. *Journal of Structural Engineering, 142*(1), 04015081.

Yang, T., Li, Y., & Leelataviwat, S. (2013). Performance-based design and optimization of buckling restrained knee braced truss moment frame. *Journal of Performance of Constructed Facilities, 28*(6), A4014007.

Appendix

Appendix A

Roof Drift ratio of Prototype 12-story Building

A 12-story prototype building located in Vancouver is designed, and the nonlinear dynamic analysis is conducted using the ground motions presented in Chapter 6. The figures in this appendix are the roof drift ratio time histories of the building subjected to maximum considered earthquake (MCE) shaking intensities.

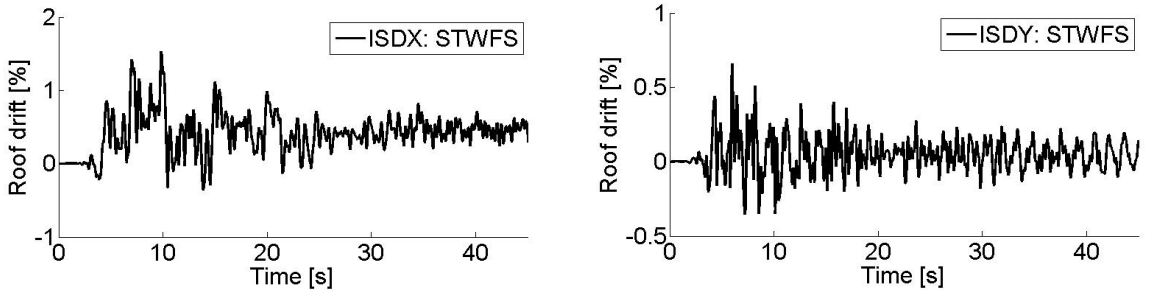

a) Roof drift ratio_RSN15

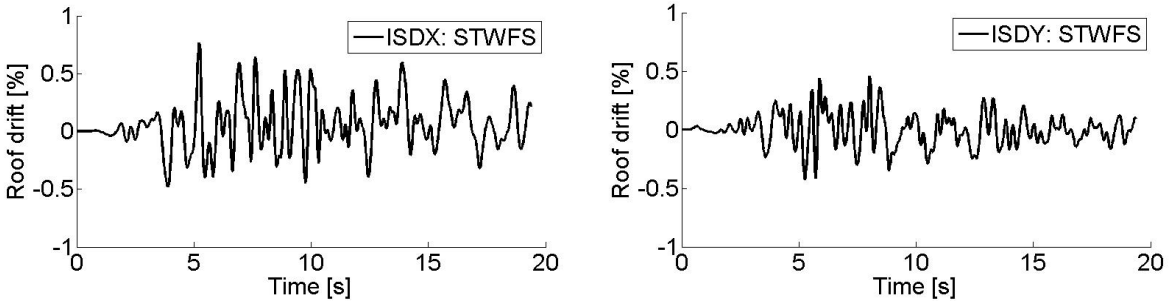

b) Roof drift ratio_RSN139

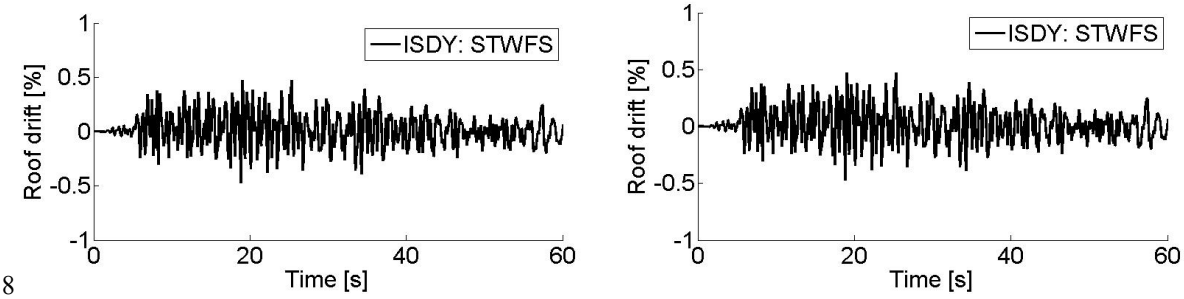

8

c) Roof drift ratio_RSN164

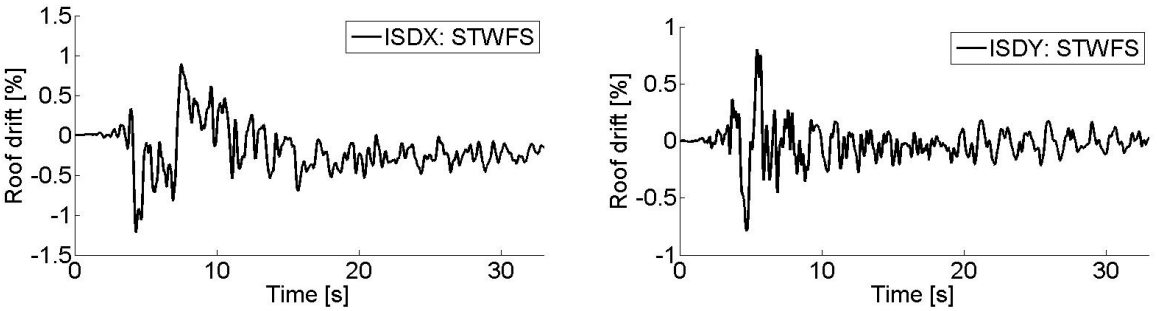

d) Roof drift ratio_RSN285

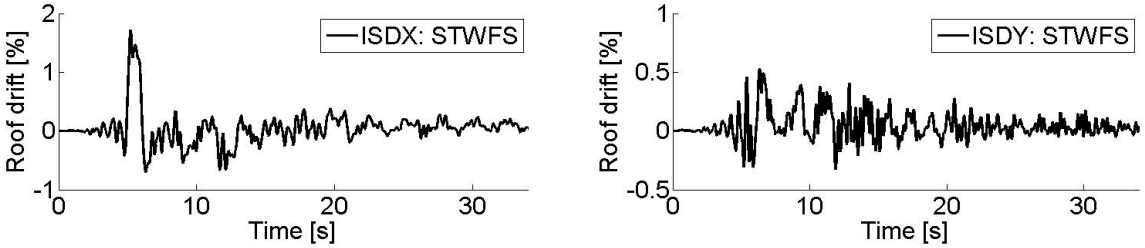

e) Roof drift ratio_RSN292

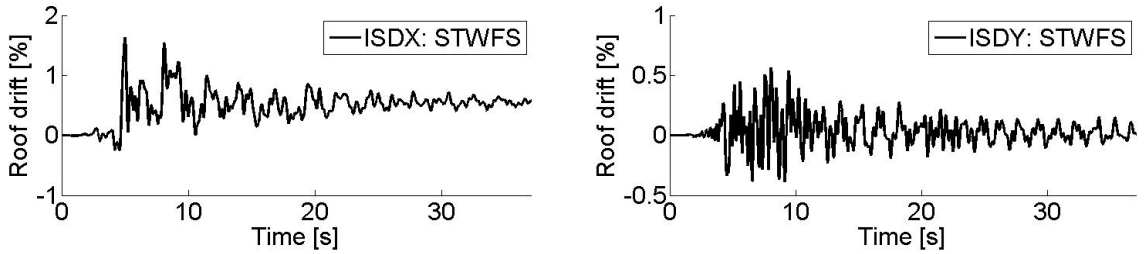

f) Roof drift ratio_RSN313

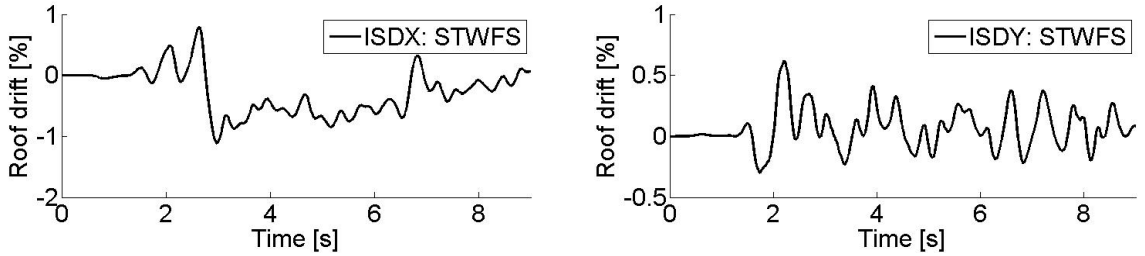

g) Roof drift ratio_RSN496

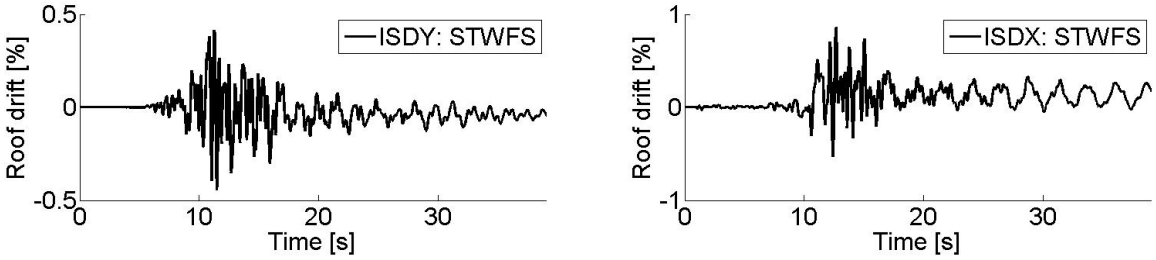

h) Roof drift ratio_RSN587

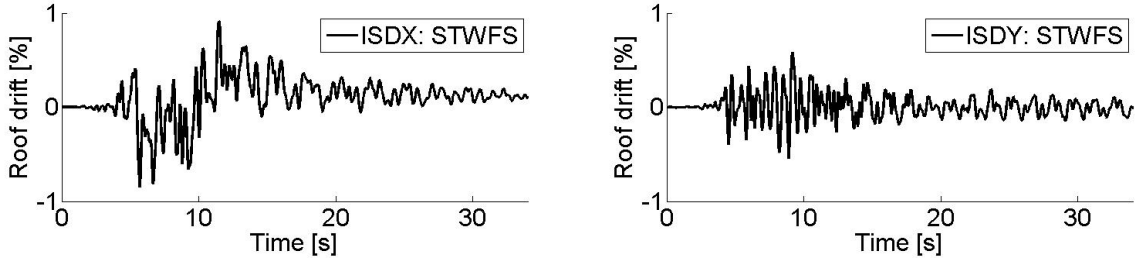

i) Roof drift ratio_RSN739

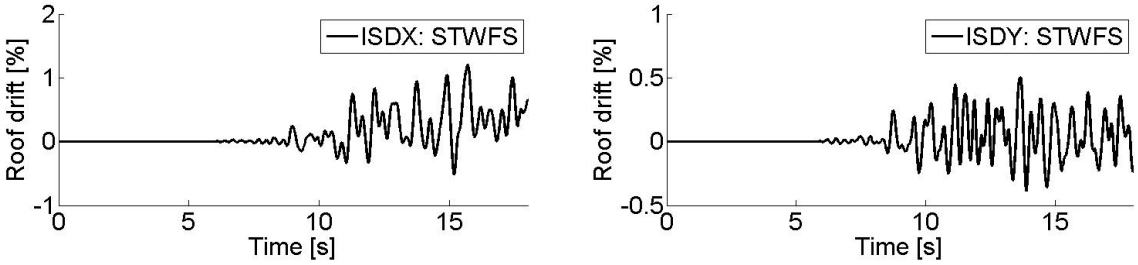

j) Roof drift ratio_RSN741

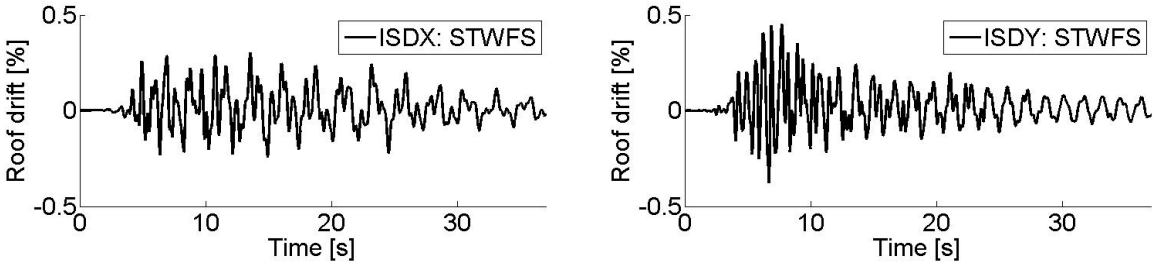

k) Roof drift ratio_RSN755

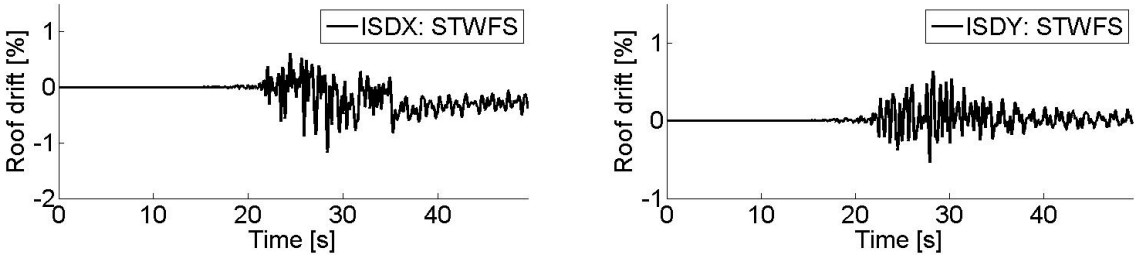

a) Roof drift ratio_ Geiyo_EHM005

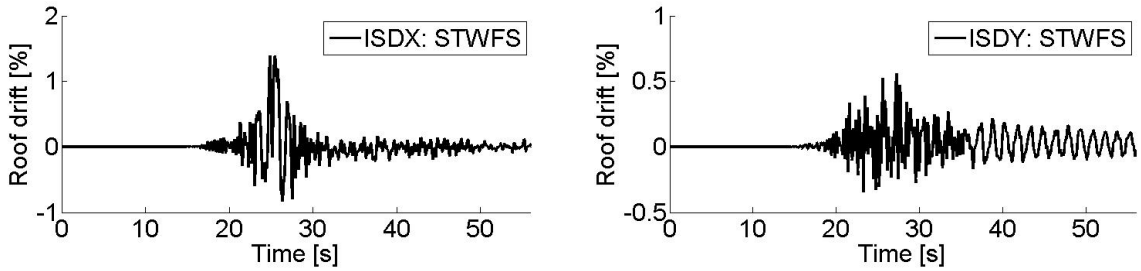

b) Roof drift ratio_ Geiyo_EHM008

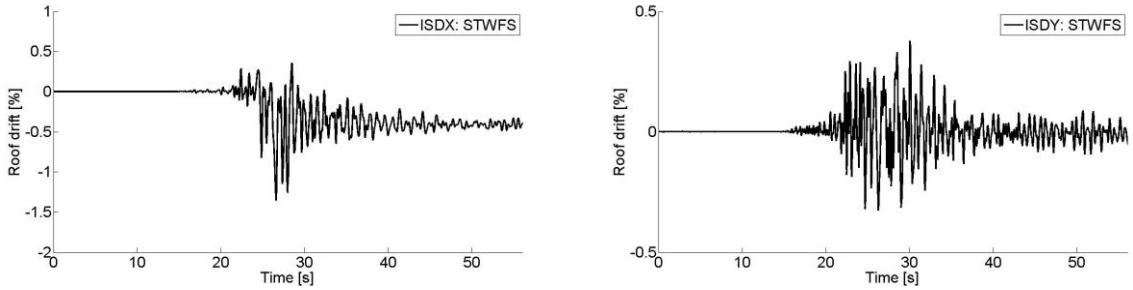

c) Roof drift ratio_ Geiyo_YMG018

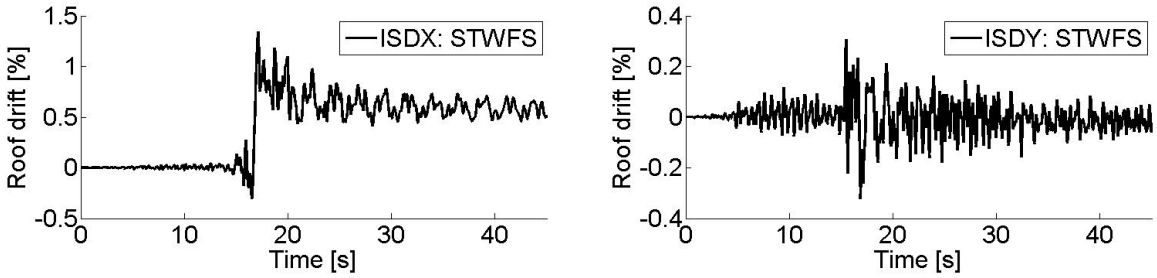

d) Roof drift ratio_ Mich_UNIO

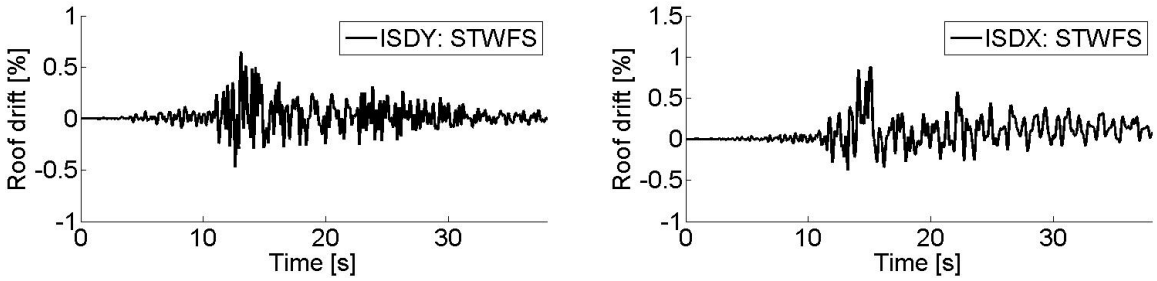

e) Roof drift ratio_ Mich_VILE

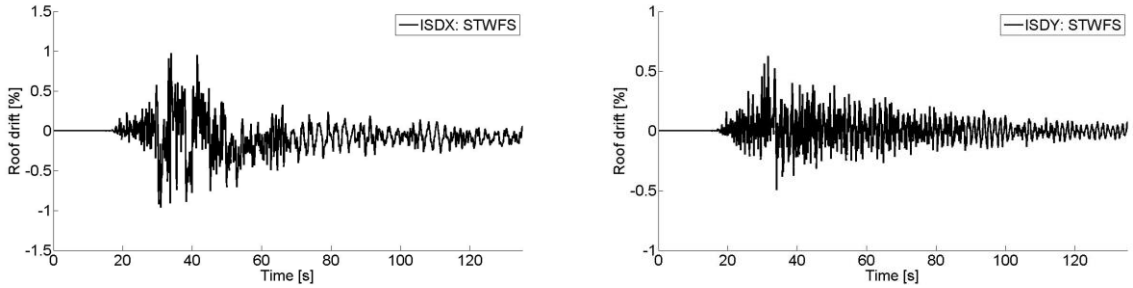

f) Roof drift ratio_ Miyagi_Oki_MYG006

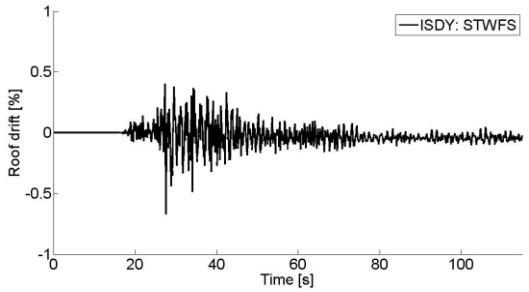

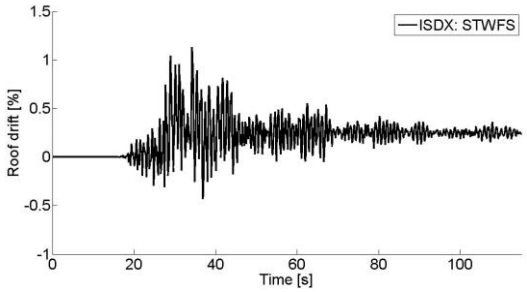

g) Roof drift ratio_ Miyagi_Oki_MYG010

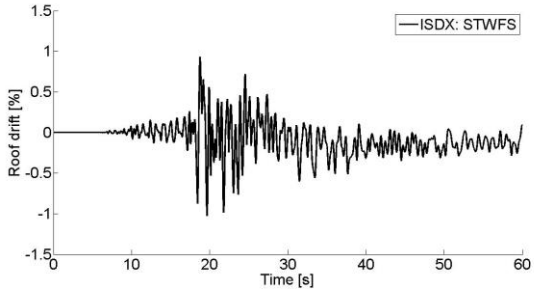

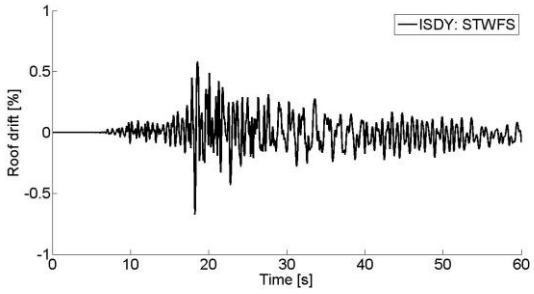

h) Roof drift ratio_ Nisqually_USGS7010

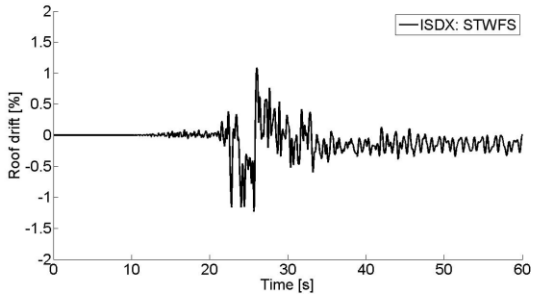

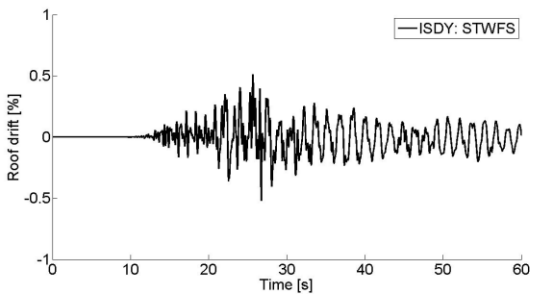

i) Roof drift ratio_ Nisqually_USGS7032

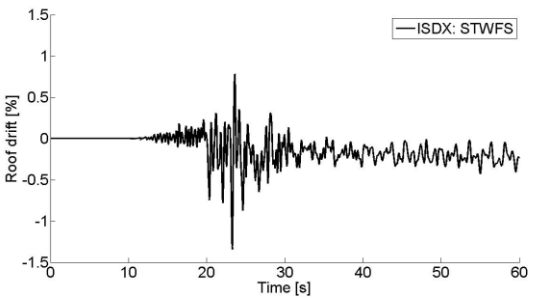

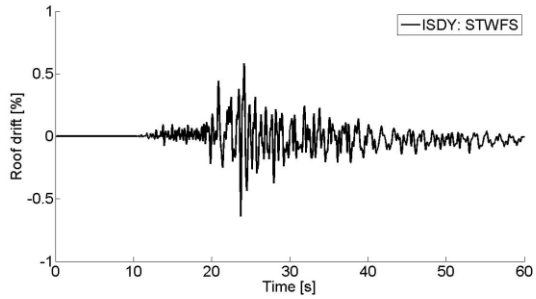

j) Roof drift ratio_ Nisqually_USG7030

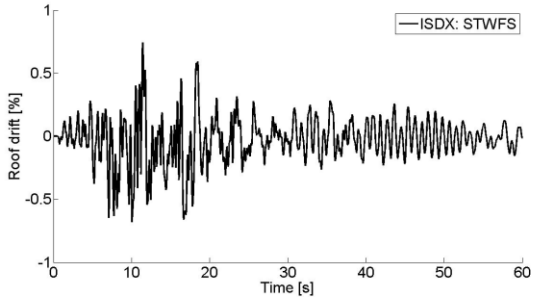

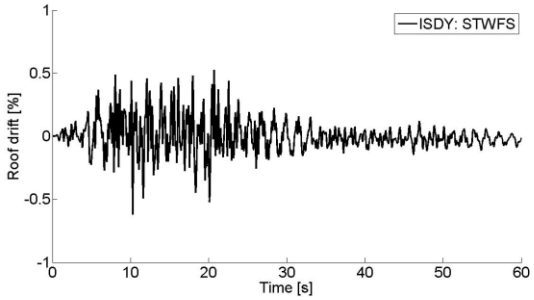

k) Roof drift ratio_ Olympia_OLY0A-

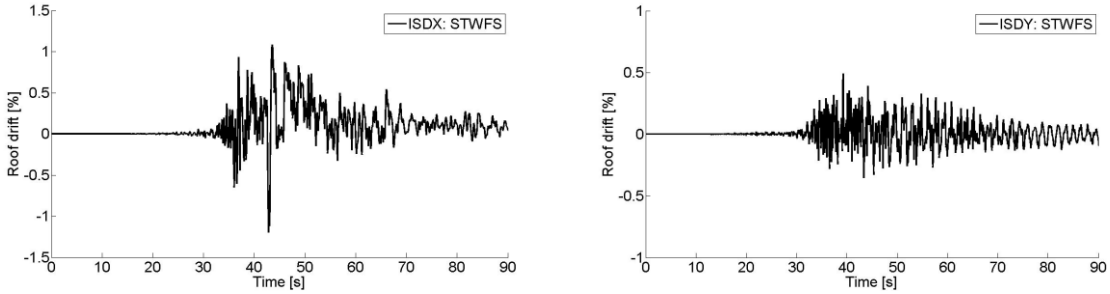

a) Roof drift ratio_ Hokkaido_HKD087

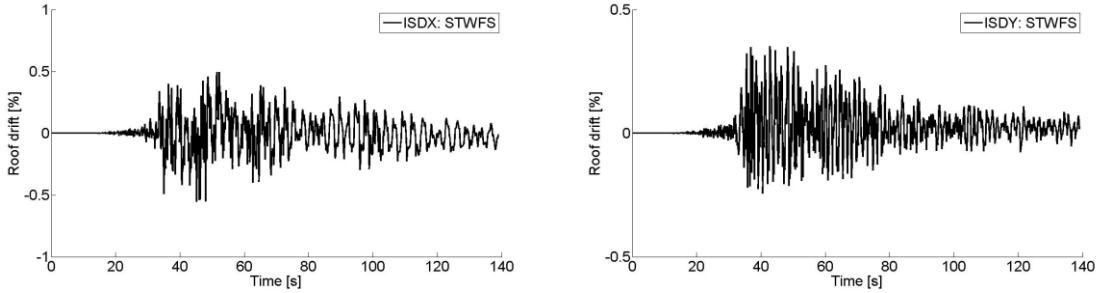

b) Roof drift ratio_ Hokkaido_HKD094

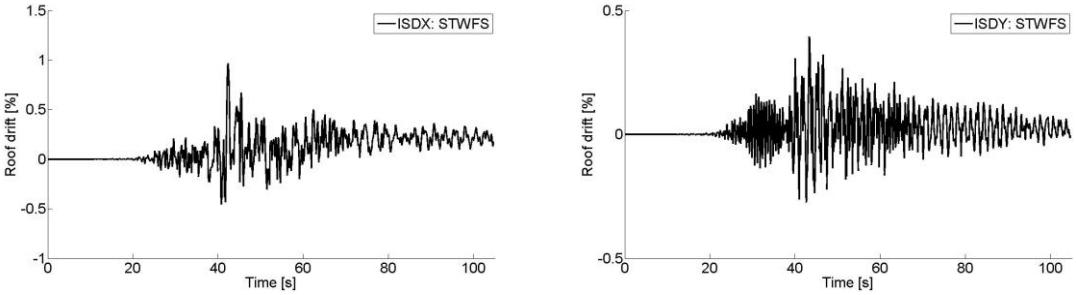

c) Roof drift ratio_ Hokkaido_HKD105

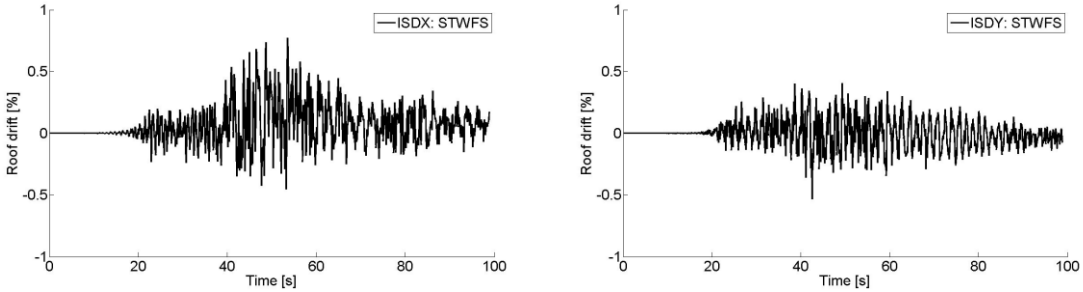

d) Roof drift ratio_ Hokkaido_HKD127

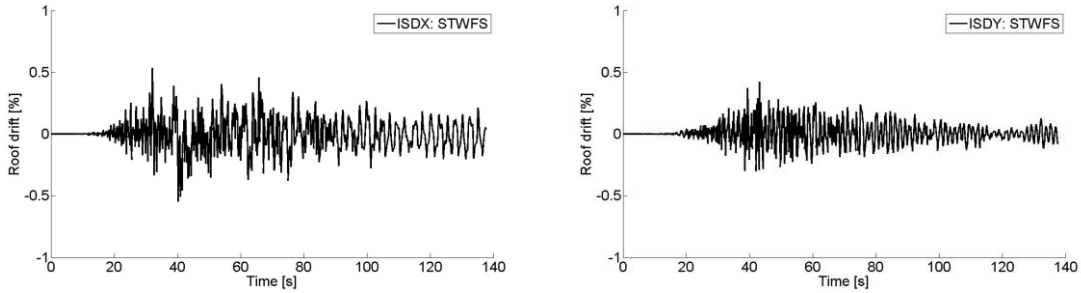

e) Roof drift ratio_ Hokkaido_HKD182

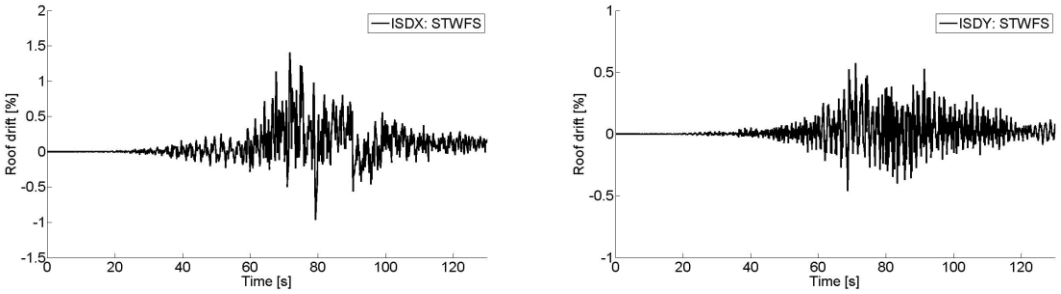

f) Roof drift ratio_ Maule_stgolaflorida

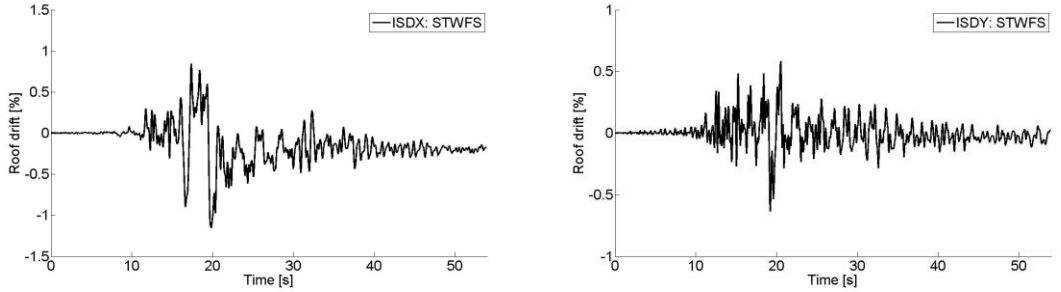

g) Roof drift ratio_ Michoacan_AZIH

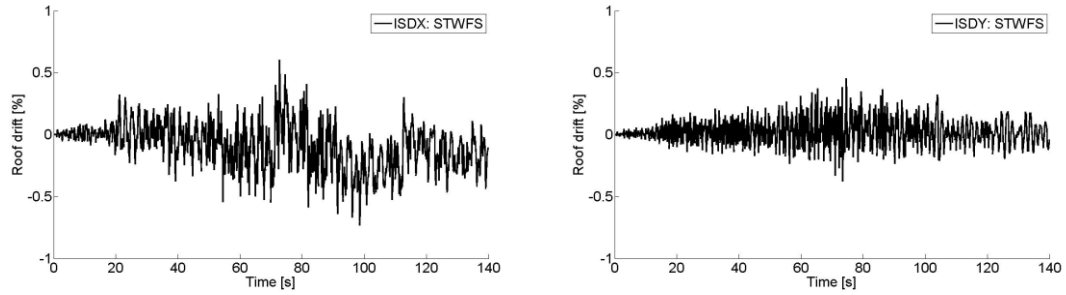

h) Roof drift ratio_ Tohoku_CHB022

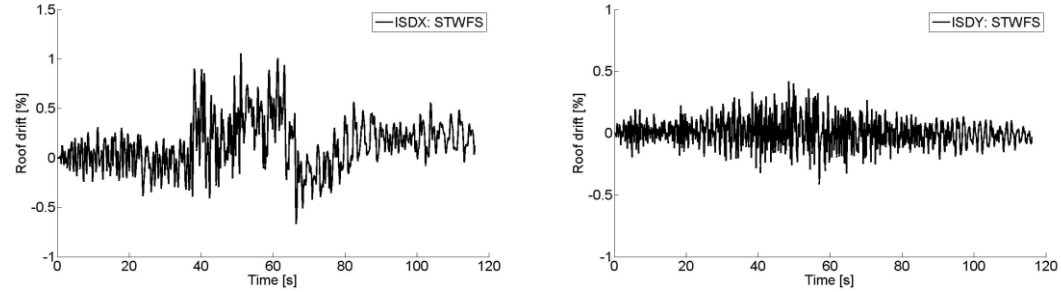

i) Roof drift ratio_ Tohoku_KNG007

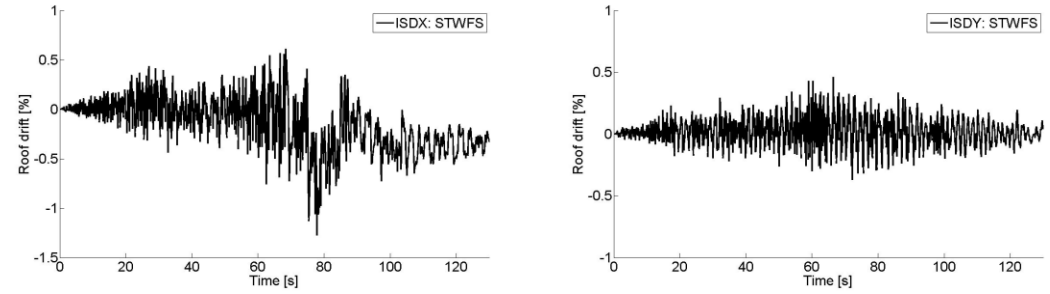

j) Roof drift ratio_ Tohoku_SIT009

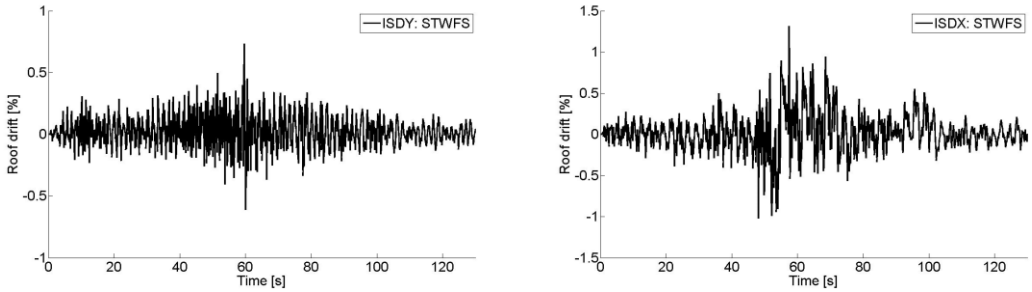

k) Roof drift ratio_ Tohoku_TKY006

Figure A.1 Roof drift ratio: 12-story BRBF building